The role of Blimp-1 transcriptional regulator in adipose-resident Tregs

by

Lisa Yuko Beppu

B.S., University of California, Davis, 2010

Submitted to the Graduate Faculty of the

School of Medicine in partial fulfillment

of the requirements for the degree of

Doctor of Philosophy

University of Pittsburgh

2021

UNIVERSITY OF PITTSBURGH

SCHOOL OF MEDICINE

This dissertation was presented

by

Lisa Yuko Beppu

It was defended on

April 15, 2021

and approved by

Amanda Poholek, PhD, Assistant Professor, Department of Immunology, Pediatrics

Greg Delgoffe, PhD, Associate Professor, Department of Immunology

Jon Piganelli, PhD, Associate Professor, Department of Immunology, Pathology, Surgery

Robert O'Doherty, PhD, Professor, Department of Medicine

Dissertation Advisor: **Louise D'Cruz, PhD**, Assistant Professor, Department of Immunology

The role of Blimp-1 transcriptional regulator in adipose-resident Tregs

Lisa Yuko Beppu, PhD

University of Pittsburgh, 2021

Adipose-resident regulatory T cells are protective against local inflammation, and are believed to play a critical role in preserving insulin sensitivity and glucose tolerance. Although their basic markers and roles have been studied, less is known about the transcriptional machinery regulating their differentiation and function.

B lymphocyte-induced maturation protein-1 (Blimp-1) is a transcriptional regulator known to be involved in development, polarization, and maintenance of various immune cells including CD4+ T cells. Using Blimp-1 reporter mice, we discovered that Blimp-1 is constitutively expressed in a subset of visceral adipose tissue (VAT) Tregs, and that Blimp-1+ VAT Tregs are phenotypically distinct from their Blimp-1- counterparts. We also found that Treg-specific Blimp-1 deletion led to reduced ST2+ KLRG1+, IL-10-producing VAT and inguinal adipose tissue (IAT) Tregs. Surprisingly, during diet-induced obesity, Blimp-1 Treg deficient mice gained less weight, had reduced body fat percentage, and exhibited improved insulin sensitivity compared to wild-type mice. Furthermore, this was accompanied by white adipocyte beiging. It has previously been shown that IL-10 can directly induce thermogenesis. Therefore, we repeated these experiments utilizing mice with Treg-specific deletion of IL-10 and found that they phenocopied the Blimp-1 Treg deficient mice. In summary, these findings reveal that Treg-adipocyte cross-talk can occur via a Blimp-1/IL-10 axis, and that the absence of Blimp-1+ Tregs increases white adipose tissue beiging and is metabolically protective against diet-induced obesity.

Table of Contents

List of Tables

List of Figures

List of Abbreviations

aTreg: adipose-resident regulatory T cell

BAT: brown adipose tissue

Blimp-1 CKO: Blimp-1 conditional knockout

DC: dendritic cell

DIO: diet-induced obesity

HFD: high fat diet

IAT: inguinal adipose tissue

ILC2: Type 2 innate lymphoid cell

iLN: inguinal lymph node

M1: classically-activated macrophage

M2: alternatively-activated macrophage

NK cells: natural killer cell

scAT: subcutaneous adipose tissue

SFD: standard fat diet

Th1: T helper 1 cell

Th2: T helper 2 cell

Th17: T helper 17 cell

Treg: regulatory T cell

VAT: visceral adipose tissue

WAT: white adipose tissue

WT: wild-type

Preface

First and foremost, I would like to thank my thesis advisor, Dr. Louise D'Cruz, for her mentorship and training throughout the course of my PhD graduate program. I would also like to thank the rest of my PhD dissertation committee, Dr. Amanda Poholek, Dr. Jon Piganelli, Dr. Greg Delgoffe and Dr. Robert O'Doherty for their significant theoretical contributions during the course of this project.

In addition, I would like to give a very special thank you to the Blimp-1 team (Xiaoyao Qu, Giovanni Marrero, Alex Finley, Allen Fooks and Zackary Mullen) as well as our collaborators (Dr. Raja Gopal Reddy Mooli, Ian Sipula, Dr. Bingxian Xie, Dr. Michael Jurczak and Dr. Sadeesh Ramakrishnan) for their tremendous expertise and assistance in carrying out the experiments especially in the midst of the COVID-19 pandemic. Also, thank you to the staff of the University of Pittsburgh Flow Cytometry Core, Center for Metabolism and Mitochondrial Medicine Core and DLAR for providing the infrastructure necessary to efficiently carry out all of our work.

Finally, I would like to thank all of my family, friends and God for their love, support and care throughout the last 5+ years in Pittsburgh. I will forever be grateful.

1.0 Introduction

1.1 Epidemiology and etiology of obesity

Obesity is a growing worldwide epidemic. Since 1975, the number of people with obesity has tripled globally, with more people now residing in a country where annual cases of obesity-related deaths exceed those due to malnutrition[1]. In the United States, obesity rates have continuously risen over the last 20 years[2, 3]. In 2017-2018, 70% of adults and 35% of children and adolescents between the ages of 2-19 were overweight or obese[2, 4]. This has translated to staggering economic costs. A recent analysis of the obesity-related medical expenditures in the United States estimated 260 billion dollars were spent in 2016 alone[5]. This did not take into account indirect costs such as loss of workplace productivity or burden to caregivers[6, 7].

Obesity is a serious medical condition because it is tied to numerous co-morbidities including Type 2 diabetes, cardiovascular disease, fatty liver disease, respiratory challenges, cancer and depression[8, 9]. Furthermore, the current SARS-CoV-2 global pandemic has once again drawn attention to the dangers of obesity, as individuals with this condition have suffered higher rates of hospitalization and case fatality[10].

Obesity is clinically defined as having a body mass index of $\geq$30kg/m^2. Fat deposition can occur at various sites within the body, but an excess of visceral fat around the abdominal organs makes individuals especially prone to developing comorbidities[8]. Although there is a tendency to attribute obesity to poor diet and a sedentary lifestyle, it is actually a multi-factorial disease with many biological, genetic, social and behavioral

contributors. These include but are not limited to: genetic predisposition, status of the gut microbiota, poor sleep quality, stress, changes in metabolism due to prescription medications or age, and socioeconomic factors[8].

Recently, researchers have found that an individual's immune system also plays an important role in obesity as well. In lean, healthy individuals, the adipose is populated by anti-inflammatory immune cells[11]. However, during obesity, the presence of pro-inflammatory immune cells has been linked to disruptions in insulin signaling and glucose tolerance[11]. Although weight loss is promoted as a means of addressing these problems, it is clear from the epidemiological data that this so far has not been a viable solution for most people. Therefore, immunological interventions have recently garnered interest as a possible alternative to combating obesity[12].

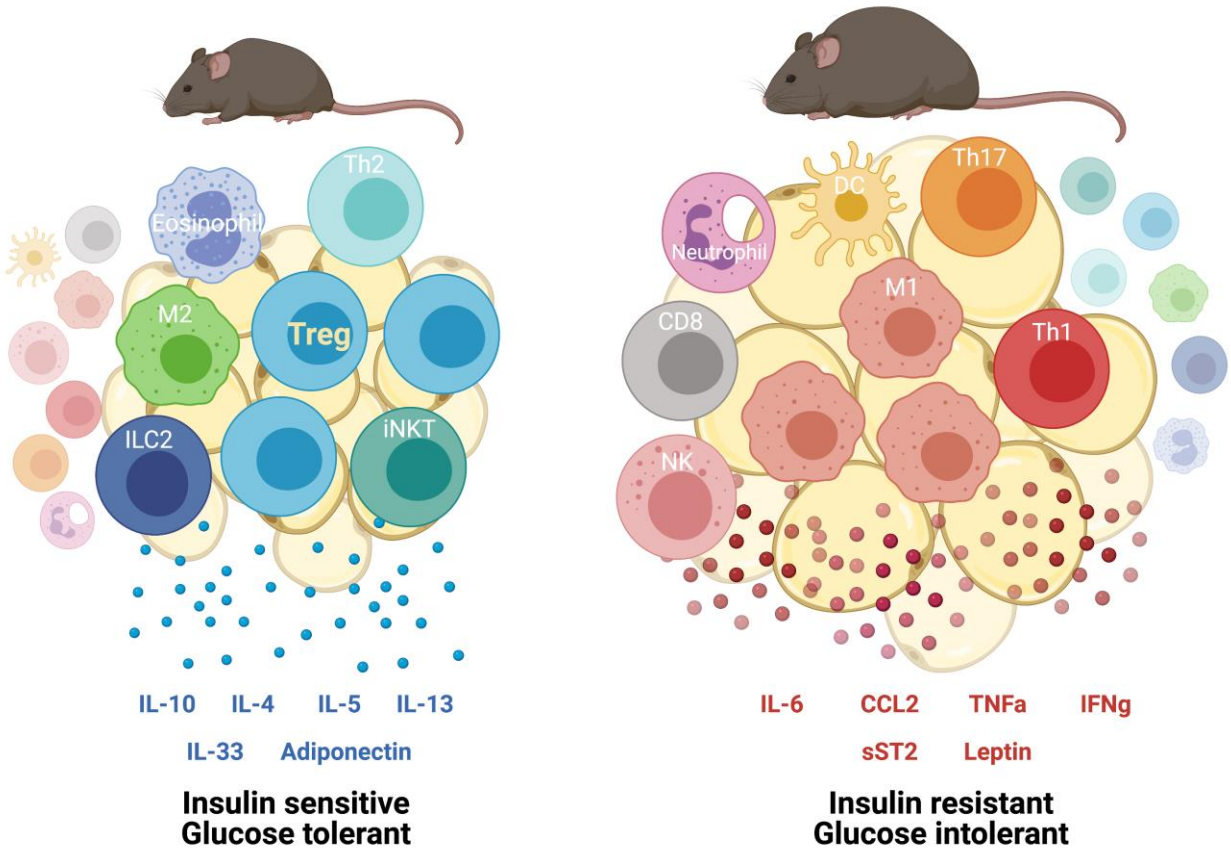

Figure 1. Adipose-resident immune cells in lean and obese adipose tissue.

In lean mice, the white adipose tissue is populated primarily by anti-inflammatory immune cells that secrete cytokines that help maintain insulin sensitivity and glucose tolerance. However, during obesity, there is a higher frequency of pro-inflammatory immune cells that release cytokines that exacerbate insulin resistance and glucose intolerance. In addition, adipocytes themselves can secrete adipokines that affect metabolic homeostasis.

1.2 Immunopathology of obesity

Adipose tissue has traditionally been viewed as energy repositories consisting of lipid-storing adipocytes. However, within the past decade, a growing body of evidence

has made it clear that the adipose is also an endocrine organ that plays a critical role in maintaining systemic metabolism. This is made possible by the fact that adipose tissue-resident immune cells as well as adipocytes themselves secrete cytokines and adipokines that allow cross-talk amongst each other as well as with the rest of the endocrine system. In this section, we will start by covering how obesity leads to adipose tissue remodeling and changes in the immune cell compartment, and then proceed to explore how these events affects 2 key processes that are critical for maintaining metabolic homeostasis- thermogenesis and insulin sensitivity.

1.2.1 Adipose tissue immune homeostasis is modulated by adipocyte morphology, the adipokine milieu and oxygen availability.

Adipose tissue can be categorized into two forms- brown adipose tissue (BAT) and white adipose tissue (WAT). Brown adipose tissue contains adipocytes with multiple small lipid droplets and abundant amounts of mitochondria that aid in energy dissipation through thermogenesis (i.e. heat production) via uncoupling protein 1 (UCP1)[11, 13]. White adipose tissue can be further subcategorized into subcutaneous adipose tissue (scAT) and visceral adipose tissue (VAT). VAT is the fat surrounding intra-abdominal organs, whereas the scAT is the fat which exists right underneath the skin[14]. In addition to scAT and VAT, WAT can also be found in more limited quantities in the bone marrow, perivascular, epicardial and mediastinal retro-orbital space[9]. White adipocytes are usually characterized by a single large triglyceride-containing lipid droplet and have fewer, variable amounts of mitochondria[13]. Initially, the WAT's sole purpose was thought to be

lipid storage[8]. However, it is now clear that the scAT also contains “beige” adipocytes that possess thermogenic potential similar to that of brown adipocytes[8].

Whether or not adipose tissue homeostasis is maintained relies on the balance between tissue-resident anti-inflammatory immune cells (e.g. alternatively activated M2 macrophages, regulatory T cells (Treg), type 2 innate lymphoid cells (ILC2), eosinophils and T helper 2 cells (Th2)) and pro-inflammatory immune cells (e.g. classical M1 macrophages, CD8 T cells, T helper 1 cells (Th1) and T helper 17 cells (Th17)), as well as how these immune cells interact with adipocytes[11]. In lean, healthy adipose tissue, white and brown adipocytes produce adiponectin[15, 16]. This adipokine induces antigen-presenting cells to secrete anti-inflammatory cytokines such as IL-10, IL-1RA, ARG1, MGL1, and Chi3l3 while also inhibiting their ability to release pro-inflammatory cytokines such as IFNg, TNFa, CCL2, IL-6, and iNOS[17, 18, 19, 20]. In addition to adipocytes, certain subclasses of mesenchymal stromal cells secrete IL-33, a cytokine that supports maintenance of Tregs and ILC2 cells[11]. ILC2-derived cytokines, such as IL-5 and IL-13, support the maintenance of eosinophils, which through secretion of IL-4 can promote M2 macrophage polarization[21, 22]. Furthermore, adipose Tregs and a $NK1.1^{NEG}$ subclass of invariant natural killer T cells (iNKT) can secrete IL-10[23, 24 10], which can further promote M2 polarization, and also prohibit inflammatory signaling in adipocytes[25].

However, during obesity, white adipocytes undergo hyperplasia (i.e. increased cell proliferation therefore resulting in more adipocytes for lipid storage) and hypertrophy (i.e. increased lipid storage per individual cell) to accommodate excess fat[8]. When the latter occurs, adipocytes that become too large can burst leading to the recruitment of macrophages whose job is to clear cellular debris[26-28]. However, the free fatty acids

released from ruptured adipocytes also induces macrophages to produce TNFa which in turn acts back on intact adipocytes to induce expression of CCL2, a chemoattractant for myeloid and lymphoid cells[29].

This immune cell infiltration turns inflammatory in nature due to alterations in the adipokine milieu during excessive fat gain. During obesity, a rise in circulating leptin exacerbates inflammation by promoting recruitment, differentiation, maintenance and function of pro-inflammatory immune cells such as macrophages, neutrophils, dendritic cells, granulocytes, NK cells, Th1 and Th17 cells while inhibiting differentiation, maintenance and function of anti-inflammatory immune cells such as Th2 and Treg cells[30]. In addition, obesity results in increased secretion of soluble ST2 (sST2) adipokine in the VAT. sST2 is a decoy receptor for IL-33. In high fat diet (HFD)-fed mice, the presence of sST2 leads to decreased frequency of Tregs and ILC2s[31].

Besides changes in adipokines, hypoxia may also worsen inflammation in expanding adipose tissue[32, 33]. Blood vessels deliver oxygen to the adipose tissue. In one study, HFD mice underwent adipose tissue-specific deletion of vascular endothelial growth factor (VEGF), a growth factor necessary for angiogenesis and delivery of oxygen to cells. This deletion resulted in adipocyte apoptosis, macrophage infiltration, and an increase in inflammatory PAI-1, TNFa and CCL2, and a decrease in anti-inflammatory adiponectin within the WAT[34]. Although these findings don't rule out the possibility that these results were attributable to other factors such as decreased macronutrient delivery, in vitro experiments with human adipocytes and immune cells have demonstrated that hypoxia can directly increase inflammatory IL-6, leptin, PAI1, CCL2, and TNFa while reducing anti-inflammatory adiponectin and IL-10[35].

White and brown adipocytes can have differential effects on immune cells. For example, BAT secretes lower levels of IL-6 compared to WAT[36]. When macrophage cell lines were co-cultured with differentiated white adipocytes, macrophages exhibited a pro-inflammatory gene signature and more IL-6 was detected in the media compared to monocultured macrophages[36]. However, this did not occur when macrophages were co-cultured with differentiated brown adipocytes[36]. The anti-inflammatory nature of BAT has also been demonstrated in transplant studies. In one study by Shankar et al. (2018), intrascapular BAT transplantation into HFD mice led to the VAT having decreased frequency of M1 macrophages and CD8 T cells, and increased frequency of Tregs[37]. In addition, when mice underwent BAT transplants, the VAT presented with decreased expression of pro-inflammatory cytokines *Mcp1, Il6, Tnfa* and *Jnk1*, while expression of anti-inflammatory cytokines *Il1b, Arg1, Chi3l3* and *Il10* simultaneously increased[37].

1.2.2 A global overview of how careful coordination between adipose depots and other endocrine organs maintains insulin sensitivity and glucose tolerance.

The body requires nutrients to meet its basal as well as active energy needs. The liver plays a major role in stabilizing glucose levels. It is the primary organ responsible for endogenous glucose production when the body is fasting[38]. Upon meal consumption, glucose triggers the pancreatic ß-cells to secrete insulin into the bloodstream[39]. Circulating insulin binds to its receptors on adipose, liver and muscle cells to upregulate glucose, fatty acid, and protein transporters nutrients can be shuttled from the blood into these organs[39]. In addition, insulin signaling halts gluconeogenesis within the liver[38].

However, during obesity, cells become insulin resistant (i.e. they stop responding to insulin), and thus lipids are not removed from the bloodstream. Reduced insulin sensitivity also increases hormone-sensitive lipase (HSL) activity within hypertrophic adipocytes causing them to undergo increased lipolysis[40]. Release of free fatty acids leads to recruitment of macrophages that secrete cytokines that further accelerate lipolysis[39]. Overall, this results in increased circulating free fatty acids. Initially, the pancreas synthesizes additional insulin as a compensatory mechanism resulting in hyperinsulinemia[41]. However, over time, prolonged exposure to high fatty acid levels induces cellular stress responses in the pancreas that cause b-cell dysfunction and apoptosis resulting in Type 2 Diabetes, a condition in which pancreatic insulin production is partially or completely abolished[41].

Besides damaging pancreatic b-cells, lipids also have a harmful effect on the liver. Livers import fatty acids to generate ATP[40]. However, any excess fatty acids are stored as triglycerides[40]. In addition, the liver imports glucose which can be utilized in de novo triglyceride synthesis[40]. Excess triglycerides accumulation leads to hepatic steatosis (i.e. fatty liver disease), which has been linked to metabolic dysfunction[42]. During the early stages of obesity, hepatic steatosis may correlate positively with hyperinsulinemia, most likely due to the liver's diminished capacity to clear plasma insulin[38]. In addition, hepatic steatosis has been associated with continued gluconeogenesis even in the fed state, which likely worsens hyperglycemia[39].

1.2.3 BAT, scAT beige adipocytes, and anti-inflammatory immune cells promote thermogenesis and is protective against insulin resistance.

BAT and scAT beige adipocytes play a critical role in preserving metabolic homeostasis. In human adults, greater BAT mass is negatively correlated with BMI and fasting glucose[43]. In addition, BAT transplantation into both lean and obese mice results in improved insulin sensitivity and glucose tolerance[44]. Furthermore, multiple studies have demonstrated that preservation of beige adipocytes curbs diet-induced obesity (DIO) in mice[45-48]. The protective capacity of brown and beige adipocytes appears to be in part due to their ability to carry out thermogenesis to maintain core body temperature. Once activated by cold exposure, exercise, thyroid hormones, ß3-adrenergic agonist, or diets rich in protein, polyunsaturated fatty acids and capsinoids, BAT and beige adipocytes tap into their intracellular triglyceride stores to free fatty acids that are then utilized in ß-oxidation for ATP and heat generation[9]. As lipids are utilized, the BAT imports exogenous fatty acids and glucose to synthesize triglycerides to replace the ones that were recently utilized[9]. This process removes nutrients from the bloodstream, and thus helps maintain normoglycemia, normolipidemia and insulin sensitivity.

Adipose-resident immune cells are believed to help regulate thermogenesis. The BAT is more resistant to inflammation compared to scAT or VAT[49, 50]. Unlike lean scAT which contains a notable amount of immune cells, CD45+ leukocytes make up less than 5% of live cells within the BAT of 8wk old mice[51]. In addition, in HFD-fed mice, marked BAT immune cell filtration does not occur until after 6 months on HFD[49, 50]. One proposed reason for this is that brown adipocytes utilize a large amount of fatty acids and glucose

to generate heat, and thus the supply of nutrients available to support immune cell maintenance and function is limited[52].

Of the known BAT immune cells, macrophages are the most well-characterized. BAT macrophage frequency and phenotype can be age and diet-dependent. For example, Peterson et al. (2017) found that F4/80+ total macrophages comprise about 30% of BAT leukocytes after 8wks on low fat diet, but only 20% of BAT leukocytes after 8wks on HFD[51]. However, in one study by Sakamoto et al. (2016), the relative expression of *F4/80* and *Tnfa* mRNA doubled in the BAT after 16wks on HFD compared to 16wks on normal diet[53]. Interestingly, a study by Wolf et al. (2017) highlighted how BAT macrophages may cross-talk with BAT-innervating neurons to regulate metabolic homeostasis. They found that CX3CR1+ macrophage-specific *Mecp2* deletion led to decreased sympathetic innervation of the BAT, homeostatic thermogenesis and energy expenditure in 6-month-old mice[54]. Furthermore, a subset of BAT macrophages were in direct contact with BAT neurons, and *Mecp2* deletion resulted in disruption of the plexin-semaforin signaling axis that modulates norepinephrine activated thermogenesis[54]. Besides macrophages, other types of immune cells such as Siglecf+ eosinophils, ILC2s and mast cells have been found in the BAT, however whether or not they play a direct role in thermogenesis remains to be determined[51, 55, 56].

In contrast to the BAT, the role of WAT macrophages, eosinophils, ILC2s and mast cells in regulating thermogenesis has been better described. During cold-induced thermogenesis, scAT adipocytes secrete adiponectin which can directly and selectively promote the proliferation of M2 macrophages over M1 macrophages[57]. In cold-challenged mice, deletion of mononuclear phagocytes by clodronate liposomes leads to

reduced scAT macrophages and decreased *Ucp-1* and *Cidea* suggesting M2 macrophages play a role in adipocyte beiging during adaptive thermogenesis[57]. M2 macrophages are supported by eosinophils. Eosinophils are the primary IL-4 producers in the scAT, and loss of IL-4 producing eosinophils, selective deletion of *Il4r* in myeloid cells, or disruption of IL-4/13 or STAT6 signaling leads to fewer M2 macrophages, and reduced scAT beige adipocyte biogenesis and thermogenesis[58, 59 60]. Besides eosinophils, ILC2s also play a major role in promoting beiging. ILC2-derived IL-13 and IL-5 support maintenance of VAT M2 macrophages and eosinophils[21]. Furthermore, in the scAT of thermoneutral mice, IL-33 activated ILC2s secrete IL-13, which works synergistically with eosinophil-derived IL-4 to induce beiging in PDGFRa+ adipocyte precursor cells[60]. Interestingly, ILC2s can also secrete methionine-enkephalin (MetEnk) to directly promote scAT beiging independently of macrophages, eosinophils or an adaptive immune response[61].

Besides ILC2s, eosinophils and macrophages, mast cells may also play a role in scAT beiging although the trends in humans and mice differ. Cold-shocked human mast cells can secrete histamine and IL-4, and each of these factors individually or in combination can induce *Ucp1* expression in differentiated adipocytes in vitro[62]. However, in mice, mast-cell derived serotonin has been found to suppress norepinephrine-induced scAT beiging[63]. In addition, in HFD mice, ablation of mast cell serotonin synthesis led to increased scAT beiging, and curtailed weight gain and insulin resistance[64].

In addition to ILC2s, eosinophils, macrophages and mast cells, Tregs have also been described for their role in maintaining metabolic homeostasis. These cells are the focus of this project and will be discussed in greater detail in the following chapters**.**

Besides thermogenesis-driven insulin sensitivity preservation, batokines (i.e. BAT-secreted cytokines) such as neuregulin 4 (NRG4), fibroblast growth factor 21 (FGF21), and IL-6 may also help maintain metabolic homeostasis[15]. For example, NRG4 is highly enriched in BAT compared to other organs, and *Nrg4* deficient HFD mice exhibit worsened hepatic steatosis as a result of increased de novo lipogenesis in hepatocytes[65]. In addition, it has previously been shown that *Fgf21* null mice have reduced lipid and glucose metabolism in the liver during the fasted state[66, 67]. Finally, IL-6 is known to perform multiple metabolically-related functions such as regulating insulin secretion by the pancreas as well as controlling insulin clearance from the liver and skeletal muscle[68-70].

1.2.4 Obesity-driven changes in the WAT immune cell compartment suppress thermogenesis.

During obesity, scAT macrophage frequency correlates positively with adipocyte hypertrophy in mice, and BMI in humans[71]. This is detrimental because during DIO, direct adhesion of macrophages to adipocytes through a4-integrin/VECAM-1 interaction can suppress UCP-1[72]. In addition, macrophages from obese tissue can secrete IL-1ß and TNFa, which dampen thermogenesis[53, 73, 74]. In contrast to macrophages, pro-thermogenic ILC2s are decreased in the scAT of obese mice compared to that of lean mice[56].

1.2.5 Additional considerations for adipose immunobiology and its role in metabolic homeostasis.

Although at first glance it may appear that lean adipose tissue is associated with anti-inflammatory immune cells, while obese adipose tissue is tied to pro-inflammatory immune cells, it is important to note that the immunopathology of obesity is much more nuanced than this simplified description. For example, adipose-resident immune cells display extreme heterogeneity. In one study, single cell RNA-seq uncovered 7 distinct macrophage subpopulations in the VAT, and all of them changed their transcriptional signatures in response to diet alteration[75]. In addition, adipose immune cells can be shaped by metabolic reprogramming of cells in response to nutrient availability[76]. Furthermore, adipocytes and immune cells can be influenced by aging and sex hormones[77]. Finally, a recent study found that the adipose tissue can possess "obesogenic memory", a condition in which HFD-induced inflammation is irreversible even after mice are placed back on standard chow and lose weight[78]. Hence, any findings within the adipose tissue must be examined carefully and understood that they are context-dependent.

1.3 The role of Tregs in adipose tissue and systemic metabolism

Many types of immune cells including macrophages, eosinophils, ILC2s and mast cells regulate adipose tissue homeostasis and systemic metabolism. However, more recently, regulatory T cells have caught the attention of adipose immunologists as an

abundance of emerging literature suggest that these cells play a critical role in metabolic homeostasis. Adipose resident regulatory T cells (aTregs) are present within both white and brown adipose tissue, and are shaped by multiple factors including diet, age and sex[11, 79-82 80]. Unless otherwise noted, this section will focus on Tregs from male C57BL/6 mice only, as they are the primary mouse model currently being used in adipose immunobiology studies, and because these were the animals that were utilized in this project. We will begin by first reviewing the role of Tregs in adipose tissue immune homeostasis, then describe how they regulate insulin sensitivity and thermogenesis.

1.3.1 The role of Tregs in adipose tissue immune homeostasis.

Tregs play an important role in maintenance of adipose tissue immune homeostasis, and loss of Tregs results in inflammation. In lean, 10wk old mice, selective deletion of Tregs by diphtheria toxin led to higher levels of pro-inflammatory mediators *Tnfa*, *Il6*, *Rantes*, and *Saa3* in the VAT[23]. The exact mechanism by which Tregs suppress adipose inflammation is undefined, however we can propose at least two ways in which this may occur. One possibility is that Tregs act directly on adipocytes. aTregs can secrete IL-10[23 10], and in vitro studies have found that IL-10 can directly suppress LPS-induced IL-6 production by 3T3-L1 adipocytes[83]. The second possibility is that aTregs favor anti-inflammatory M2 macrophage polarization. In the VAT, macrophages are the primary cells capable of MHCII mediated interactions with T cells in both lean and obese mice[84]. Loss of PPARγ+ Tregs in lean mice has been shown to increase pro-inflammatory CD11b+ CD11c+ F4/80+ macrophages and CD11b+ Ly6c^{hi} monocytes in the VAT[85]. Furthermore, it has previously been shown that Tregs can promote M2 macrophages

during both human and mouse in vitro experiments, and in mouse models of acute lung injury[86-88].

1.3.2 The role of Tregs in insulin sensitivity and thermogenesis.

Besides suppressing inflammation, Tregs also play a critical role in controlling insulin sensitivity and glucose tolerance[89-91]. For example, in lean, 10wk old mice, selective deletion of Tregs by diphtheria toxin led to increased fasting insulin[23]. In HFD-fed mice, VAT Treg maintenance is reliant on IL-33/ST2 signaling, and disruption of this pathway leads to insulin resistance and glucose intolerance[31, 91, 92]. Interestingly, fat Tregs appear to exacerbate age-associated insulin resistance in mice, as loss of PPARg+ Tregs leads to reduced fasting insulin and glucose, and improved sensitivity during glucose tolerance and insulin tolerance tests[93].

In addition to regulating insulin, recent studies in nontraditional mouse models (i.e. not male C57BL/6 mice) have uncovered a potential role for Tregs in regulating thermogenesis. In one study, Medrikova et al. (2015) utilized female C57BL/6 mice and found that BAT Tregs possess a temperature-sensitive gene signature that differs from splenic or VAT Tregs[82]. When these mice underwent Treg depletion and were cold-challenged, the Treg-deficient mice exhibited decreased oxygen consumption, body heat and BAT thermogenic gene expression[82]. In a breakthrough study by Kalin et al. (2017), male BALB/c mice were either cold challenged, underwent ß3-adrenergic stimulation or fed high sugar high fat (HSHF) diet to investigate the capacity of WAT and BAT Tregs to be induced from naïve CD4 T cells, and to see how this potentially affected thermogenesis[94]. In response to short-term cold acclimation, BAT, scAT and VAT Tregs

were all inducible from naïve CD4 T cells[94]. In response to ß3-adrenergic stimulation, BAT and scAT Treg induction potential was greater than VAT Treg induction potential from naïve CD4 T cells[94]. Next, 6wk old C57BL/6 or 8wk old BALB/c mice were placed on high-fat/high-sugar (HFHS) diet for 2 weeks[94]. The result was increased BAT Tregs and decreased VAT Tregs in both C57CL/6 and BALB/c mice compared to standard chow control mice[94]. In addition, in HFHS BALB/c mice, scAT Tregs were reduced in comparison to standard chow control mice[94]. During longer periods on HFHS diet (8wks for C57BL/6 mice, 16wks for BALB/c mice), both strains exhibited reduced frequency of VAT Tregs, but not scAT or BAT Tregs[94]. Treg depletion in BALB/c mice followed by ß-adrenergic stimulation or short-term HFHS diet led to decreased thermogenesis, lipolysis and ß-oxidation compared to mice that had their Tregs intact[94]. Gain-of-function experiments with in vivo Treg transfer or in situ expansion of Tregs via subcutaneous IL-2 injection led to increased thermogenesis, lipolysis and ß-oxidation in the BAT and scAT[94]. In the end, they found that ß-adrenergic signaling induced BAT naïve CD4 T cells into becoming Treg through a STAT6/PTEN axis, and that these BAT Tregs in turn enhanced thermogenesis, ß-oxidation, lipolysis and adipocyte differentiation[94]. Similar observations were also made to smaller degrees in scAT and VAT[94]. To note, these BALB/c mice had higher frequencies of scAT and BAT Tregs than VAT Tregs, which is the opposite of what is found in C57BL/6 mice[94]. However, in support of the findings in BALB/c mice, studies using humanized mice also found that ß-adrenergic signaling enhanced the induction potential of VAT Tregs from naïve CD4 T cells in vitro, and led to increased VAT Treg frequency and thermogenesis in vivo[95].

1.4 Adipose tissue-resident Treg development, differentiation and maintenance

1.4.1 VAT Treg development, differentiation and maintenance

In lean mice, VAT Tregs reach a peak frequency of 40% of total CD4 T cells at ~25wks of age, before falling to about 10% by 40wks of age[79, 96]. In contrast, VAT Tregs comprise only about 10% of total CD4 T cells in mice that received HFD for 8-29wks[23, 79]. The transcriptional signature of VAT Tregs from lean mice differs from that of VAT Tregs of obese mice, or Tregs found in other peripheral tissues and secondary lymphoid organs[79, 97]. Canonical markers of lean VAT Tregs include: FOXP3, GATA3, PPARγ, KLRG1, CCR2, ST2, NRP1 and IL-10[91, 96, 98].

VAT Treg maintenance and differentiation is driven by TCR stimulation, iNKT-derived IL-2[99], and PDGFRa+ Sca-1+ mesenchymal stromal cell-derived IL-33[19]. In VAT Tregs, TCR signaling in the presence of IL-2 induces the transcription factors BATF and IRF4 to directly bind *Pparg* and *Il1rl1* (the gene encoding ST2) to upregulate their expression[92, 100]. TCR signaling in the presence of IL-2 is sufficient to induce ST2 expression, however the addition of IL-33 further promotes its expression[92]. IL-33/ST2 signaling in VAT Tregs requires the adaptor protein MyD88[92], and is especially important for VAT Treg maintenance[91, 92]. Disruption of IL-33/ST2 signaling by soluble ST2 (sST2), an alternative isoform which behaves as a IL-33 decoy receptor, leads to decreased VAT Treg frequency[31]. ST2+ Tregs are reduced in obese adipose tissue compared to lean adipose tissue, but administration of IL-33 can recover these cells[91]. While ST2 plays an important role in maintenance, cooperation between the transcription factors PPARγ and

Foxp3 drives the VAT Treg signature, especially the genes involved in lipid metabolism that are distinctly upregulated in VAT Tregs compared to muscle or colon Tregs[85, 97].

Two landmark studies by Kolodin et al. (2015) and Li et al. (2018) have provided key insight into how the pathways above are spatially and temporally organized to dictate VAT Treg development, differentiation and maintenance. In Kolodin's study, it was determined that VAT Tregs are likely thymically-derived, as they found little evidence of VAT Tregs being acquired from circulating peripheral Tregs or from conversion of VAT Foxp3- CD4+ T effector cells into VAT Tregs[96]. Tregs seeded the VAT prior to 3wks of age, as mice that underwent thymectomies after this point exhibited no differences in VAT Treg frequency[96]. Within lean 15-week-old mice, there was a higher frequency of VAT Tregs compared to VAT CD4 T effector or splenic Tregs that was attributable to slower cellular turnover of VAT Tregs relative to the other two populations[96]. At 25 weeks of age, VAT Tregs exhibited substantial clonal expansion compared to VAT CD4 T effector cells or lymph node Tregs[96]. In addition, total MHCII-deficient mice had fewer VAT Tregs indicating that antigen presentation was important for either thymic selection of VAT-destined Tregs, and/or for maintenance of VAT Tregs once they were within the tissue[96]. Furthermore, they identified these MHCII+ cells as being macrophages and dendritic cells[96]. Finally, they demonstrated utilizing total ST2-deficient mice as well as through IL33 injections that IL33-ST2 signaling played a significant role in VAT Treg expansion independent of TCR-MHCII interactions[96].

In a follow-up study by the same lab, Li et al. (2018) utilized VAT Treg TCR transgenic, PPARγ reporter or VAT Treg/TCR transgenic-PPARγ dual reporter mice to propose that VAT Treg development and differentiation is a 2-step process[100]. Their

findings suggested that thymic Tregs first trafficked to the spleen where those possessing VAT antigen-specific TCRs become activated to express low levels of PPARγ, KLRG1, CD44 and Blimp-1[100]. From there, these specific cells proceeded to infiltrate the VAT, where they underwent further chromatin remodeling to acquire the entirety of their VAT Treg signature which included high expression of PPARγ and ST2[100]. Utilizing conditional knockout mice lacking ST2 specifically in Tregs, they proved that cell-intrinsic IL33-ST2 signaling was critical for VAT Treg maintenance[100]. Furthermore, it appeared that VAT Treg accumulation was Foxp3 dependent, as clonotype+ CD4 T effector cells were present within the VAT at very low frequencies, but adoptively transferred CD4 T effector cells retrovirally transduced to overexpress Foxp3 become enriched in the VAT[100].

Beyond PPARg and Foxp3, ID2 and KLF10 also play important roles in VAT Treg maintenance, differentiation and function. ID2 is a positive regulator of ST2, CCR2, KLRG1 and GATA3 expression, and loss of ID2 leads to increased cell apoptosis and decreased IL-10 and IL-13 production[101]. In both humans and mice, KLF10 is decreased in VAT and scAT Tregs from obese subjects compared to lean subjects[102]. In HFD-fed mice, adoptively transferred KLF10-deficient splenic Tregs migrated less to the VAT compared to adoptively transferred wild-type Tregs. In induced Tregs, loss of KLF10 resulted in defective glycolysis and oxidative phosphorylation, and decreased TGFB3 production[102]. With respect to systemic metabolism, mice lacking KLF10+ CD4 T cells exhibited greater weight gain, insulin resistance and hepatic steatosis[102].

Besides ID2 and KLF10, there are a number of other candidate transcription factors that may shape the VAT Treg compartment. In obese *Stat3*$^{f/f}$ CD4-Cre+ mice, loss of STAT3 signaling skewed VAT T cells towards a Th1 phenotype over a Treg

phenotype, and coincided with increased expression of inflammatory *Socs3*, *Saa3*, and *Ifng* within the tissue[90]. However, because these mice are CD4-Cre, we cannot rule out the possibility that these aTregs were affected in a cell-extrinsic manner by CD8 T cells or NKT cells. In addition, single cell RNA-seq and ATAQ-seq studies have offered the bZIP, ETS and NR transcription factor families as possible VAT Treg regulators[97].

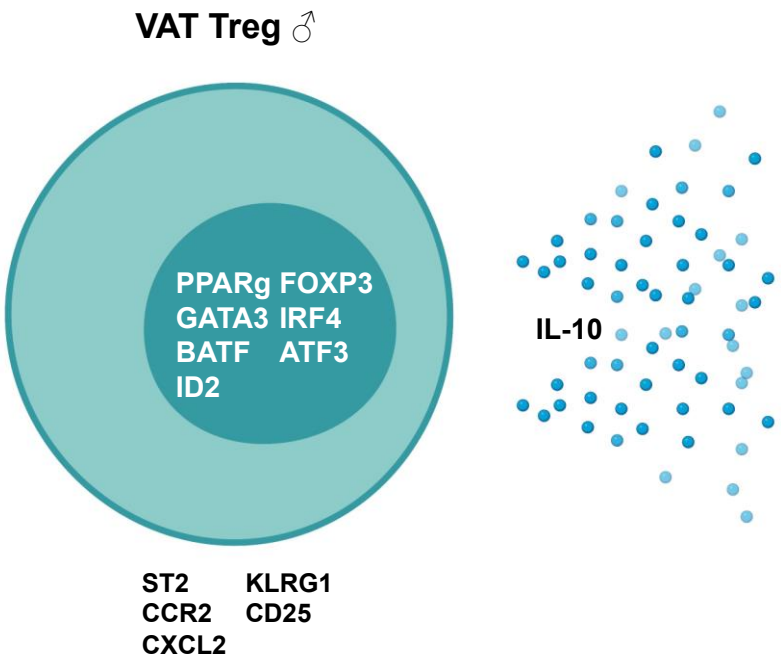

Expression (Obese VS Lean)	
GATA3	↓
IL-10	↓
ST2	↓
KLRG1	↓
CCR2	↓
CD25	No change
PPARg	No change
CXCL2	?
ID2	?
ATF3	?

Figure 2. Phenotype of visceral adipose tissue-resident Tregs in male mice.

Visceral adipose tissue Tregs in male mice are characterized by the transcription factors: PPARg, FOXP3, GATA3, IRF4, BATF, ATF3 and ID2. In addition, they exhibit a number of extracellular surface markers including: ST2, KLRG1, CCR2, CD25 and CXCL2. VAT Tregs carry out their effector function through secretion of IL-10. Expression of VAT Treg canonical markers can vary depending on whether they reside in lean or obese adipose tissue.

1.4.2 scAT and BAT Treg development, differentiation and maintenance

Compared to VAT Tregs, less is known about scAT and BAT Treg development, differentiation and maintenance. However, some studies suggest that scAT Tregs are less affected by age and obesity. In one study, the frequency of scAT Tregs only underwent a miniscule increase over time from ~10% of CD4 T cells at 5wks of age to ~15% of CD4 T cells at 20wks of age, unlike the VAT compartment which increased from ~10% at 5wks of age to ~50% at 20wks of age[23]. In addition, in 13wks old leptin-deficient obese mice, there was no difference in the scAT Treg frequency between $Lep^{ob/+}$ and $Lep^{ob/ob}$ mice[23]. Maintenance of scAT Tregs does not appear to be PPARγ driven, as treatment of mice with pioglitazone, a PPARγ agonist, resulted in no differences in scAT Treg frequency between treated and untreated mice[85]. However, similar to VAT Tregs, KLF10 is decreased in scAT Tregs from obese humans and mice compared to lean subjects, and loss of KLF10 disrupts trafficking of Tregs into the scAT[102]. With respect to BAT Tregs, as mentioned in the earlier sections, naïve CD4 T cells are induced into Tregs through the STAT6/PTEN axis in response to ß-adrenergic signaling[94].

1.5 The role of Blimp-1 transcriptional regulator in Treg development, differentiation and function

B lymphocyte-induced maturation protein-1 (Blimp-1) is a zinc finger motif containing transcriptional regulator encoded by the gene positive regulatory domain 1 (Prdm1)[103] that was initially recognized for its role in suppressing IFNß gene

expression[103], and for regulating plasma cell differentiation[104]. However, it is now clear that Blimp-1 plays a critical role in development, differentiation, and maintenance of various myeloid and lymphoid immune cells including macrophages, dendritic cells and T cells[105-107].

Blimp-1 has a far-reaching role in T cells. During early T cell development, Blimp-1 deficient mice have fewer thymic T cells at the double-positive and single-positive T cell stage, and double-positive cells are more prone to apoptosis[108]. In addition, Blimp-1 is critical for peripheral T cell homeostasis as loss of Blimp-1 leads to uncontrolled T cell expansion and a lethal lymphocyte hyperproliferative syndrome[109]. In CD8 T cells, Blimp-1 determines whether proliferating CD8 T effector cells become terminally differentiated into short-lived effector cells, or form into memory precursor effector cells[110-112]. Blimp-1 also positively regulates the expression of cytolytic genes such as *Gzmb*, *Gzmk*, and *Prf1*, while repressing expression of *Tnfa* and *Ifng*[110, 111]. Blimp-1 is not required for CD8 memory T cell maintenance, but is critical for an efficient memory recall response during viral infections[110, 111]. In CD4 T cells, Blimp-1 plays a critical role in CD4 T cell differentiation by promoting the transcriptional signature of some subsets, while repressing those of others. In particular, Blimp-1 favors the development, differentiation and function of regulatory T cells.

In an early study by Cretney et al. (2011), *Blimp1*$^{+/GFP}$ reporter mice and Ly5.1+ wild-type Ly5.2+ *Blimp-1*$^{GFP/GFP}$ mixed bone marrow chimera mice possessing both wild-type and Blimp-1 deficient Tregs were utilized to study the role of Blimp-1 in effector Tregs[113]. They found that Blimp-1 was dispensable for splenic effector Treg development[113]. However, there was a higher frequency of Blimp-1- Tregs than Blimp-

1+ Tregs in the Peyer's patches, epithelium and lung, indicating that Blimp-1 is required for peripheral Treg homeostasis[113]. When infected with influenza, Blimp-1- lung Tregs failed to upregulate ICOS pointing towards a role for Blimp-1 in effector Treg activation[113]. In addition, through a series of in vitro and in vivo experiments involving IL-2—anti-IL-2 antibody complex injections into *Blimp-1*$^{+/GFP}$ mice, they demonstrated that IL-2 induced Blimp-1, and that its expression could be further enhanced by IL-12, IL-6 and IL-4[113]. Functionally, Blimp-1 was required for IL-10 production[113]. Beyond experiments in Blimp-1 mice, they utilized Ly5.1+ wild-type Ly5.2+ *Irf-/-* mixed bone marrow chimera mice to show that IRF4 directly bound Blimp-1 to positively regulate its expression in Tregs, in line with previous observations made in plasma cells, CD8 T cells and total CD4 T cells[114, 115]. IRF4-deficient mesenteric lymph node Tregs had decreased ICOS, CTLA4 and CD103 expression indicating that IRF4 is important for Treg differentiation[113]. In addition, during influenza infection, Tregs required IRF4 to upregulate ICOS and traffic from the mediastinal lymph node to the lungs[113]. Finally, microarrays confirmed that although Blimp-1 and IRF4 worked in concert to dictate effector Treg fate, Blimp-1 was requisite for activation, IL-10 production and maintenance in peripheral tissues, whereas IRF4 was required for differentiation[113].

In a different study, Bankoti et al. (2017) focused on the role of Blimp-1 in effector Treg maintenance, differentiation and function under non-inflammatory conditions. Utilizing Blimp-1 reporter mice, they found that Blimp-1 was expressed in ~20-30% of splenic, mesenteric lymph node (MLN), and large intestines lamina (LI-LP) Tregs, but in only ~5% of thymic Tregs[116]. In order to elucidate the role of Blimp-1 in Treg maintenance, differentiation and function, they utilized *Prdm1*$^{f/f}$ Foxp3-Cre+ mice that lacked Blimp-1

specifically in Tregs. Loss of Blimp-1 had no effect of thymic Treg frequency[116]. However, in the absence of Blimp-1, greater proliferation and decreased cell death resulted in higher Treg frequency in the spleen, MLN, and LI-IP[116]. In addition, loss of Blimp-1+ Tregs increased splenic and MLN CD4 Teffector and CD8 T cells[116]. Blimp-1 deficient splenic Tregs produced less IL-10[116]. However, this was countered by an increase in IL-10 producing CD4 Teffector cells[116]. Loss of Blimp-1+ Tregs had no effect on IL-17 production by CD4 T cells[116]. Hence, in terms of immunopathology, loss of Blimp-1+ Tregs led to only mild intestinal inflammation[116]. Finally, utilizing microarrays and qPCR, they compared how Blimp-1 modulated the transcriptomes of peripheral Tregs versus CD4 T effector cells. Genes that were commonly upregulated by Blimp-1 included: *Batf3*, *Bcl6*, *Prdm1*, *Slc2a6* and *Tox*[116]. Genes that were commonly down-regulated by Blimp-1 included: *Cd5*, *Grap2*, *Il10*, *Notch1* and *Trib2*[116]. Genes that were uniquely upregulated in Blimp-1- Tregs included: *Ccr6*, *Hif1a*, *Il17f*, *Stat4* and *Tcf7*[116]. Genes that were uniquely down-regulated in Blimp-1- Tregs included: *Ctla4*, *Maf, Socs2*, *Tbx21* and *Tnfrsf18*[116]. *Tnfrsf18* is the gene which encodes GITR[116]. Interestingly, Blimp-1 and GITR appears to form an auto-regulatory loop. In a study by Vasanthakumar et al. (2017), GITR activated the transcription factor RelA, and RelA positively regulated Blimp-1 expression independent of TCR signaling or IRF4 in effector Tregs[117].

In a follow-up to their 2015 study, Cretney et al. (2018), further examined the cell-intrinsic effects of Blimp-1 deletion in Tregs, and for the first time described immunopathological changes that occurred in older mice that lacked Blimp-1+ Treg. Utilizing 8wk old *Foxp3*^{RFP}*Prdm1*$^{GFP/+}$ reporter mice, they found that Blimp-1+ Treg frequency was greatest in the colon and small intestines[118]. However, Blimp-1+ Tregs

were also present in the thymus, blood, spleen, liver, lung, mesenteric and peripheral lymph nodes, and Peyer's patches[118]. In addition, from 8wks to 6months of age, the frequency of Blimp-1+ Tregs significantly increased in the liver, and decreased in the small intestine epithelium[118]. Utilizing *Prdm1*$^{f/f}$ Foxp3-Cre+ mice, they also found that Treg-specific deletion of Blimp-1 led to increased blood, thymic, splenic, mesenteric and peripheral lymph nodes, lung, Peyer's patches, and small intestinal epithelium Tregs frequency[118]. Surprisingly, Blimp-1 deficient splenic Tregs exhibited more of an activated phenotype with a higher fraction expressing CD103 or ICOS, and a lower fraction expressing CD62L[118]. Loss of Blimp-1 led to increased frequency of ICOS+ Tregs in the blood, liver, lungs, mesenteric and peripheral lymph nodes, and Peyer's patches as well[118]. These findings went against the data in their earlier paper suggesting that Blimp-1 is required for effector Treg activation[113]. However, it was mentioned that their mice exhibited "Foxp3-Cre leakiness", with all of their animals displaying some degree of non-specific Cre activity in B cells, CD4 T effector cells or CD8 T cells. With regard to immunopathology in aged mice, *Prdm1*$^{f/f}$ Foxp3-Cre+ mice started to become ill at ~110 days of age, and none survived past 650 days of age. In contrast, most wild-type mice remained alive[118]. In addition, they found higher concentrations of serum antinuclear antibodies in 1yr or older knockout mice compared to age-matched wild-type mice[118]. Furthermore, as knockout mice aged, they began exhibiting variable amounts of abnormal immunopathology especially in their salivary glands, gastrointestinal tract, and pancreas[118].

Expanding on the many known functions of Blimp-1 in Tregs, Ogawa et al. (2018) found that it also suppresses IL-17 production in Foxp3+ RORγt+ Helios- microbiota-

specific intestinal mucosa Tregs, and that this occurred independently of IL-10 production status[119]. In these cells, binding of Blimp-1 to the *Il17a* and *Il17f* genes did not prevent the positive transcriptional regulator RORγt from binding to these genes[119]. However, Blimp-1 caused inhibitory histone modifications within the *Il17* gene[119]. In the absence of Blimp-1, IRF4 and p300 bound to these genes, and together with RORγt upregulated IL17a and IL17f. The end result was failure to prevent gastrointestinal inflammation or adoptively transferred colitis[119].

Besides its role in intestinal homeostasis, Garg et al. (2019) found that Blimp-1 can indirectly protect Foxp3 expression in central nervous system (CNS) Tregs[120]. During autoimmune Type 1 diabetes, it was previously shown that Foxp3 could be down-regulated in Tregs, and that these cells would become pathogenic[121]. However, in this study, Garg et al. noted that during experimental autoimmune encephalitis, CNS Tregs maintained Foxp3 expression as well as their capacity to produce IL-10 despite being in an inflammatory environment. It was also observed that a higher percentage of CNS Tregs were Blimp-1+ compared to Tregs from non-inflamed spleen. It was previously shown that, during homeostasis, *Foxp3* must be demethylated for it to be stably expressed in splenic Tregs[122]. In their study, Garg et al. demonstrated that in the absence of Blimp-1, DNA methylating enzyme DNMT3A was expressed in an IL-6/STAT3 dependent manner[120]. This reduced chromatin accessibility to *Foxp3* leading to destabilization of the Treg signature[120]. These findings reiterated the importance of Blimp-1 in maintaining Treg identity.

Recently, a study by Vasanthakumar et al. (2020) discovered that male and female mice retain distinct VAT Treg signatures. Blimp-1 was more highly expressed in male

VAT Tregs compared to female VAT Tregs[80]. In male mice, Treg-specific Blimp-1 deletion led to fewer VAT Tregs, accompanied by decreased ST2, KLRG1, CCR2 and TIGIT expression, and increased CD62L and CD103 expression[80]. In addition, loss of Blimp-1+ Tregs led to increased glucose intolerance compared to WT mice[80]. RNA-seq analysis of male VAT Tregs identified numerous genes that were either positively regulated (*Klrg1*, *Il1rl1*, *Il10ra*, *Ccr2*, *Il10*, *Areg*, *Cd69*, *Ctla4*, *Gata3*, *Pparg*, *Il5*) or negatively regulated (*Tcf7*, *S1pr1*, *Ccr7*, *Sell*, *Cxcr3*, *Icos*) by Blimp-1[80]. ChIP-seq data revealed that Blimp-1 directly bound *Il10*, *Ccr2*, *Il1rl1*, *Ccr7*, *Tcf7*, *Klf2*, *Cxcr5*, *S1pr1*, *Myc* and *Bcl6* in VAT Tregs but with different degrees of chromatin accessibility between male and female mice[80]. In male VAT, IL-6 was produced primarily by dendritic cells, and to a lesser degree by ILC2s and macrophages[80]. IL-6 induced Blimp-1 expression in vitro, and *Il6* deficient mice had fewer ST2+ KLRG1+ CCR2+ VAT Tregs[80]. *Il6* deficient mice also had fewer IL-33 producing stromal cells[80]. Injection of IL-33 into *Il6* deficient mice increased VAT Treg frequency[80]. Taken together, this suggested that dendritic cells, macrophages and ILC2-derived IL-6 sustained IL-33 producing stromal cells, and that IL-33/ST2 signaling promoted VAT Treg maintenance.

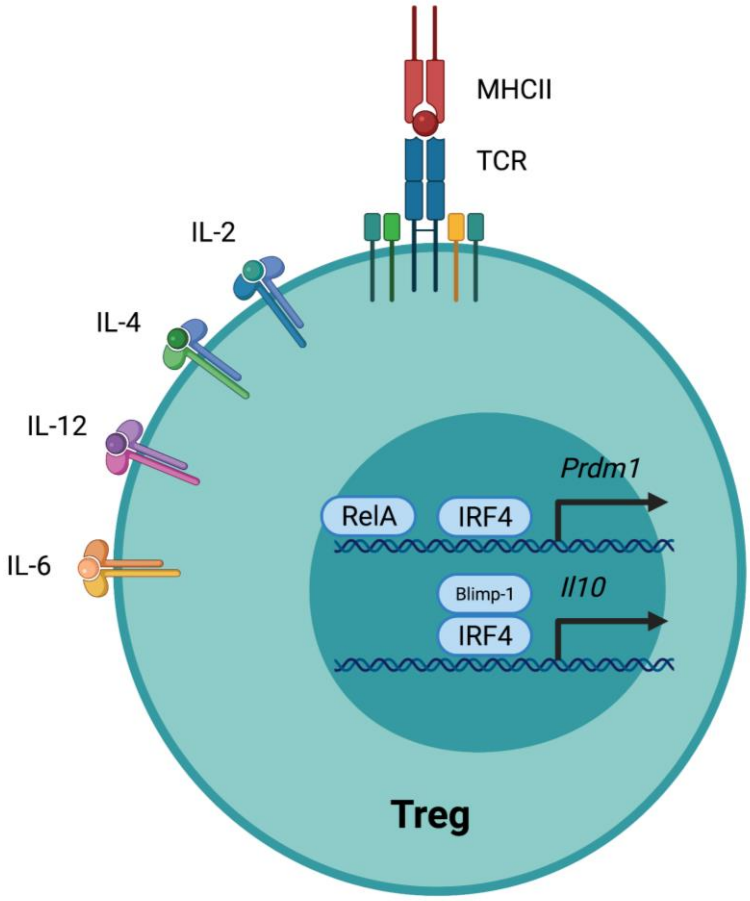

Figure 3. Phenotype of Blimp-1+ Tregs.

B lymphocyte-induced maturation protein-1 (Blimp-1) is induced by T cell receptor activation in the presence of IL-2. However, its expression can be enhanced by additional cytokines including IL-4, IL-12 and IL-6. Blimp-1 is encoded by the gene *Prdm1*, and its transcription is regulated by RelA and IRF4. Furthermore, dual binding of Blimp-1 and IRF4 can induce IL-10 expression in Tregs.

2.0 The role of Blimp-1 in adipose-resident Tregs

2.1 Introduction

Adipose-resident Tregs protect against systemic inflammation and metabolic disease by limiting expansion of pro-inflammatory cells, preserving insulin sensitivity and maintaining glucose tolerance. Although their basic markers and roles have been studied, less is known about the transcriptional machinery regulating their differentiation and function. For this project, I decided to investigate the role of B lymphocyte-induced maturation protein-1 (Blimp-1) transcriptional regulator since it interacts with Id proteins, which our lab has previously found a role for in adipose Treg survival and maintenance. To study this question, we placed male *Prdm1*$^{f/f}$ Foxp3-YFP-Cre+ conditional knockout mice (CKO) lacking Blimp-1 specifically in Tregs and wild-type (WT) litter mate controls on either standard chow (SFD) or high fat diet (HFD), aged them out to 26-28wks, then compared Tregs from various adipose depots as well as the metabolic phenotype of the different mice. I hypothesized that: 1) Blimp-1 is required for adipose Treg maintenance, differentiation and function, and that 2) Blimp-1+ Tregs help preserve insulin sensitivity and glucose tolerance.

Portions of the following chapter are taken or adapted from the publication: Beppu, L. Y., Mooli, R., Qu, X., Marrero, G. J., Finley, C. A., Fooks, A. N., Mullen, Z. P., Frias, A. B., Jr, Sipula, I., Xie, B., Helfrich, K. E., Watkins, S. C., Poholek, A. C., Ramakrishnan, S. K., Jurczak, M. J., & D'Cruz, L. M. (2021). Tregs facilitate obesity and insulin resistance

via a Blimp-1/IL-10 axis. *JCI insight*, *6*(3), e140644. https://doi.org/10.1172/jci.insight.140644

2.2 Materials and methods

2.2.1 Study design

The objective of this study was to interrogate the function of IL-10 and Blimp-1 expression by adipose-resident Tregs in mice on SFD and HFD. To do this, we used a combination of in vivo and ex vivo assays on mouse samples. We designed and performed the experiments predominantly using flow cytometry and metabolic indices for our analysis. The number of replicates for each experiment is indicated in the figure legends.

2.2.2 Mice

C57BL/6 mice were purchased from The Jackson Laboratory. Blimp-1–YFP (commercially available at Jackson, stock number 008828), Foxp3-RFP (commercially available at Jackson, stock number 008374)[123], and *Blimp-1*$^{fl/fl}$ mice (commercially available at Jackson, stock number 008100)[124] were donated by A. Poholek (University of Pittsburgh). *Il10*$^{fl/fl}$ mice were donated by D. Vignali (University of Pittsburgh). Foxp3-YFP-Cre mice were purchased from The Jackson Laboratory (stock number 016959)[125]. All experiments were approved by the University of Pittsburgh Institutional Animal Care

and Use Committee. All mice used in experiments were age-matched littermate males between 26 and 28 weeks of age. Male mice were used due to the hormonal fluctuations that occur in female mice. Where indicated, mice were fed either SFD (standard chow) or HFD (60% kcal fat, Teklad, Envigo, TD06414) from 8 weeks of age until 26–28 weeks of age. Male animals were assigned to groups of 3–7 mice per experiment where possible, and at least 2 independent experiments were performed throughout the study. Mice were bred and housed in specific pathogen–free conditions in accordance with the Institutional Animal Care and Use Guidelines of the University of Pittsburgh. Mice were maintained at approximately 22°C room temperature as standard.

2.2.3 Cell isolation

Murine epididymal, inguinal, and brown adipose single-cell suspensions were prepared as previously described (45). Briefly, tissue was harvested, weighed, finely chopped with a razor blade, and digested with Liberase TM and DNase I (MilliporeSigma) at 37°C with shaking for 30 minutes before filtering through a 70 μm nylon mesh and centrifugation for 5 minutes at 4°C. The supernatant was removed and the SVF was isolated and processed for flow cytometry. Single-cell suspensions of spleen and iLN cells were made by processing murine spleens between 2 glass slides.

2.2.4 Flow cytometry

Antibodies against murine CD4 (RM4-5, AF700, BV650), CD8 (53-6.7, APC/Fire 750, BV785), CCR2 (SA203G11, BV421), CD11c (N418, APCCy7, Pe/Cy5), CD206

(C068C2, APC), CD11b (M1/70, BV421), F4/80 (BM8, BV510, BV711, FITC), TCRβ (H57-597, BV605), and NK1.1 (PK136, BV650) were purchased from BioLegend. Antibodies against CD4 (GK1.5, BUV395) and ST2 (U29-93, BV480) were purchased from BD Biosciences. Antibodies against B220 (RA3-6B2, AF488), CD11c (N418, e450, PE-Cy5.5), CD25 (PC61.5, PE-Cy7), CD4 (GK1.5, APC-eFluor 780, Super Bright 645), CD45 (30-F11, Pacific Orange), Foxp3 (FJK-16s, APC, e450, FITC), GITR (DTA-1, Super Bright 600), IL-10 (JES5-16E3, PE), KLRG1 (2F1, APC, APC-eFluor 780, PE-eFluor 610), NK1.1 (PK136, PE), and ST2 (RMST2-2, PE, PerCP-eFluor710) were purchased from eBioscience, Thermo Fisher Scientific. Viability dyes (e506, near IR, UV) were purchased from Invitrogen, Thermo Fisher Scientific. Extracellular flow staining was performed in 2% FBS-PBS in the presence of BioLegend's TruStain FcX for 30 minutes at 4°C. Fixation, permeabilization, and intracellular staining were performed using eBioscience's (Thermo Fisher Scientific) Foxp3/transcription factor staining buffer set per manufacturer's directions. Flow data were collected using a Cytek Aurora or BD Biosciences LSR and analyzed using FlowJo.

2.2.5 Intracellular cytokine analysis

For intracellular cytokine staining total SVF was stimulated with PMA (50 ng/mL) (MilliporeSigma) and ionomycin (1 nM) (MilliporeSigma) for 5 hours. Brefeldin A (eBioscience, Thermo Fisher Scientific) was added to the culture at the recommended concentration. Cells were surfaced stained, before fixing, permeabilizing, and intracellular staining according to the manufacturer's instructions (eBioscience, Thermo Fisher Scientific, Foxp3/transcription factor staining kit).

2.2.6 Determination of fasting blood glucose, glucose tolerance testing (GTT), and insulin tolerance testing (ITT)

Mice were fasted overnight before fasting blood glucose and insulin levels were measured. Blood glucose was measured using a handheld glucometer (Bayer Contour Next), and plasma insulin was measured by ELISA (Alpco). For the GTTs, we administered glucose (2 g/kg of body weight) by i.p. injection after an overnight fast. We measured changes in plasma insulin at 15, 30, and 120 minutes and blood glucose at 15, 30, 45, 60, and 120 minutes after glucose injection. For the ITT, mice were fasted for 6 hours before intravenous injection with 0.75 U/kg of body weight Novolin-R human recombinant insulin (Henry Schein). After insulin injection, blood glucose was measured at 15, 30, 45, 60, and 120 minutes.

2.2.7 Indirect calorimetry and body composition measurements

Indirect calorimetry was performed using the Promethion Multiplexed Metabolic Cage System (Sable Systems) by the University of Pittsburgh Center for Metabolism and Mitochondrial Medicine. Animals were placed individually in chambers for 24 hours to acclimate followed by 48 hours at ambient room temperature with 12-hour light/12-hour dark cycles for analysis. Animals had free access to food and water. Respiratory measurements (VO2 /VCO2) were made at 5-minute intervals. Food intake was measured in metabolic chambers during the 48-hour period. Body composition including fat and LM was determined using by EchoMRI. Mice were weighed twice per month to determine weight increases over time on SFD and HFD.

2.2.8 Tissue H&E staining

Tissues were placed in cassettes and submerged in 10% formalin solution overnight. Tissue cassettes were washed with tap water for 15 minutes and stored in 70% ethanol at room temperature. Paraffin embedment and sectioning (4–5 μm thickness) was performed by StageBio. Slides were deparaffinized and rehydrated using ethanol and PBS, respectively. H&E staining was performed using hematoxylin for 5 minutes followed by eosin for 15 seconds. The images were acquired by using an Evos fluorescence inverted microscope.

2.2.9 Reverse transcription quantitative PCR analysis

Total RNA was extracted using RNeasy Lipid Tissue Mini Kit (Qiagen) as per the manufacturer's instructions. First 1 μg of total RNA was reversed-transcribed using Mu-MLV reverse transcriptase (Promega). Gene expression was evaluated by quantitative real-time PCR using SYBR Green Mastermix (Radiant Molecular Tools) with a Quant Studio 3 Station quantitative PCR machine (Applied Biosystems, Thermo Fisher Scientific). The results were expressed as fold change using the 2-ΔΔCT method, and β-actin was used as an internal normalization control. A list of the primer sequences used is provided in Supplemental Table 1.

Table 1. Real-time PCR primers

Gene	Forward (5'-3')	Reverse (5'-3')
Ucp1	GGCCTCTACGACTCAGTCCA	TAAGCCGGCTGAGATCTTGT
Prdm16	CAGCACGGTGAAGCCATTC	GCGTGCATCCGCTTGTG
Cidea	ATCACAACTGGCCTGGTTACG	TACTACCCGGTGTCCATTCT
Dio2	CATGCTGACCTCAGAAGGGC	CCCAGTTTAACCTGTTTGTAGGCA
AdipoQ	GCACTGGCAAGTTCTACTGCAA	GTAGGTGAAGAGAACGGCCTTGT
Fabp4	ACAAGCTGGTGGTGGAATGTG	CCTTTGGCTCATGCCCTTT
Plin2	CTCAGGAGGAGCTGGAGATG	TCAATCAGGTGGACAGTGGA
Pparg	AGGCGAGGGCGATCTTGACAG	AATTCGGATGGCCACCTCTTTG
β-actin	TATTGGCAACGAGCGGTTCC	GGCATAGAGGTCTTTACGGATGT

2.2.10 Western blotting

Protein extracts were prepared as previously described[126]. In brief, the adipose tissue samples were lysed in radioimmunoprecipitation assay lysis buffer (50 mM Tris pH 7.4, 150 mM NaCl, 5 mM EDTA, 1% NP-40) supplemented with protease and phosphatase inhibitors (MilliporeSigma). The protein content was measured by using protein assay kit (Bio-Rad). The protein lysates (20–25 μg) were resolved on 9%–12% polyacrylamide gels and transferred to nitrocellulose membranes. Membranes were blocked with 5% skim milk powder in Tris-buffered saline containing 0.01% Tween 20 and probed with primary antibodies (UCP1, PAI-24894, Invitrogen, Thermo Fisher Scientific; PRDM16, NBP1-77096, Novus Biologicals; β-actin, 66009-I-Ig, Proteintech) overnight at

4°C. Membranes were then probed with respective secondary antibodies — anti-rabbit IgG (H+L) DyLight800, Cell Signaling Technology, catalog 5151S, and anti-mouse IgG (H+L) DyLight680, Cell Signaling Technology, catalog 5470S) and visualized using Odyssey CLx Imaging System (LI-COR). The Western blot images were quantified by using ImageJ software (NIH, Bethesda, Maryland, USA).

2.2.11 Cell culture and IL-10 in vitro assay

Mouse inguinal adipose-derived SVF preadipocytes (Kerafast, Inc.) were provided in-house (University of Pittsburgh). Cells were grown to confluence in DMEM/F12 with 10% FBS and 1% penicillin-streptomycin. One day prior to differentiation, cells were subcultured into a 12-well plate at 70% confluence and allowed to rest overnight. The cells were differentiated into brown adipocytes with the cocktail of 0.5 mM isobutylmethylxanthine, 125 nM indomethacin, 2 µg/mL dexamethasone, 850 nM insulin, 1 nM T3, and 0.5 µM rosiglitazone. After 2 days, cells were placed into postdifferentiation maintenance media consisting of complete media with 850 nM insulin, 1 nM T3, and 0.5 µM rosiglitazone. After an additional 2 days, cells were treated for 16 hours with 100 ng/mL recombinant mouse IL-10 (R&D Systems, Bio-Techne) for downstream real-time PCR analysis.

2.2.12 Statistics

All graphs were created using GraphPad Prism 8, and statistical significance was determined with the 2-tailed paired or unpaired Student’s t test or using 1-way ANOVA

adjusted for multiple comparisons where appropriate. We used a P value of less than 0.05 as statistically significant. The graphical abstract was created using BioRender.com.

2.2.13 Study approval

All rodent breeding and experimental procedures were approved by and performed in accordance with the guidelines of the Institutional Animal Care and Use Committee of the University of Pittsburgh and complied with the NIH Guide for the Care and Use of Laboratory Animals (National Academies Press, 2011).

2.3 Results

2.3.1 Blimp-1+ Tregs are present in the adipose tissue and are phenotypically distinct from their Blimp-1- counterparts

Previously published research has found that Blimp-1 is highly expressed in visceral adipose tissue (VAT) Tregs compared to Tregs from secondary lymphoid organs or other peripheral tissues[92, 127]. To verify these data, epididymal VAT Tregs and splenic Tregs were isolated from male Blimp-1^{YFP}Foxp3^{RFP} dual reporter mice. Whereas, 25% of splenic Tregs were positive for Blimp-1, 50% of VAT Tregs were positive for Blimp-1 **(Fig. 1A)**. Next, Blimp-1+ versus Blimp-1- VAT Tregs were compared for expression of canonical effector Treg markers. ST2 is the receptor for IL-33, which is known to play an important role in maintenance and expansion of adipose Tregs (aTreg)[91, 92, 96, 128]. KLRG1

is a marker of antigen-experienced Tregs[129], and is known to be highly expressed in aTregs relative to splenic Tregs[85]. There was a statistically significant increase in KLRG1, and a trend towards increased ST2 in the Blimp-1+ VAT Tregs compared to their Blimp-1- counterparts **(Fig. 1B)**. CD25, the alpha portion of the IL-2 receptor, has also been previously shown to be highly expressed in VAT Tregs compared to splenic Tregs[23]. In addition, CD25 has been shown to play a critical role in maintaining peripheral Treg identity and protection from apoptosis[130]. Furthermore, it has previously been shown in peripheral lymphoid Tregs that Blimp-1 expression correlates negatively with CD25 expression[113]. Similarly, our Blimp-1+ VAT Tregs expressed lower levels of CD25 compared to Blimp-1- VAT Tregs **(Figure 1C)**. Taken together, these data suggested that Blimp-1+ Tregs are a unique subpopulation of VAT effector Tregs.

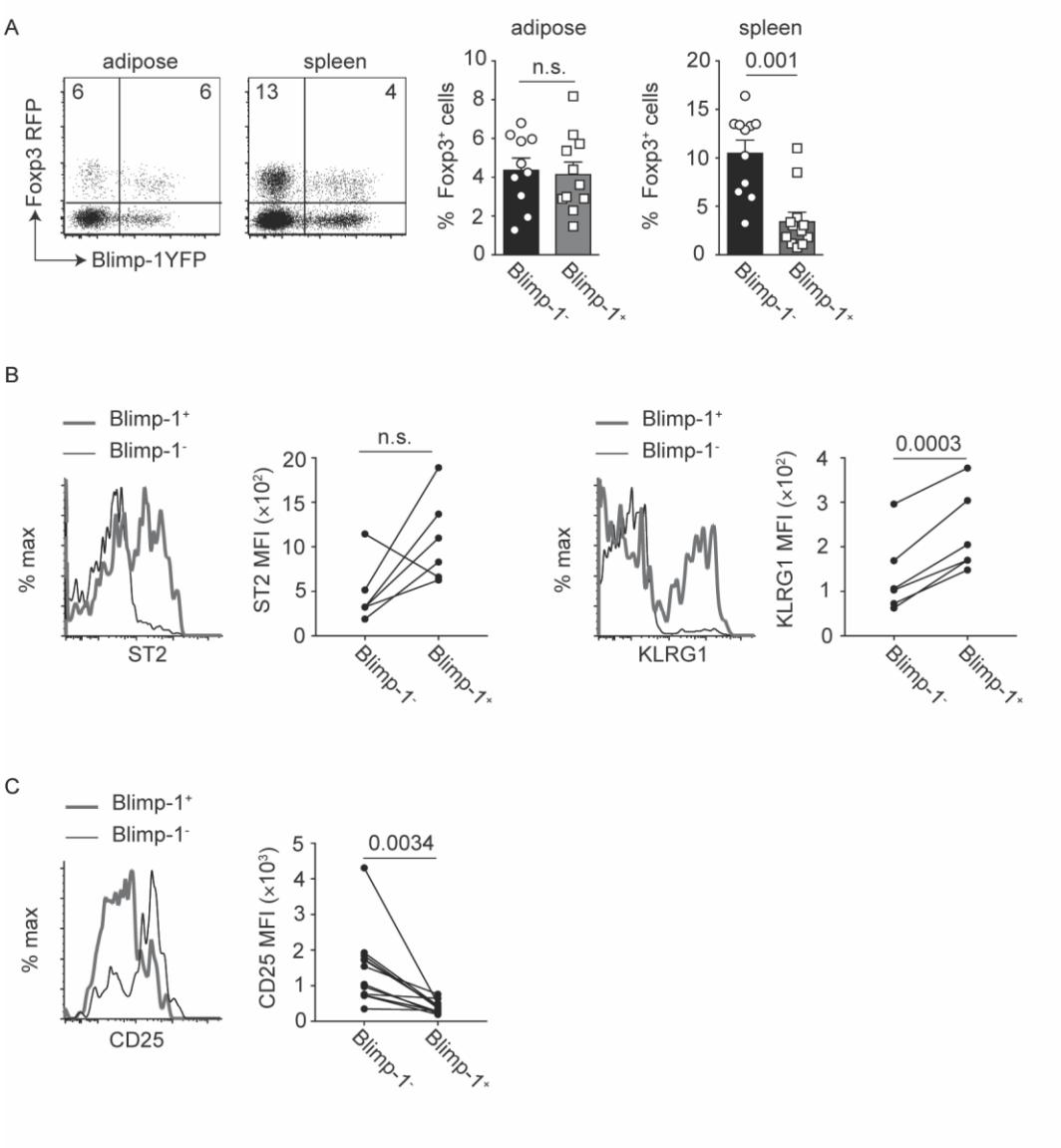

Figure 4. Blimp-1+ VAT Tregs possess a unique effector Treg signature.

Analysis of visceral adipose tissue (VAT) and splenic Tregs from 15-week-old male Blimp-1^{YFP}Foxp3^{RFP} dual reporter mice on 20% standard fat diet. (A) Representative flow plots and frequency of Blimp-1+ versus Blimp-1- Foxp3+ Tregs in VAT versus spleen. Cells were gated off total CD4 T cells. (B-C) Representative histograms and MFI quantification of ST2, KLRG1 and CD25 expression by Blimp-1+ (grey line) versus Blimp-1- (black line) VAT Tregs. Cells were gated off CD4+ Foxp3+ T cells. Data are presented as means ± SEM for n = 11 mice per group (A, C) or n = 6 mice per group (B), pooled from four independent experiments. Paired Student's t-test was used (n.s. = not significant).

2.3.2 The role of Blimp-1 in adipose Treg maintenance, differentiation and function

Next, we wanted to determine whether or not Blimp-1 plays a critical role in VAT Treg maintenance, differentiation and function. To do so, we utilized *Prdm1*$^{f/f}$ CD4-Cre+ mice lacking Blimp-1 in all CD4 and CD8 T cells. There were no differences in VAT or splenic Treg frequency or total cell count between *Blimp1*$^{f/f}$ CD4-Cre+ VS wild-type control mice **(Fig. 2A)**. However, loss of Blimp-1 led to reduced ST2 and KLRG in VAT Tregs but not splenic Tregs **(Fig. 2B)**. In addition, CCR2, a chemokine receptor known to be highly expressed in VAT Tregs compared to lymphoid Tregs[23, 85] was also downregulated in the absence of Blimp-1 **(Fig. 2B)**. Although these data suggested Blimp-1 may play an important role in maintaining the VAT Treg signature, the use of the CD4-Cre system (and thus loss of Blimp-1 in all conventional T cells) prevented us from determining whether this was occurring in a cell-intrinsic or cell-extrinsic manner.

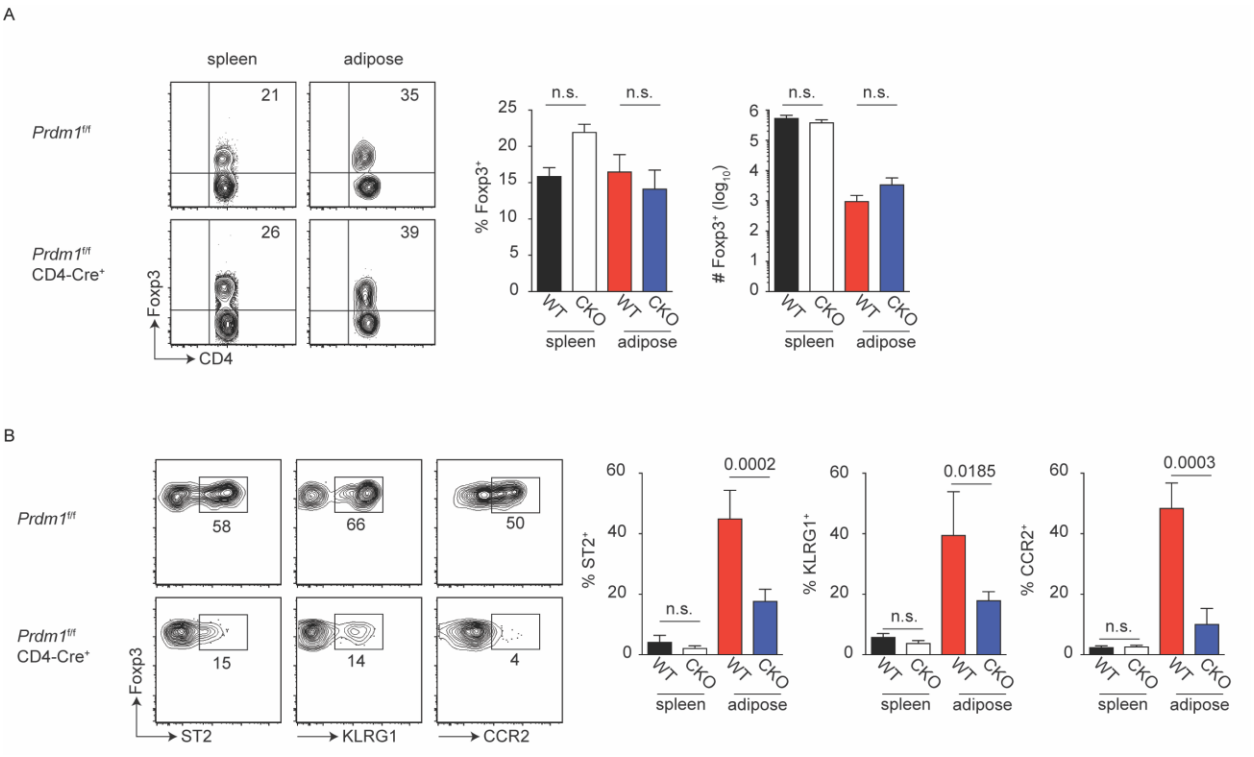

Figure 5. Loss of Blimp-1 disrupts the VAT Treg signature in *Prdm1*$^{f/f}$ CD4-Cre+ mice.

Analysis of VAT and splenic Tregs from 26-28-week old male *Prdm1*$^{f/f}$ CD4-Cre+ (CKO) or wild-type littermate control (WT) mice on 20% standard fat diet. (A) Representative flow plots and quantification of VAT and splenic Treg frequency and total cell count. Cells gated off total CD4 T cells. (B) Representative flow plots of VAT Tregs expressing ST2, KLRG1, and CCR2 (left), and frequency of these markers in VAT and splenic Tregs (right). Cells gated off CD4+ Foxp3+ T cells. Data are presented as means ± SEM for n = 10 mice per group (A) or n = 6 mice per group (B), pooled from four independent experiments. Unpaired Student's t-test was used (n.s. = not significant).

To determine whether Blimp-1 maintained the VAT Treg signature in a cell-intrinsic manner, we next analyzed *Prdm1*$^{f/f}$ Foxp3-YFP-Cre+ conditional knockout (CKO) mice lacking Blimp-1 in all Tregs under standard fat diet (SFD) and high fat diet (HFD) conditions. Under SFD conditions, Treg-specific deletion of Blimp-1 led to reduced frequency of VAT Tregs but not splenic Tregs **(Fig. 3A)**. When comparing CKO mice to

their WT counterparts, the former had fewer ST2+ and KLRG1+ VAT Tregs but exhibited no differences in splenic Tregs **(Fig. 3B)**. In addition to ST2 and KLRG1, the frequency of CCR2+ and GITR+ Tregs were examined as well. CCR2 is a chemokine receptor important for leukocyte migration into peripheral tissue, and has been shown to be more highly expressed in aTregs compared to splenic Tregs or conventional T cells in either tissue[23]. GITR has been shown to be important in Treg expansion and function[131], and is known to be up-regulated in Tregs when co-cultured in the presence of adipose tissue macrophages[132]. The absence of Blimp-1 led to reduced GITR+ and CCR2+ aTregs but not splenic Tregs **(Fig. 3B)**. Finally, we wanted to see whether Blimp-1 plays a role in VAT Treg function. Blimp-1 has previously been shown to positively regulate IL-10 expression in Tregs[113, 116]. To test whether Blimp-1 is required for IL-10 production in VAT Tregs, we isolated the stromal vascular fraction from the VAT, and stimulated it ex vivo. As expected, Blimp-1 deficiency led to diminished IL-10 production by VAT Tregs **(Fig. 3C)**. Taken together, these data indicated that Blimp-1 can regulate the VAT Treg signature under SFD conditions in a cell-intrinsic manner, and that Blimp-1 can uniquely alter the Treg phenotype in VAT compared to secondary lymphoid organs.

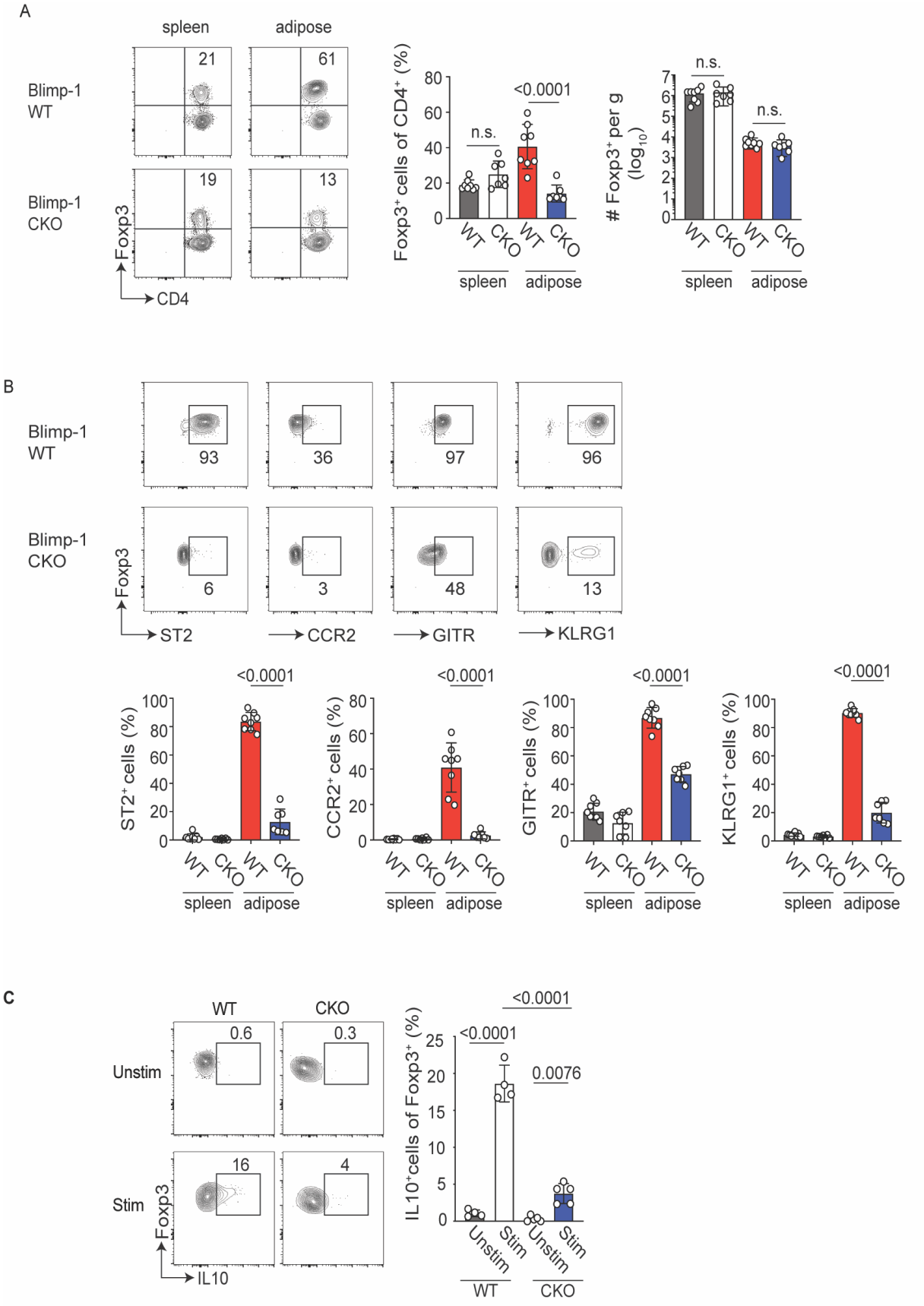
A
spleen
adipose
Blimp-1 WT
Blimp-1 CKO
21
61
19
13
Foxp3
CD4
Foxp3+ cells of CD4+ (%)
n.s.
<0.0001
WT
CKO
spleen
adipose
Foxp3+ per g (log10)
B
93
36
97
96
6
3
48
13
ST2
CCR2
GITR
KLRG1
ST2+ cells (%)
CCR2+ cells (%)
GITR+ cells (%)
KLRG1+ cells (%)
C
WT
CKO
Unstim
Stim
0.6
0.3
16
4
IL10
IL10+cells of Foxp3+ (%)
0.0076

Figure 6. Loss of Blimp-1 disrupts the VAT Treg phenotype in lean *Prdm1*$^{f/f}$ Foxp3-YFP-Cre+ mice. Analysis of VAT and splenic Tregs were from 26-28wk old male *Prdm1*$^{f/f}$ Foxp3-YFP-Cre+ (CKO) or wild-type littermate controls (WT) mice on 20% standard fat diet (SFD). (A) Representative flow plots and quantification of Treg frequency and total cell count per gram tissue. Cells gated off total CD4 T cells. (B) Representative flow plots and frequency of ST2, CCR2, GITR and KLRG1 positive Tregs. Cells gated off CD4+ Foxp3+ T cells. (C) Total VAT stromal vascular fraction was stimulated ex vivo for 5 hours with PMA and ionomycin. Representative flow plots and quantification of IL-10 producing VAT Tregs. Cells gated off CD4+ Foxp3+ T cells. Data are presented as means ± SEM and are pooled from 2-3 independent experiments with n=4-8 per group. Unpaired Student's t-test or one-way ANOVA were used (n.s. = not significant).

In addition to VAT, immune cells also reside in the subcutaneous inguinal white adipose tissue (iWAT)[94, 133-135] as well as the interscapular brown adipose tissue (BAT)[82, 94]. Thus, we decided to analyze Treg frequency and markers in these tissues as well. In the absence of Blimp-1, there was no difference in the frequency of iWAT or BAT Tregs **(Fig. 4A)**. However, there was an increase in Treg frequency within the inguinal lymph node (iLN) **(Fig. 4A)**. In addition, loss of Blimp-1 led to reduced frequency of ST2+ iWAT, BAT and iLN Tregs **(Fig. 4B)**. Furthermore, Blimp-1 deficiency led to decreases in KLRG1+ iWAT and BAT Tregs **(Fig. 4C)**. We also measured IL-10 production in IAT and iLN Tregs, and observed reductions in IL-10 production in the absence of Blimp-1 **(Fig. 4D)**. Although we attempted to measure IL-10 production in BAT Tregs, we did not have enough viable cells post-stimulation to make definitive conclusions.

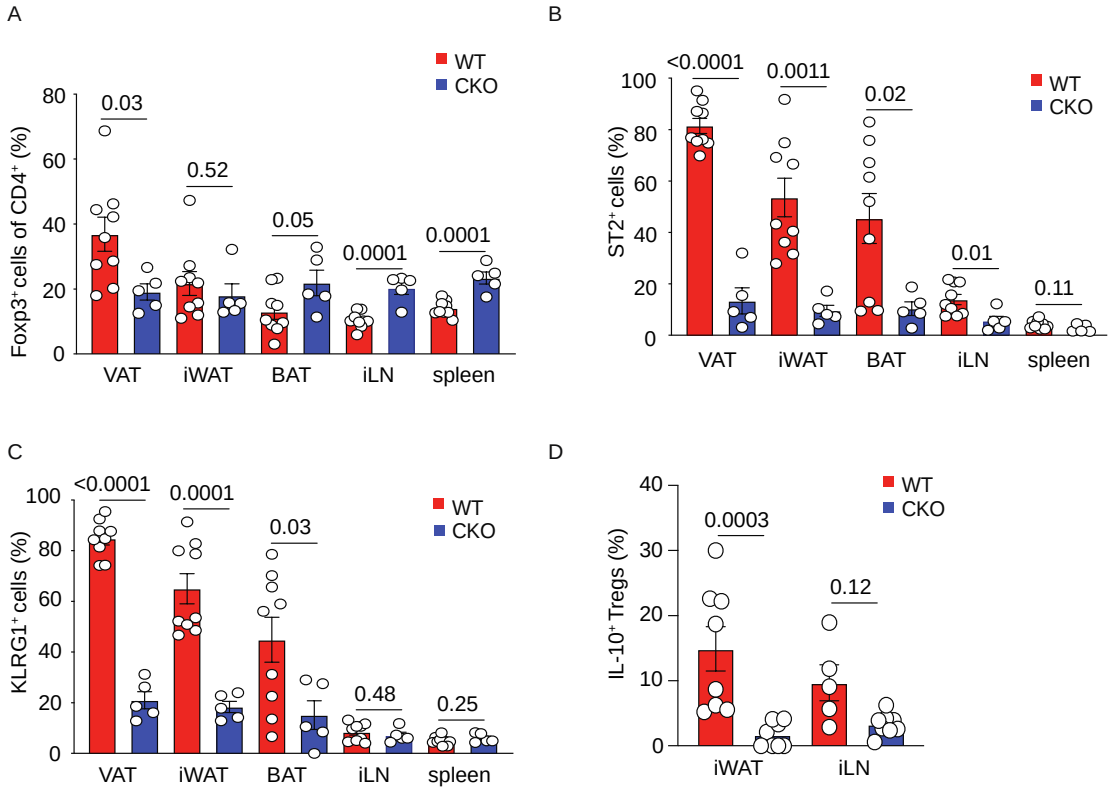

Figure 7. Loss of Blimp-1 disrupts the IAT and BAT Treg phenotype in lean *Prdm1*$^{f/f}$ Foxp3-YFP-Cre+ mice.

Analysis of IAT, BAT and iLN Tregs from 26-28wk old male *Prdm1*$^{f/f}$ Foxp3-YFP-Cre+ (CKO) or wild-type littermate controls (WT) mice on 20% standard fat diet (SFD). (A) Treg frequency in indicated tissue. Cells gated off total CD4+ T cells. (B-C) Frequency of ST2+ and KLRG1+ Tregs in indicated tissue. Cells gated off CD4+ Foxp3+ T cells. (D) Total IAT and iLN stromal vascular fractions were stimulated ex vivo for 5 hours with PMA and ionomycin. Quantification of IL-10 producing IAT and iLN Tregs. Cells gated off CD4+ Foxp3+ T cells. Data are presented as means ± SEM and are pooled from 2 independent experiments with n=5-9 per group for (A-C) and n=5-8 per group for (D). One-way ANOVA was used (n.s. = not significant).

Next, we compared the VAT Treg signature of Blimp-1 CKO mice VS WT mice on HFD. Eight-week-old mice were placed on 60% HFD and analyzed at 26-28wks of age. Treg-specific deletion of Blimp-1 did not result in any changes in VAT or splenic Treg frequency **(Fig. 5A)**. However, lack of Blimp-1 in splenic Tregs lead to decreased absolute

total number of Tregs **(Fig. 5A)**. Similar to the Blimp-1 deficient VAT Tregs from lean mice, Blimp-1 deficient VAT Tregs from obese mice had decreased levels of ST2, CCR2, GITR, and KLRG1 **(Fig. 5B)**. Finally, Blimp-1 deficient VAT Tregs produced less IL-10 **(Fig. 5C)**.

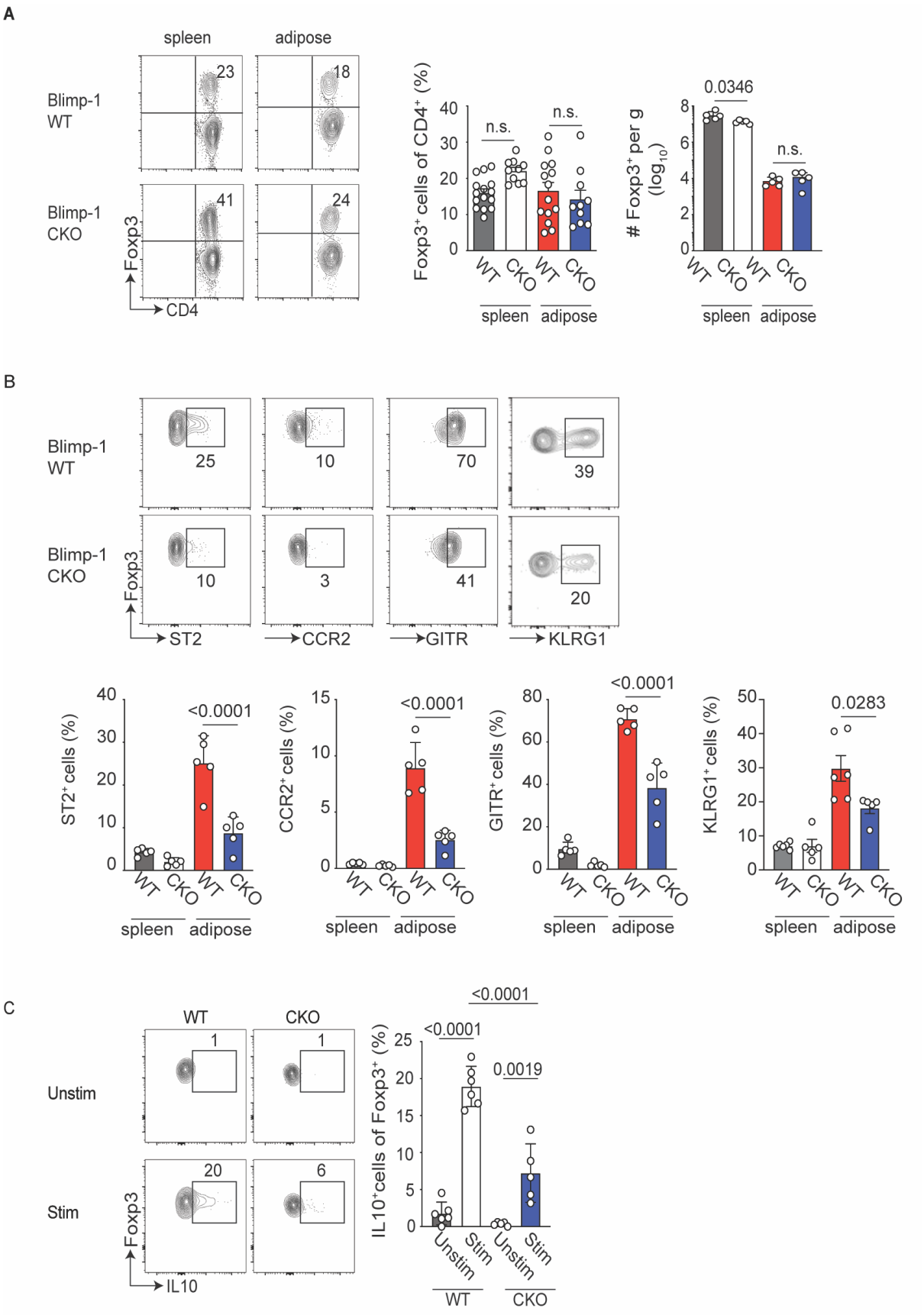
A
spleen
adipose
Blimp-1 WT
Blimp-1 CKO
23
18
41
24
Foxp3
CD4
Foxp3+ cells of CD4+ (%)
n.s.
n.s.
WT
CKO
WT
CKO
spleen
adipose
Foxp3+ per g (log10)
0.0346
n.s.
B
Blimp-1 WT
Blimp-1 CKO
25
10
70
39
10
3
41
20
Foxp3
ST2
CCR2
GITR
KLRG1
ST2+ cells (%)
<0.0001
CCR2+ cells (%)
<0.0001
GITR+ cells (%)
<0.0001
KLRG1+ cells (%)
0.0283
C
WT
CKO
Unstim
Stim
1
1
20
6
Foxp3
IL10
IL10+cells of Foxp3+ (%)
<0.0001
<0.0001
0.0019
Unstim
Stim
Unstim
Stim
WT
CKO

Figure 8. Loss of Blimp-1 disrupts the VAT Treg phenotype in obese *Prdm1*$^{f/f}$ Foxp3-YFP-Cre+ mice.

Prdm1$^{f/f}$ Foxp3-YFP-Cre+ (CKO) or wild-type littermate control (WT) male mice were placed on 60% high fat diet (HFD) starting at 8wks of age and analyzed after 18-20wks on HFD. (A) Representative flow plots and quantification of splenic and VAT Treg frequency and total cell count per gram tissue. Cells gated off total CD4 T cells. (B) Representative flow plots of ST2, CCR2, GITR and KLRG1 positive VAT Tregs (top) and quantification of markers expressed by splenic and VAT Tregs (bottom). Cells gated off CD4+ Foxp3+ T cells. (C) Total VAT stromal vascular fraction was stimulated ex vivo for 5 hours with PMA and ionomycin. Representative flow plots and quantification of IL-10 producing VAT Tregs. Cells gated off CD4+ Foxp3+ T cells. Data are presented as means ± SEM and are pooled from 2-3 independent experiments with n=5-14 per group. Unpaired Student's t-test or one-way ANOVA were used (n.s. = not significant).

In addition to analyzing VAT Tregs, we also analyzed Tregs from the IAT, BAT and iLN of HFD-fed mice. Whereas loss of Blimp-1 had no effect on IAT Treg frequency, BAT and iLN Treg frequency increased in the absence of Blimp-1 **(Fig. 6A)**. Similar to IAT and BAT Tregs from lean mice, Blimp-1 deficiency led to decreased frequency of ST2+ IAT and BAT Tregs **(Fig. 6B)**. In addition, loss of Blimp-1 led to a lower percentage of KLRG1+ IAT Tregs **(Fig. 6C)**. Finally, loss of Blimp-1 led to decreased IL-10 production by IAT and iLN Tregs **(Fig. 6D)**.

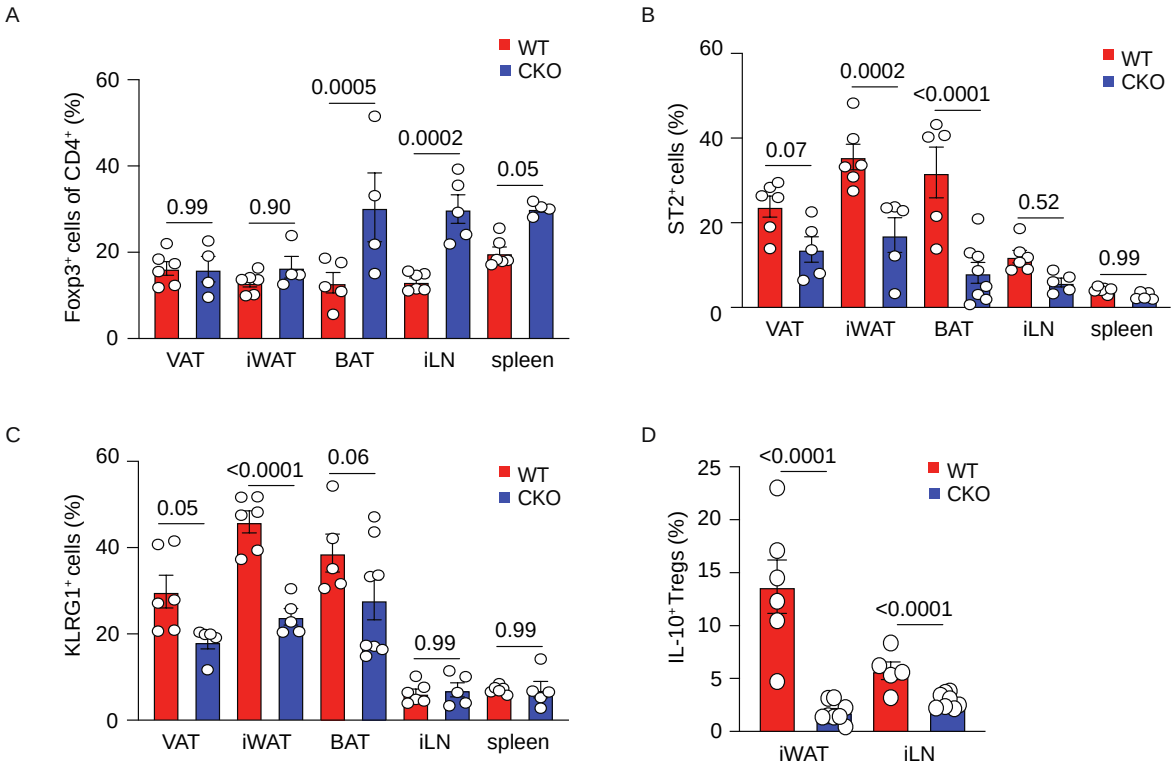

Figure 9. Loss of Blimp-1 disrupts the IAT and BAT Treg phenotype in obese *Prdm1*$^{f/f}$ Foxp3-YFP-Cre+ mice

Prdm1$^{f/f}$ Foxp3-YFP-Cre+ (CKO) or wild-type littermate control (WT) male mice were placed on 60% high fat diet (HFD) starting at 8wks of age and analyzed after 18-20wks on HFD. (A) Treg frequency in indicated tissue. Cells gated off total CD4+ T cells. (B-C) Frequency of ST2+ and KLRG1+ Tregs in indicated tissue. Cells gated off CD4+ Foxp3+ T cells. (D) Total IAT and iLN stromal vascular fractions were stimulated ex vivo for 5 hours with PMA and ionomycin. Quantification of IL-10 producing IAT and iLN Tregs. Cells gated off CD4+ Foxp3+ T cells. Data are presented as means ± SEM and are pooled from 2 independent experiments with n=4-8 per group for (A-C) and n=5-8 per group for (D). One-way ANOVA was used (n.s. = not significant).

2.3.3 The role of Blimp-1+ Tregs in protection against obesity

Previous research have suggested that VAT Tregs play an important role in protection against systemic inflammation and metabolic disease[11]. Importantly, VAT

Tregs have been implicated in helping maintain insulin sensitivity and glucose tolerance in obese mice[23, 91, 92, 128, 136]. Prior to visiting the role of VAT Tregs in maintaining metabolic homeostasis in obese mice, we decided to first examine how our *Prdm1*$^{f/f}$ Foxp3-YFP-Cre+ mice fared under standard chow. In 26-28wk old mice, the CKO mice appeared slightly leaner **(Fig. 7G)**, but overall, there was no statistically significant difference in body weight, fasting insulin or fasting glucose levels between the two experimental groups **(Fig. 7A-C)**. However, when a intraperitoneal glucose tolerance test was conducted after a 6hr fast, CKO mice exhibited lower levels of circulating glucose from 45 minutes to 2 hours post-injection, and lower levels of circulating insulin at 2 hours post-injection **(Fig. 7D-E)**. In addition, an insulin tolerance test after a 6 hour fast was performed. The CKO mice exhibited lower levels of circulating glucose as early as 15 minutes post-injection with insulin **(Fig. 7F)**.

Next, EchoMRI was utilized to analyze the body fat composition of the mice were analyzed using EchoMRI. CKO mice had a slightly lower overall body weight compared to WT mice although the difference was not statistically significant **(Fig. 7I)**. However, fat mass of CKO mice was less than their WT counterparts, and hence CKO mice had a percent body composition consisting of higher lean mass, and lower fat mass compared to WT mice **(Fig. 7I)**.

Next, mice were housed in metabolic cages to analyze their metabolism over the course of 48hrs. We observed that the CKO mice ate more **(Fig. 7J)**. However, they were also more active than the WT mice during the light cycle **(Fig. 7K)**. Respiratory exchange ratio (RER) is the ratio of CO2 volume exhaled to the oxygen volume inhaled, and can be used to determine the type of substrate being utilized during aerobic respiration where

values closer to 1 indicate glucose oxidation, and values closer to 0.7 mark fatty acid oxidation[137]. The CKO mice had a higher RER compared to WT mice during both the light and dark cycles indicating that they were utilizing glucose as their main energy source **(Fig. 7L)**.

Finally, we examined the gross anatomy of the mice. The inguinal white adipose tissue (IAT) was slightly smaller, and the VAT were clearly smaller in the CKO mice compared to the WT mice **(Fig. 7G)**. In addition, the liver of the CKO mice was a darker color of red compared to the WT mice suggesting that these mice had less hepatic steatosis **(Fig. 7G)**. Taken together, these observations suggested that mice lacking Blimp-1+ Tregs had less fat deposition. However, one concern we had was that this could be due to poor nutrient absorption. As demonstrated in **Fig. 3**, Blimp-1 deficient Tregs produce less IL-10. It has previously been shown that total IL-10 deficiency and Treg-specific IL-10 deletion can lead to colitis[125, 138-140]. Thus, we measured the colon length of our Blimp-1 CKO mice for signs of inflammation but we observed no difference between the WT and CKO mice **(Fig. 7H)**. From these data combined, we concluded that Blimp-1+ Tregs play an important role in regulating insulin sensitivity, glucose tolerance and fat deposition.

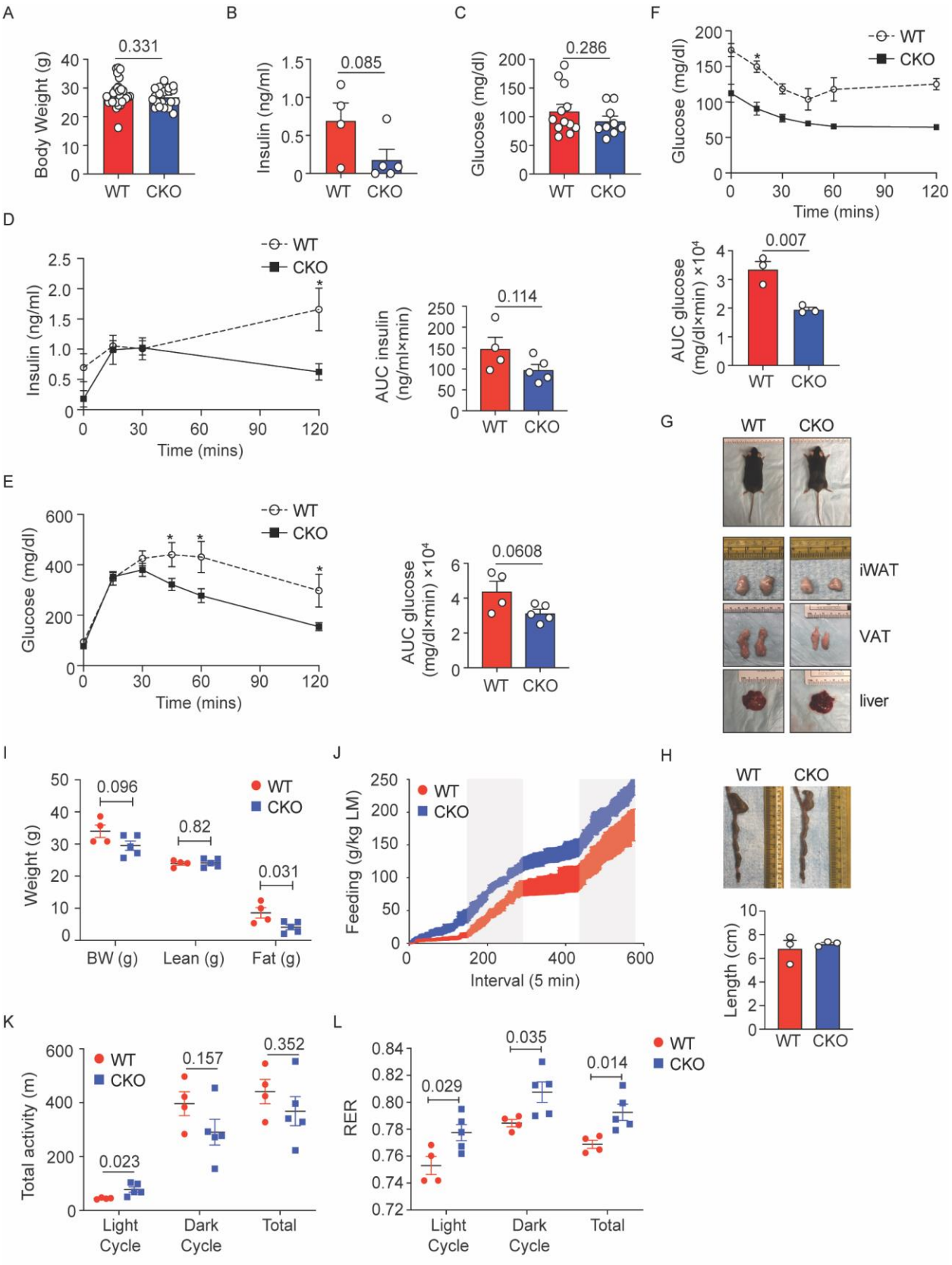
A
Body Weight (g)
0.331
WT
CKO
B
Insulin (ng/ml)
0.085
C
Glucose (mg/dl)
0.286
F
Glucose (mg/dl)
Time (mins)
D
Insulin (ng/ml)
AUC insulin (ng/ml×min)
0.114
AUC glucose (mg/dl×min) ×10⁴
0.007
E
Glucose (mg/dl)
AUC glucose (mg/dl×min) ×10⁴
0.0608
G
iWAT
VAT
liver
I
Weight (g)
0.096
0.82
0.031
BW (g)
Lean (g)
Fat (g)
J
Feeding (g/kg LM)
Interval (5 min)
H
Length (cm)
K
Total activity (m)
0.023
0.157
0.352
Light Cycle
Dark Cycle
Total
L
RER
0.029
0.035
0.014

Figure 10. Treg-specific deletion of Blimp-1 leads to decreased fat mass and improved insulin sensitvity in lean mice.

Eight-week-old *Prdm1*$^{f/f}$ Foxp3-YFP-Cre+ (CKO) or wild-type littermate control (WT) male mice were placed on 20% standard fat diet (SFD) for 18-20 weeks prior to metabolic analysis. (A) Body weight of 26-28-week-old WT and CKO mice. (B-C) Fasting plasma insulin and glucose levels. (D-E) Intraperitoneal glucose tolerance test. Plasma insulin and blood glucose levels over time post-glucose injection. Bar graphs represent area under the curve (AUC). (F) Intraperitoneal insulin tolerance test. Plasma glucose over time post-insulin injection. Bar graph indicates AUC. (G) Gross appearance, inguinal WAT (iWAT), epididymal visceral WAT (VAT) and livers. (H) Photographs and quantification of colon length. (I) Body composition as measured by EchoMRI. (J-L) Mice were placed in Promethion Multiplexed Metabolic Cage System for 48hrs and measurements recorded in 5-minute increments during 12hr light/dark cycles. (J) Food intake in grams (g) per kilogram (kg) lean mass (LM). (K) Total activity in meters (m) over 48 hours. (L) Respiratory exchange ratio (RER) where 0.7 indicates fatty acid oxidation and 1.0 indicates glucose oxidation. Data are presented as means ± SEM and are pooled from 2-3 independent experiments for A-G. Each dot represents one mouse. Unpaired Student's t-test or one-way ANOVA were used (*=P value <0.05).

We next moved on to analyzing *Prdm1*$^{f/f}$ Foxp3-YFP-Cre+ mice in a diet-induced obesity model. We first placed 8-week-old male mice on 60% high fat diet (HFD), and measured weight gain over time. Up until 4 wks on HFD, both WT and CKO mice gained weight at the same rate. However, from that point forward, CKO mice gained weight at a slower rate than their WT counterparts **(Fig. 8)**.

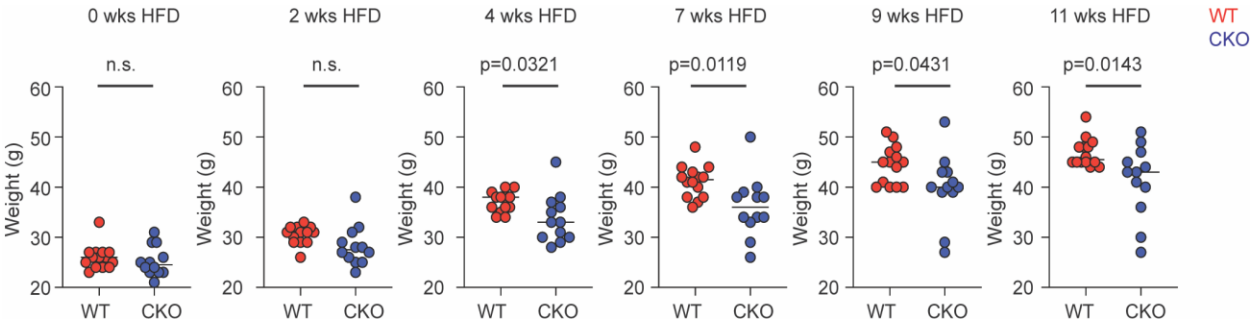

Figure 11. Weight gain in WT and *Prdm1*$^{f/f}$ Foxp3-YFP-Cre+ mice over time.

Eight-week-old *Prdm1*$^{f/f}$ Foxp3-YFP-Cre+ (CKO) or wild-type littermate control (WT) male mice were placed on 60% high fat diet (HFD), and their weight gain tracked over time. Data are presented as means ± SEM with n=12-14 per group pooled from two independent experiments. Unpaired Student's t-test was performed (n.s.= not significant).

At 26-28wks of age, the CKO mice exhibited lower body weight compared to the WT mice **(Fig. 9A)**. Analysis of body weight composition by EchoMRI confirmed this difference in body weight, and revealed that it was attributable to decreases in fat mass **(Fig. 9H)**. These differences were also observable by looking at the gross anatomy of the mice. The CKO mice were visible leaner than their WT counterparts **(Fig. 9L)**. In addition, their inguinal and visceral fat pads were smaller than those of the WT mice **(Fig. 9L)**. In addition, the liver of the CKO mice were darker in color suggesting less hepatic steatosis **(Fig.9L)**. Examination of the colon revealed no signs of inflammation, or differences in colon length between WT and CKO mice suggesting that the difference in weight was unlikely to be a result of colitis or nutrient malabsorption **(Fig. 9M)**.

When fasting glucose and insulin were measured, both were lower in the CKO mice resulting in overall decreased fasting insulin resistance as measured by HOMA-IR **(Fig. 9B-D)**. During glucose tolerance tests, circulating insulin was greater in the WT mice compared to CKO mice **(Fig. 9E)**. In addition, circulating plasma glucose was slightly

lower in the CKO mice throughout the time course, although it was not statistically significant **(Fig. 9F)**. We also performed an insulin tolerance test, but we did not see a difference in circulating glucose **(Fig. 9G)**. Because the HFD-fed mice displayed hyperinsulinemia compared to the SFD-fed mice **(Fig. 7D, Fig. 9E)**, this suggested that perhaps a higher dose of glucose needed to be injected during the glucose and insulin tolerance tests to see an observable difference in circulating glucose uptake.

Finally, mice were house in metabolic chambers for 48hrs. CKO mice ate less, but exhibited no differences in activity compared to the WT mice **(Fig. 9I-J)**. During the light cycle, CKO mice had a lower RER indicating that fat oxidation was preferential to carbohydrate use **(Fig. 9K)**.

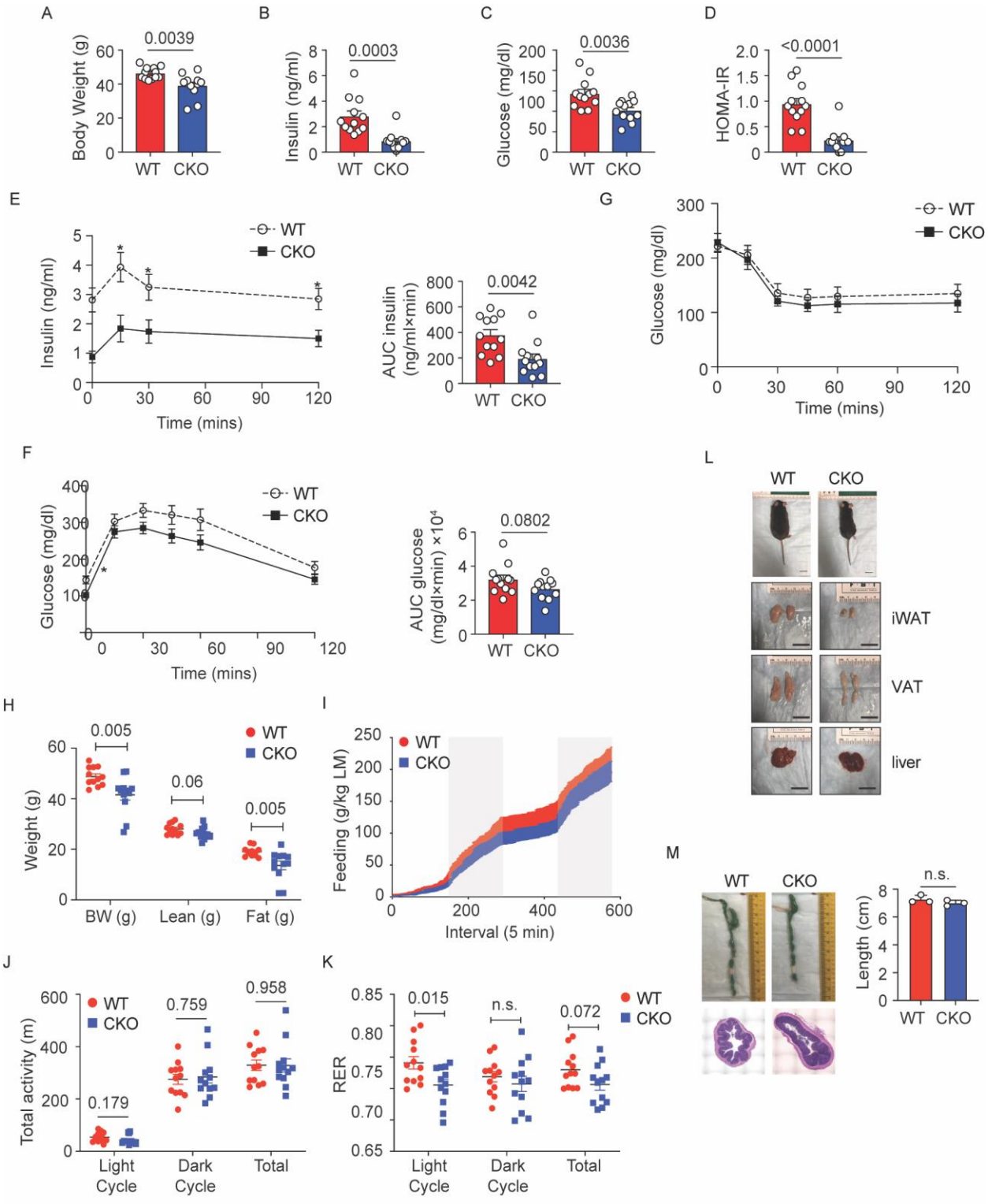

Figure 12. Loss of Blimp-1+ Tregs protects mice against diet-induced obesity.

Eight-week-old *Prdm1*$^{f/f}$ Foxp3-YFP-Cre+ (CKO) or wild-type littermate control (WT) male mice were placed on 60% high fat diet (HFD) for 18-20 weeks prior to metabolic analysis. (A) Body weight of 26-28-week old

HFD-fed WT and CKO mice. (B-C) Fasting plasma insulin and glucose levels in WT and CKO mice. (D) Fasting insulin resistance as measured by homeostatic model assessment of insulin resistance (HOMA-IR) in WT and CKO mice. (E-F) Intraperitoneal glucose tolerance test. Plasma insulin and blood glucose levels over time post-glucose injection. Bar graphs represent area under the curve (AUC). (G) Intraperitoneal insulin tolerance test. Plasma glucose over time post-insulin injection. Bar graph indicates area under the curve (AUC). (H) Body composition as measured by EchoMRI. (I-K) Mice were placed in Promethion Multiplexed Metabolic Cage System for 48hrs and measurements recorded in 5-minute increments during 12hr light/dark cycles. (I) Food intake in grams (g) per kilogram (kg) lean mass (LM). (J) Total activity in meters (m) over 48 hours. (K) Respiratory exchange ratio (RER) where 0.7 indicates fatty acid oxidation and 1.0 indicates glucose oxidation. (L) Gross appearance, inguinal WAT (iWAT), epididymal visceral WAT (VAT) and livers. (M) Top: Photographs and quantification of colon length. Bottom: H&E stain of colon cross-section. Data are presented as means ± SEM and are from 2–3 independent experiments with 3–12 mice, where each dot represents 1 mouse, and an unpaired 2-tailed Student's t test or 1-way ANOVA was performed to determine significance (*=P value <0.05).

2.3.4 The role of Blimp-1+ Tregs in maintenance of other adipose-resident immune cells

Initially, we hypothesized that disruption of the aTreg signature would lead to increased inflammation and poor metabolic outcomes as Tregs have been shown to be critical for glucose tolerance and insulin sensitivity[23, 89-91, 93]. However, our data indicated that disrupting the aTreg signature led to reduced body weight and improved insulin sensitivity. We also observed that loss of Blimp-1 in VAT, iWAT and BAT Tregs lead to reduced ST2, the receptor for IL-33, on these cells. ST2 is expressed by a multitude of innate and adaptive immune cells across multiple inflammatory disease models[141]. In adipose tissue, it has been shown that macrophages express ST2, and that IL-33

administration can reduce total VAT F4/80+ cell frequency in HFD mice[91]. In *ob/ob* mice, IL-33 administration can increase the frequency of total F4/80+ cells in the VAT, and lead to higher accumulation of alternatively activated CD206+ M2 macrophages compared to classical TLR2+ M1 macrophages[136]. In short-term HFD fed mice, total IL-33 deficient mice also exhibit increased total VAT macrophages and dendritic cells[20]. Recent research have found that macrophages can directly impact insulin resistance and glucose tolerance[142-145]. Hence, we hypothesized that Blimp-1-deficient Tregs lacking ST2 may uptake less IL-33, which could divert more of this cytokine to. However, when total F4/80+ macrophages were analyzed, there was no difference in their frequency between CKO and WT mice **(Fig. 10B)**. Adipose tissue macrophages have classically been categorized as M1 pro-inflammatory or M2 anti-inflammatory macrophages with the former linked to insulin resistance, and the latter associated with insulin resistance[146]. When we examined the relative frequencies of CD11c+ M1 macrophages, and CD206+ M2 macrophages, we observed no differences in the ratio between CKO and WT mice **(Fig. 10B)**.

Besides macrophages, we decided to interrogate other types of adipose-resident immune cells that could express ST2 as well. In the absence of Blimp-1+ Tregs, there was no difference in the percentage of adipose-resident ST2+ non-Treg leukocytes **(Fig. 10A)**. It was previously shown that IL-33 promotes IL-2 secretion by dendritic cells, and that this facilitates expansion of ST2+ Tregs[147]. In addition, DCs have been shown to directly suppress VAT inflammation and assist in metabolic homeostasis[148]. However, when we examined the F4/80- $CD11b^{med}$ CD11c+ dendritic cell compartment, we saw no changes between Blimp-1 CKO and WT mice **(Fig. 9C)**. In addition, different B cell subsets have been implicated in either promotion or protection from insulin resistance[149],

and IL-10 producing ST2+ B cells have been identified during gut inflammation[150]. When we examined total B220+ B cells in our mice, we did not see any changes in their frequency between WT and CKO mice **(Fig. 9C)**.

Interestingly, we did observe fewer adipose-resident NK cells and a higher percentage of CD8 T cells **(Fig. 9D-E)**. The decrease in NK cells was promising as they are known to be pro-inflammatory and enhance insulin resistance when present[151]. In contrast, the increase in CD8 T cells was concerning at first as they are believed to contribute towards insulin resistance[152]. However, our preliminary data indicate that in the absence of Blimp-1+ Tregs, adipose-resident CD8 T cells express more PD-1 exhaustion marker. Thus, additional studies are required to determine whether these cells are actually functional.

Hence, although there were a few changes in the adipose immune cell compartment, these differences did not provide a clear and convincing argument for the improved metabolic outcomes in CKO mice.

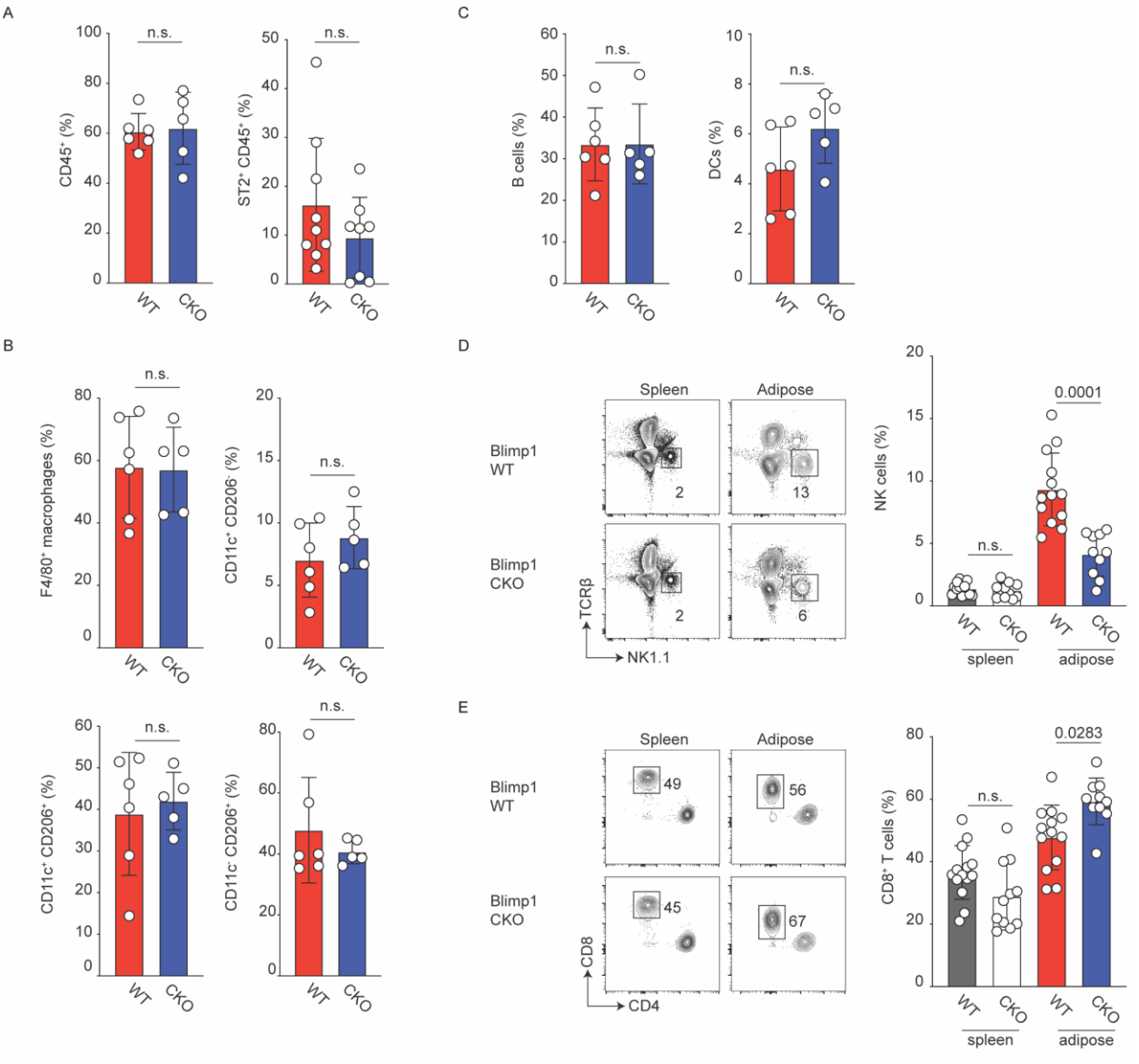

Figure 13. Changes in the VAT immune cell landscape with loss of Blimp-1+ Tregs.

Eight-week-old *Prdm1*$^{f/f}$ Foxp3-YFP-Cre+ (CKO) or wild-type littermate control (WT) male mice were placed on 60% high fat diet (HFD) for 18-20 weeks prior to global immunophenotyping of the visceral adipose tissue by flow cytomtery. (A) Frequency of leukocytes, and ST2+ leukocytes in the presence and absence of Blimp-1+ Tregs. (B) Total frequency of F4/80+ CD11b+ macrophages as a percentage of innate immune cells. Frequency of CD11c+ M1 macrophage, CD206+ M2 macrophage, and CD11c+ CD206+ heterogeneous macrophage populations as a percentage of the total macrophage population. (C) Frequnecy of B220+ B cells, and F4/80- CD11b^{med} CD11c+ dendritic cells. (D-E) Representative flow plots and quantification of NK cells and CD8 T cells in spleen and adipose. Data are presented as means ± SEM

and are pooled from at least 2 independent experiments with n=5-14. Each dot represents one mouse. Unpaired Student's t-test was utilized (n.s.= not significant).

2.3.5 The role of Blimp-1+ Tregs in thermogenesis

A recent study by Rajbhandari et al. (2018) found that *Il10* null mice were protected from age-associated and HFD- induced obesity, and that they had improved glucose tolerance compared to WT mice[153]. In addition, they determined that inguinal white adipocytes transduced in vitro with shIL-10Rα adenovirus expressed less thermogenesis genes such as *Ucp1*, *Cox8b*, and *Cidea*[44], and that administration of IL-10Rα anti-sense oligonucleotide-specific to adipose tissue could lead to increased expression of thermogenic genes *Ucp1*, *Cidea*, *Cox8b* and *Otop1* in the iWAT, and decreased fat mass[153]. Hence, we hypothesized that decreased IL-10 production by Blimp-1-deficient Tregs may lead to increased thermogenesis and protection from obesity.

We first tested this hypothesis by examining the brown and white adipose depots of mice on SFD. Utilizing real-time PCR, we found that Treg-specific *Prdm1* deletion had no effects on thermogenic genes (*Ucp1*, *Prdm16*, *Cidea*, *Dio2*) in the IAT **(Fig. 11A)**. We also utilized western blotting to measure UCP1 and PRDM16. Although there was a slight increase in protein expression, the differences were not statistically significant **(Fig. 11B)**. In addition to thermogenesis markers, we also measured a number of genes characteristic of white adipose tissue (*AdipoQ*, *Fabp4*, *Plin2*, *Pparg*), however expression of these genes remained stable **(Fig 11A)**. We next examined the VAT by real-time PCR. Unlike the inguinal adipose tissue, we found that loss of Blimp-1+ Tregs led to increased expression of *Ucp1* in this tissue **(Fig. 11A)**. Finally, we examined the BAT, but did not

detect any changes in thermogenesis genes or WAT-associated genes **(Fig. 11A)**. However, in vitro treatment of differentiated beige cell lines with IL-10 demonstrated that this cytokine is able to directly suppress *Ucp1* **(Fig. 11C)**. In addition to analyzing thermogenic genes and proteins, we also measured energy expenditure by these mice over the course of 48hrs, as well as their rectal temperatures but we did not detect any changes (**Fig. 11D-E)**. Taken together, these data suggested that in SFD mice, Blimp-1 Treg deficiency leads to limited, localized adipocyte beiging in the VAT only.

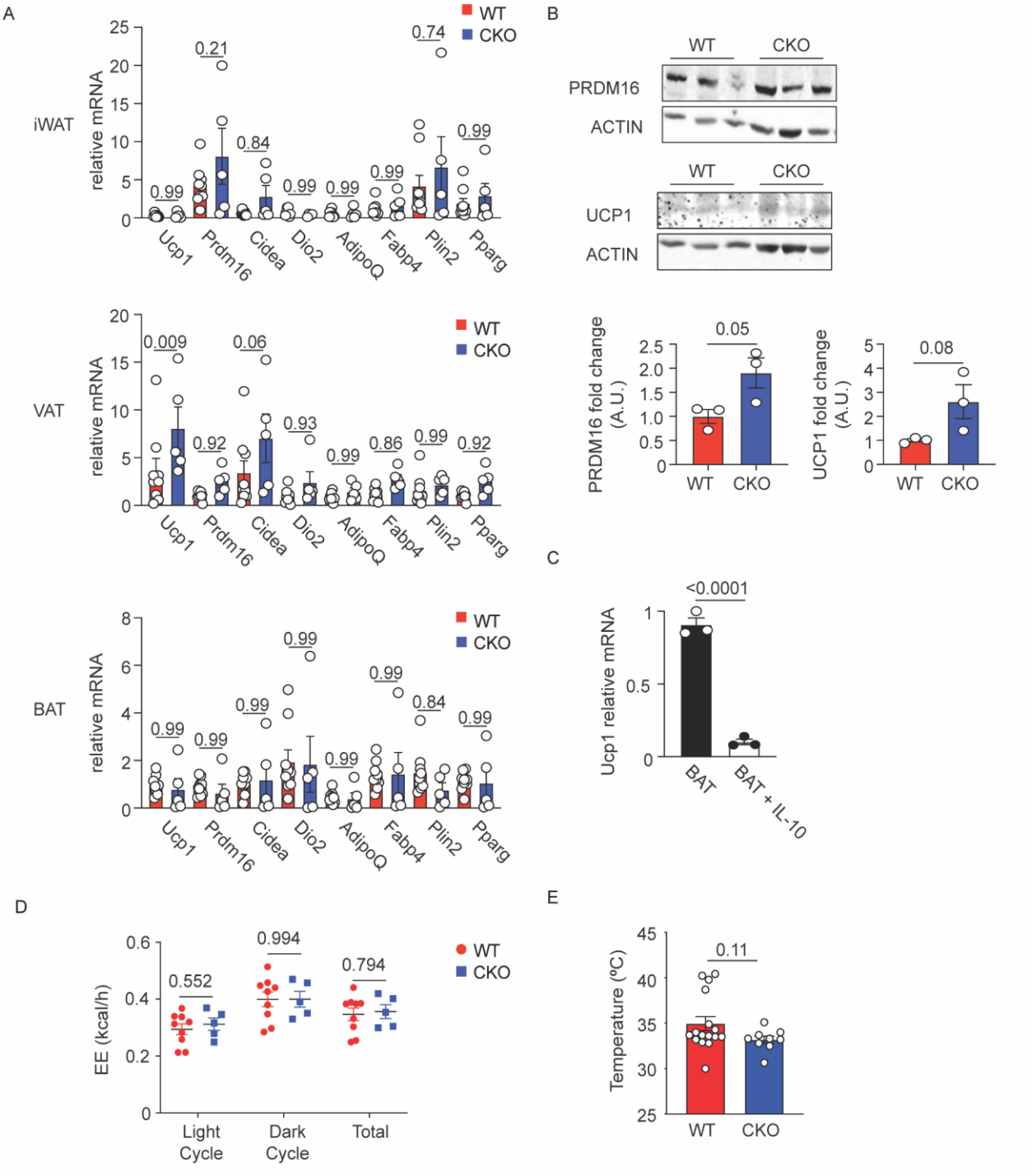

Figure 14. Loss of Blimp-1+ Tregs has limited effect on thermogenesis in lean mice.

Eight-week-old *Prdm1*$^{f/f}$ Foxp3-YFP-Cre+ (CKO) or wild-type littermate control (WT) male mice were placed on 20% standard fat diet (SFD) for 18-20 weeks prior to analysis. (A) Inguinal white adipose tissue (iWAT), visceral adipose tissue (VAT) and brown adipose tissue (BAT) were isolated and analyzed via real-time

PCR. (B) Western blots of total iWAT, and quantification of bands normalized to beta-actin (A.U.= arbitrary units). Each lane represents one biological replicate. (C) Real-time PCR of in vitro differentiated beige adipocyte cell lines treated for 48 hours with recombinant IL-10. Each dot represents a technical replicate and are representative of two independent experiments. (D) Mice were placed in Promethion Multiplexed Metabolic Cage System for 48hrs, and energy expenditure (EE) was recorded during 12hr light/dark cycles. (E) Rectal temperature. Data from (A), (D) and (E) are presented as means ± SEM, and are from pooled from 2-3 independent experiments with n=3-16 mice, where each dot represents one mouse. Unpaired Student's t-test or one-way ANOVA was utilized.

We next examined how loss of Blimp-1+ Tregs affects thermogenesis in HFD mice. We observed that CKO mice had increased expression of *Ucp1*, *Prdm16* and *Dio2* in IAT, as well as increased expression of *Dio2* in BAT **(Fig. 12A)**. In addition, we observed a substantial increase in UCP1 protein expression in CKO mice compared to WT mice **(Fig. 12B)**. Similarly to SFD mice, we did not observe any changes in energy expenditure or rectal temperature **(Fig. 12C-D)**. Taken together, we concluded that loss of Blimp-1+ Tregs increased thermogenesis and adipocyte beiging in HFD mice.

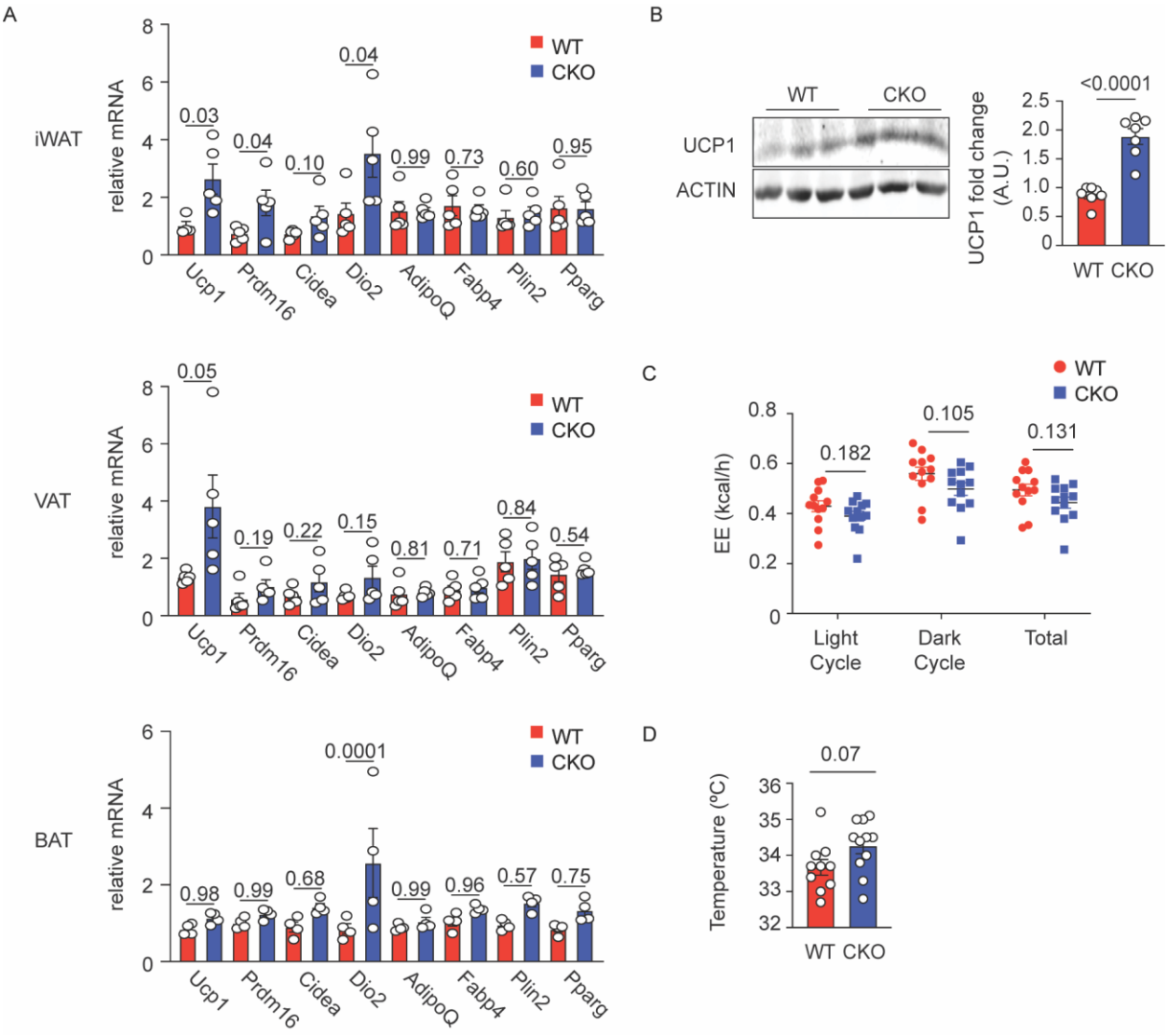

Figure 15. Loss of Blimp-1+ Tregs leads to increased thermogenesis in obese mice.

Eight-week-old *Prdm1*$^{f/f}$ Foxp3-YFP-Cre+ (CKO) or wild-type littermate control (WT) male mice were placed on 60% high fat diet (HFD) for 18-20 weeks prior to analysis. (A) Inguinal white adipose tissue (iWAT), visceral adipose tissue (VAT) and brown adipose tissue (BAT) were isolated and analyzed via real-time PCR. (B) Western blot of total iWAT, and quantification of bands normalized to beta-actin (A.U.= arbitrary units). Each lane represents one biological replicate. (C) Real-time PCR of in vitro differentiated beige adipocyte cell lines treated for 48 hours with recombinant IL-10. Each dot represents a technical replicate and are representative of two independent experiments. (D) Mice were placed in Promethion Multiplexed Metabolic Cage System for 48hrs, and energy expenditure (EE) was recorded during 12hr light/dark cycles. (E) Rectal temperature. Data are presented as means ± SEM, and are from pooled from 2-3 independent

experiments with n=4-12, where each dot represents one mouse. Unpaired Student's t-test or one-way ANOVA was utilized.

One question that remained was whether the changes in insulin sensitivity and thermogenesis in obese mice were directly caused by loss of Blimp-1+ Tregs, or if they were secondary to weight loss. Thus, to address this question, we decided to analyze *Prdm1*$^{f/f}$ Foxp3-YFP-Cre+ mice after they were on HFD for only 3 weeks. This was the timepoint that we previously identified that after which body weight begins to diverge **(Fig. 8)**. As expected, Blimp-1 CKO mice exhibited no change in body weight, and lean and fat mass remained the same **(Fig. 13A, 13G)**. Blimp-1 Treg deficient short-term HFD mice had no changes in fasting insulin, but decreased fasting glucose, leading to overall decreased insulin resistance **(Fig. 13B-D)**. However, when a glucose tolerance test was performed, there were no differences in circulating insulin or glucose between the two experimental groups **(Fig. 13E-F)**. Metabolic chamber analyses over the course of 48hrs found no differences in feeding behavior or activity level **(Fig. 13H-I)**. There was a trend towards elevated glucose oxidation in the CKO group during the light cycle, although it was not statistically significant **(Fig 13J)**.

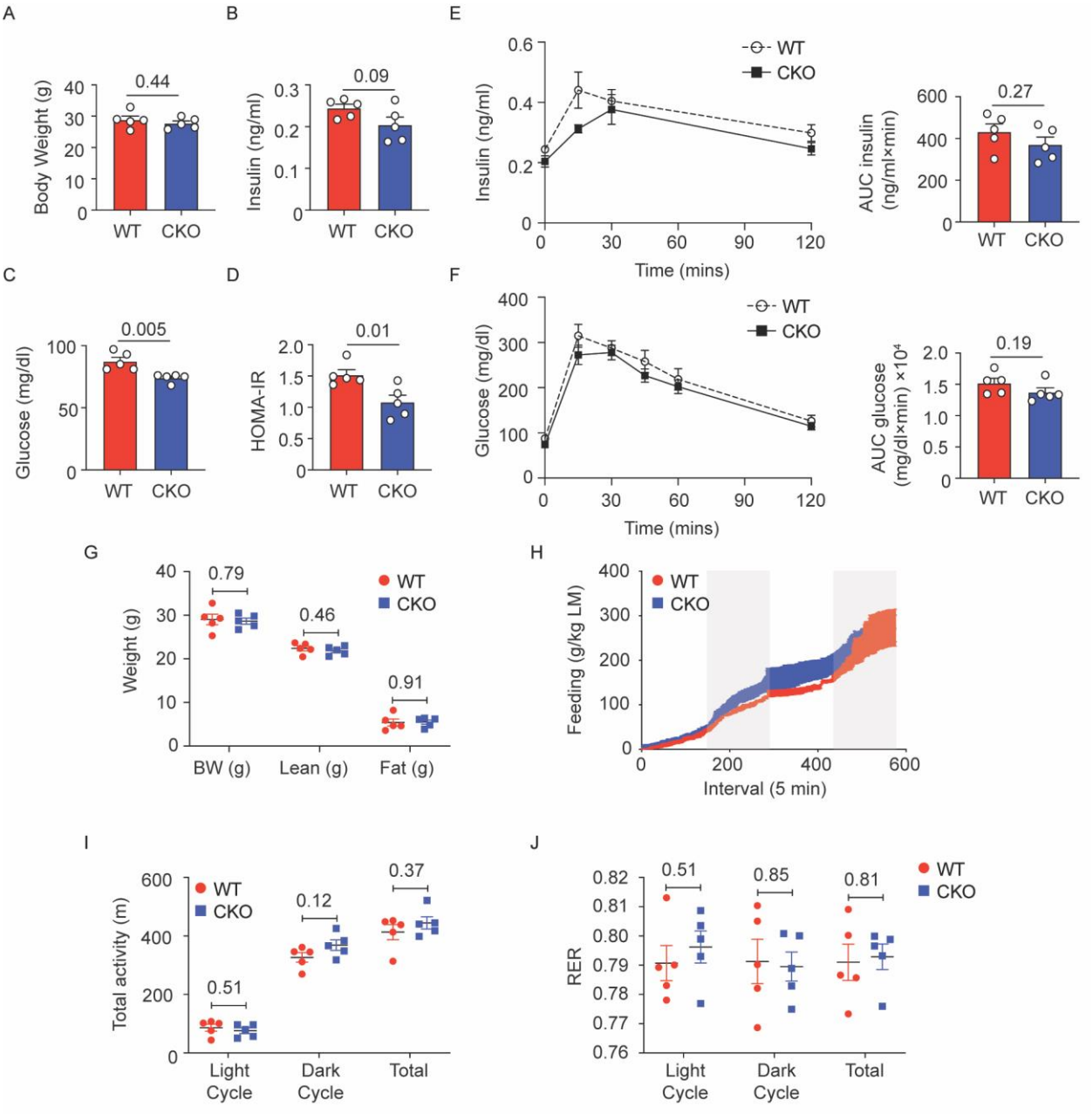

Figure 16. Loss of Blimp-1+ Tregs protects against insulin resistance in short-term HFD mice.

Eight-week-old *Prdm1*$^{f/f}$ Foxp3-YFP-Cre+ (CKO) or wild-type littermate control (WT) male mice were placed on 60% high fat diet (HFD) for 3 weeks prior to metabolic analysis. (A) Body weight of 11-week old HFD-fed WT and CKO mice. (B-C) Fasting plasma insulin and glucose levels in WT and CKO mice. (D) Fasting insulin resistance as measured by homeostatic model assessment of insulin resistance (HOMA-IR) in WT and CKO mice. (E-F) Intraperitoneal glucose tolerance test. Plasma insulin and blood glucose levels over time post-glucose injection. Bar graphs represent area under the curve (AUC). (G) Body composition as

measured by EchoMRI. (H-J) Mice were placed in Promethion Multiplexed Metabolic Cage System for 48hrs and measurements recorded in 5-minute increments during 12hr light/dark cycles. (H) Food intake in grams (g) per kilogram (kg) lean mass (LM). (I) Total activity in meters (m) over 48 hours. (J) Respiratory exchange ratio (RER) where 0.7 indicates fatty acid oxidation and 1.0 indicates glucose oxidation. Data are presented as means ± SEM and are pooled from 2 independent experiments with n=5 per group. Each dot represents one mouse. Unpaired Student's t-test or one-way ANOVA was used.

Analyses of Tregs within the various adipose depots found that Blimp-1 CKO mice had increased total Tregs in the VAT and BAT **(Fig. 14A)**. In addition, loss of Blimp-1 led to numerous changes in the signature of VAT, BAT and IAT Tregs **(Fig. 14A)**, and IL-10 production was perturbed in Blimp-1 deficient VAT, IAT, and lymphoid Tregs **(Fig. 14B)**.

Finally, when we examined thermogenic and white adipose tissue-associated genes, we found that thermogenic genes such as *Prdm16*, *Cidea* and *Dio2* were up-regulated in IAT and VAT **(Fig. 15A-B)**. We detected no changes in the BAT **(Fig. 15C)**. Systemically, the total energy expenditure between the two groups were the same **(Fig. 15D)**. Thus, taken together, our short-term HFD data supported the notion that Blimp-1 deficient Tregs can directly protect mice from metabolic dysfunction and induce adipocyte beiging and thermogenesis irrespective of weight during HFD feeding.

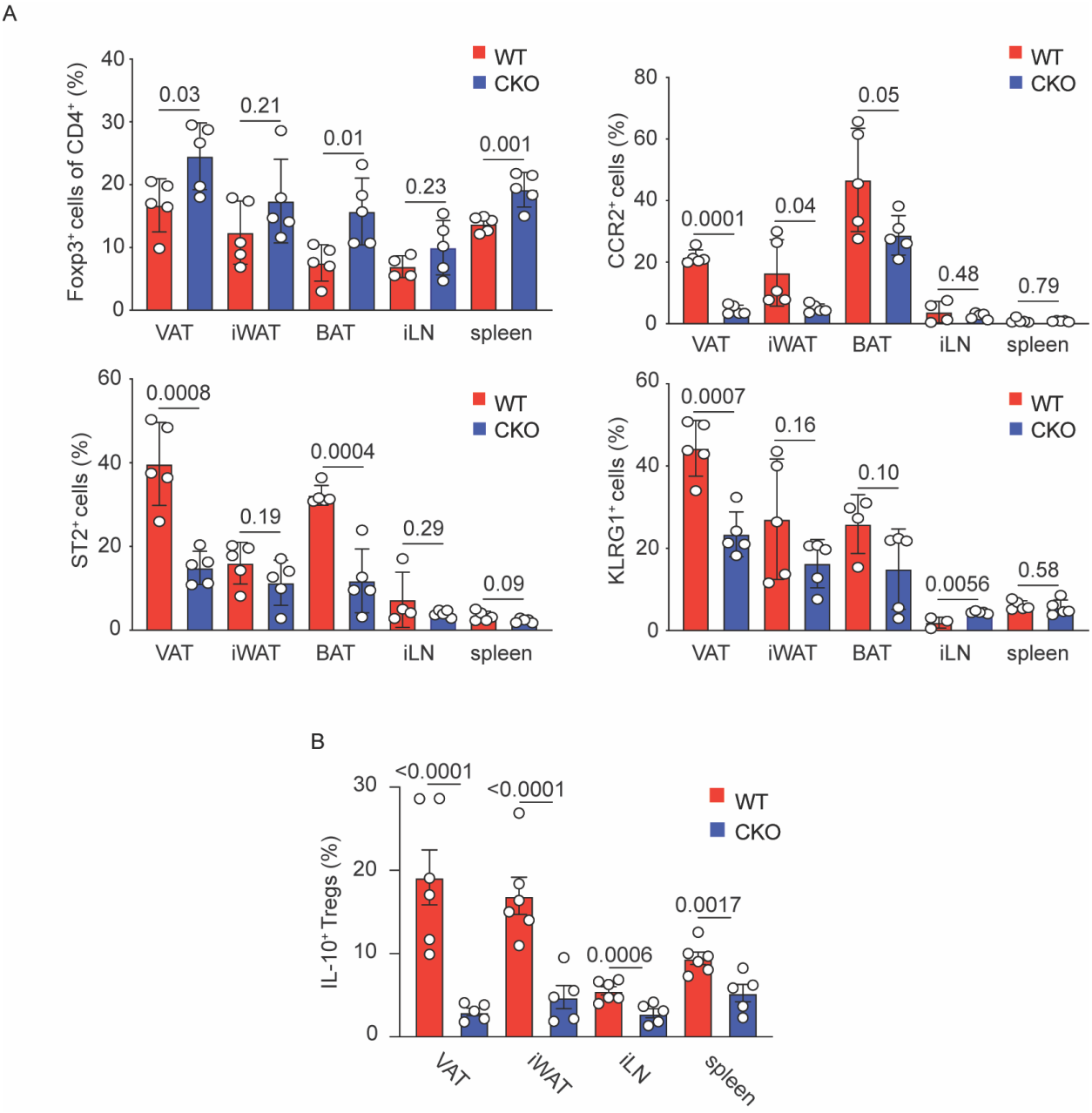

Figure 17. Blimp-1-deficient Tregs from short-term HFD mice exhibit altered adipose Treg signature. Eight-week-old *Prdm1*$^{f/f}$ Foxp3-YFP-Cre+ (CKO) or wild-type littermate control (WT) male mice were placed on 60% high fat diet (HFD) for 3 weeks prior to Treg analysis by flow cytometry. (A) Frequency of CD4+ Foxp3+ Tregs and adipose Treg markers on the cells. (B) Total adipose and secondary lymphoid organ stromal vascular fractions were stimulated ex vivo for 5 hours with PMA and ionomycin. Quantification of IL-10 producing Tregs. Cells gated off CD4+ Foxp3+ T cells.

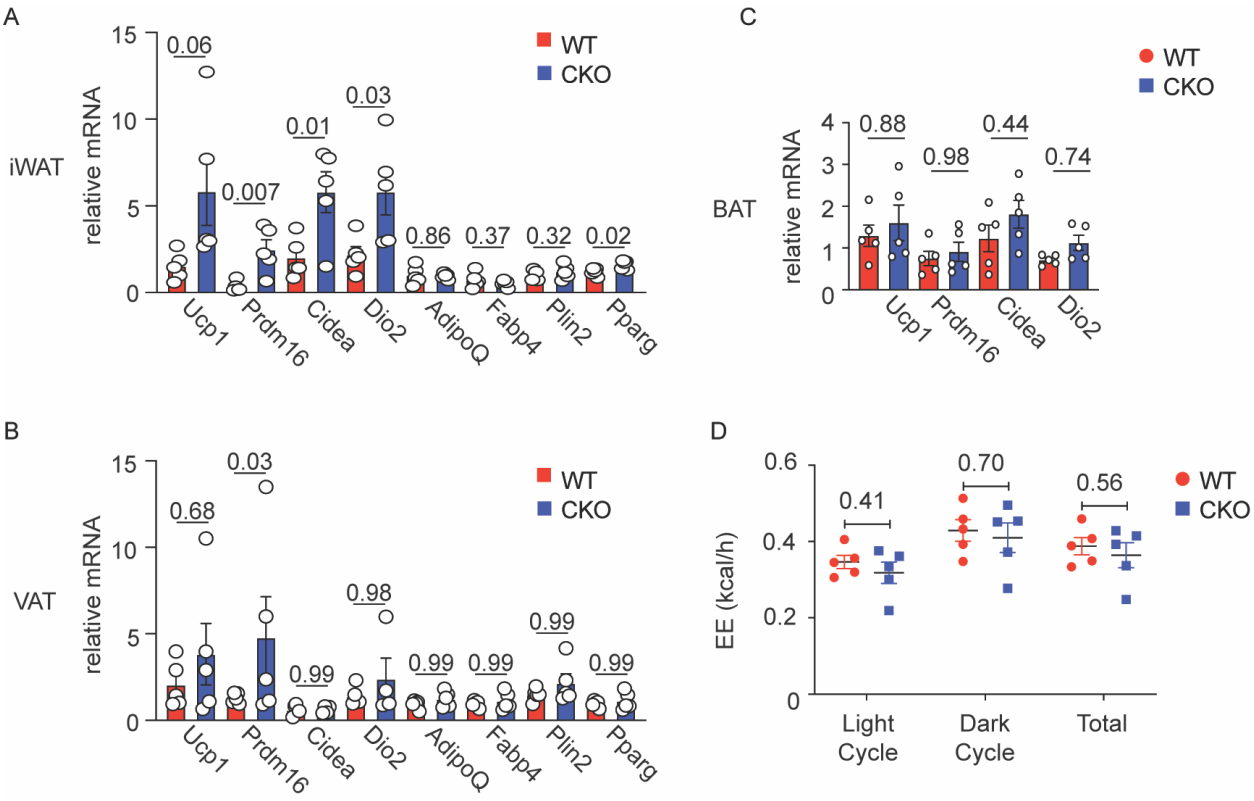

Figure 18. Loss of Blimp-1+ Tregs leads to increased adipocyte beiging in short-term HFD mice.

Eight-week-old *Prdm1*$^{f/f}$ Foxp3-YFP-Cre+ (CKO) or wild-type littermate control (WT) male mice were placed on 60% high fat diet (HFD) for 3 weeks prior to analysis. A) Inguinal white adipose tissue (iWAT), (B) visceral adipose tissue (VAT), and (C) brown adipose tissue (BAT) were isolated and analyzed via real-time PCR. (D) Mice were placed in Promethion Multiplexed Metabolic Cage System for 48hrs, and energy expenditure (EE) was recorded during 12hr light/dark cycles.

Next, to confirm that increased thermogenesis in Blimp-1 deficient mice was mediated by IL-10, we generated *Il10*$^{f/f}$ Foxp3-YFP-Cre+ mice lacking IL-10 on all Tregs. Similarly, to what was observed in the Blimp-1 CKO mice, these mice weighed less **Fig. 16A)**. Upon examination of their gross morphology, their inguinal and visceral fat pads appeared smaller, and their livers were darker in color suggesting less hepatic steatosis **(Fig. 16G)**. EchoMRI analysis confirmed that the difference in body weight between the

CKO and WT mice were a result of reduced fat mass and not lean mass **(Fig. 16I)**. Changes in body weight and composition were not attributable to nutrient malabsorption as histological analyses of the colon indicated no changes in inflammation or colon length **(Fig. 16H)**.

Metabolically, the CKO mice fared better than their WT counterparts. CKO mice had lower fasting insulin and glucose levels, and reduced insulin resistance **(Fig. 16B-D)**. In addition, there was less circulating insulin and glucose in the blood during glucose tolerance testing **(Fig. 16E-F)**. When the mice were placed in metabolic chambers for 48hrs, there were no changes in feeding behavior or activity between the two groups **(Fig. 16J-K)**. However, during the light cycle, the CKO mice had increased RER indicating greater glucose oxidation **(Fig. 16L)**. Finally, thermogenic markers were compared between WT and IL-10 Treg deficient mice. CKO mice had increased expression of thermogenic markers such as *Ucp1, Prdm16, Cidea* and *Dio2* at the gene and protein level in the inguinal and visceral white adipose tissue **(Fig. 16M, Fig.17A-B)**.

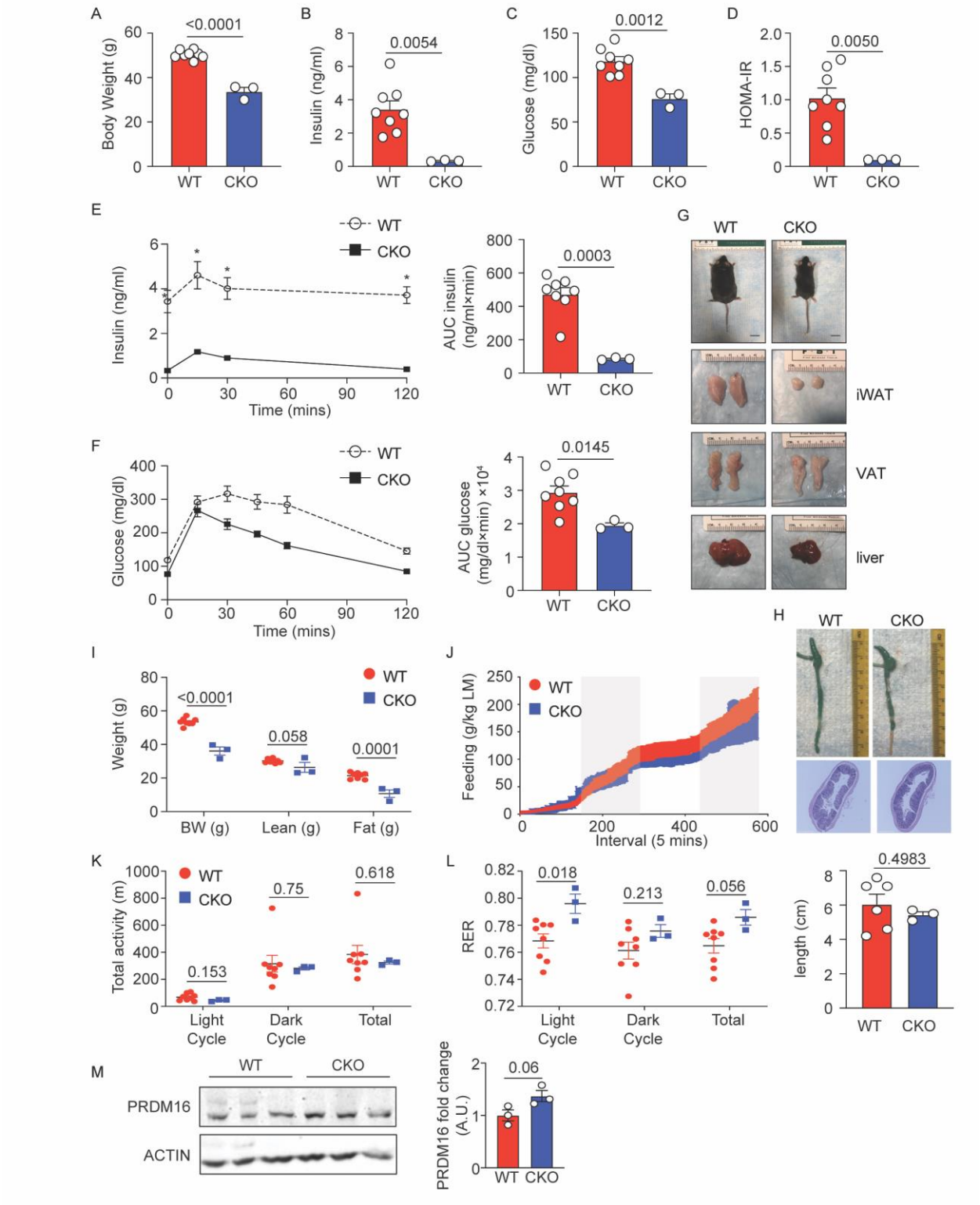

Figure 19. Loss of IL-10+ Tregs protects mice from diet-induced obesity.

Eight-week-old *Il10*$^{f/f}$ Foxp3-YFP-Cre+ (CKO) or wild-type littermate control (WT) male mice were placed on 60% high fat diet (HFD) for 18-20 weeks prior to metabolic analysis. (A) Body weight of 26-28-week old HFD-fed WT and CKO mice. (B-C) Fasting plasma insulin and glucose levels in WT and CKO mice. (D) Fasting insulin resistance as measured by homeostatic model assessment of insulin resistance (HOMA-IR) in WT and CKO mice. (E-F) Intraperitoneal glucose tolerance test. Plasma insulin and blood glucose levels over time post-glucose injection. Bar graphs represent area under the curve (AUC). (G) Gross appearance, inguinal WAT (iWAT), epididymal visceral WAT (VAT) and livers. (H) Top: Photographs and quantification of the colon length in WT and CKO mice after 18-20 weeks on HFD. Bottom: H&E stain of colon cross-section. (I) Body composition as measured by EchoMRI. (J-L) Mice were placed in Promethion Multiplexed Metabolic Cage System for 48hrs and measurements recorded in 5-minute increments during 12hr light/dark cycles. (J) Food intake in grams (g) per kilogram (kg) lean mass (LM). (K) Total activity in meters (m) over 48 hours. (L) Respiratory exchange ratio (RER) where 0.7 indicates fatty acid oxidation and 1.0 indicates glucose oxidation. (M) Western blot of total iWAT, and quantification of bands normalized to beta-actin (A.U.= arbitrary units). Each lane represents one biological replicate. Data are presented as means ± SEM and are pooled from 3 independent experiments with n=3-8 mice per group. Each dot represents one mouse. Unpaired Student's t-test or one-way ANOVA was used (*=P value <0.05).

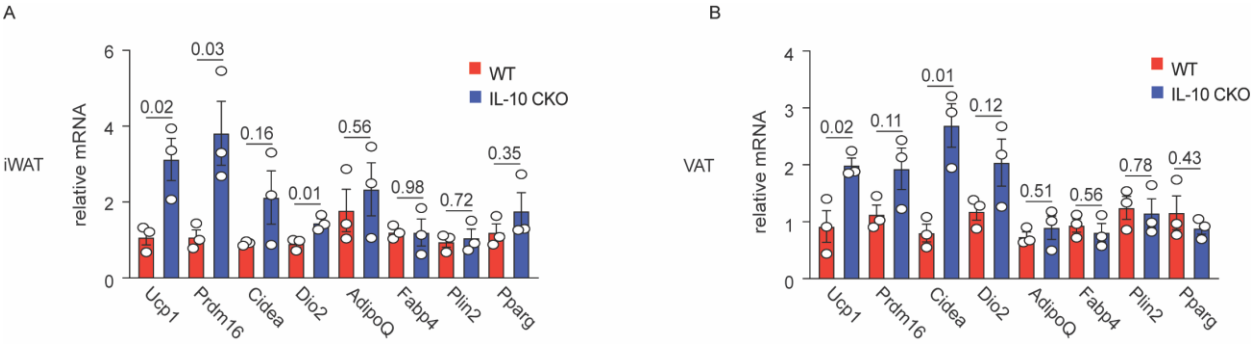

Figure 20. Loss of IL-10+ Tregs leads to increased thermogensis and beiging in obese mice.

8-week-old male Foxp3-YFP-Cre+ (WT) and IL-10$^{f/f}$ Foxp3-YFP-Cre+ mice (IL-10 CKO) were placed on 60% high fat diet (HFD) for 18-20 weeks prior to real-time PCR analysis. Bar graphs showing relative mRNA expression from total (A) iWAT and (B) VAT. Values were normalized to beta-actin. Data are presented as means ± s.e.m. for n = 3 mice per group. An unpaired Student's t-test was performed to determine significance and the P values are indicated on the graphs.

2.3.6 The Role of Tregs and IL-10 during human obesity

Finally, we attempted to check whether a correlation existed between Tregs and human obesity. To do so, we utilized publicly available data from the Metabolic Syndrome in Men (METSIM) study. This cross-sectional population-based longitudinal study utilized microarrays to analyze gene expression in abdominal subcutaneous adipose tissue from randomly selected Finnish men ages 45-70yrs old[154]. Alongside, these data, clinical features associated with obesity were also collected[154]. Using these data, we correlated BMI to Foxp3 expression by T cells and found that there was a negative correlation between the two **(Fig. 17A)**. In addition, subjects with increased BMI had higher levels of IL-10r and total IL-10 **(Fig. 17B-C)**. Of the IL-10 being expressed, the portion due to adipose Tregs also positively correlated with BMI **(Fig. 17D)**. Combining these data with the previously described pre-clinical findings supports further investigation into the role of adipose Treg-derived IL-10 in maintaining metabolic homeostasis in humans, and provides a possible therapeutic target in restoring insulin sensitivity during obesity.

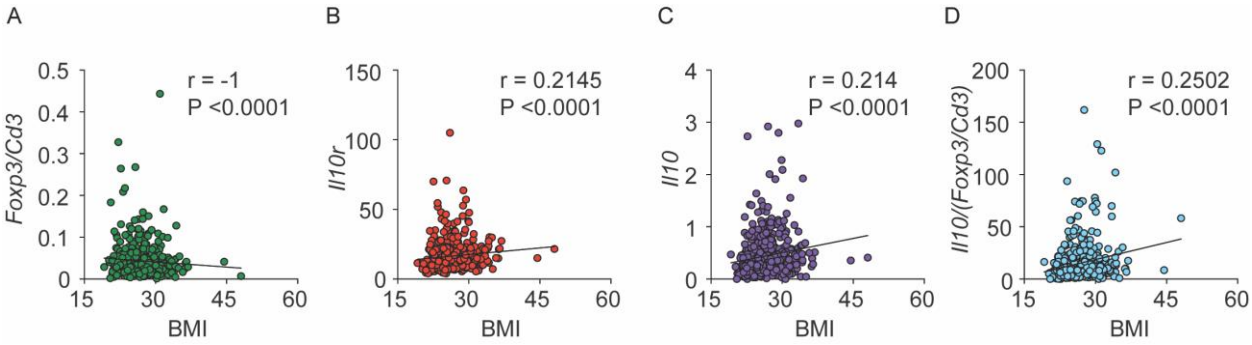

Figure 21. Clinical correlation of IL-10+ Tregs to increased body mass index.

Publicly available data from the Metabolic Syndrome in Men (METSIM) study were analyzed to identify possible correlations between Treg IL-10 and obesity. This cross-sectional population-based longitudinal study utilized microarrays to analyze gene expression in abdominal subcutaneous adipose tissue from randomly selected Finnish men ages 45-70yrs old.

2.4 Discussion

The role of Tregs in peripheral tissues has been extensively explored over the past decade, with most publications delineating a role for these cells in suppressing local inflammation and maintaining tissue homeostasis[23, 79, 80, 85, 91, 92, 96, 97, 100, 127]. However, recent publications have revealed that the function of peripheral Tregs is more complex than initially reported and is tissue and context dependent. For example, aTregs have been shown to be pathogenic in age-associated obesity[93, 155]. In addition, WT female mice, which have reduced aTreg frequency and IL-10 secretion, are protected from glucose intolerance and fat gain, relative to age-matched male mice, although whether glucose tolerance and fat reduction in female mice are driven through an IL-10–deficient aTreg axis has not yet been established[80]. Similarly, the role of Blimp-1 in the immune system is highly context dependent and tissue specific. For example, it was recently

shown that Blimp-1 is an unexpected positive regulator of Th2 responses in the lung, facilitated through an IL-10/STAT3 axis[156].

Treg-secreted IL-10 is known to suppress inflammatory immune cells and for the maintenance of tissue homeostasis, particularly at barrier surfaces[157, 158]. In this present study, we show that Treg IL-10 is also critical for suppressing adipocyte beiging in male mice. Loss of IL-10 expression by Tregs resulted in mice that were protected from DIO and showed improved insulin sensitivity. Mechanistically, Treg-intrinsic loss of Blimp-1 led to reduced IL-10 production, resulting in increased expression of PRDM16 and UCP1 by adipocytes, proteins that are critical for upregulation of the beiging program[153, 159, 160]. One puzzling aspect of our findings was that whole-body energy expenditure did not increase with loss of IL-10 or Blimp-1 by Tregs, despite an increase in beige gene expression in the visceral and inguinal adipose tissue depots. IL-10 is, however, secreted by other B and T cell populations in the adipose tissue[133], and it may be that IL-10 from these additional cells counters an increase in whole-body expenditure in our model.

It is well established that IL-10 secretion by Tregs is essential for preventing gut inflammation and colitis[116, 119, 125]. However, in our system, we found no evidence of Treg-specific deletion of IL-10 or Blimp-1 resulting in colitis and influencing the weight loss phenotype we observed. Mice on HFD gained weight, albeit at a slower rate than their WT counterparts. Possible factors for these distinctions may include the animal's microbiota and the variety of chow used across studies, as well as the age and subtle differences in the background of the mice. We were encouraged to see our phenotype was consistent with that of the recently published germline IL-10–deficient animals[153] and

that colitis was likely not a factor underlying the weight loss and IR we observed in the Treg-specific IL-10– and Blimp-1–deficient animals.

Finally, we consider our findings in the context of previously reported aTreg functions in DIO. Prior data have shown a clear correlation between reduced aTreg frequency and increased body mass and that temporal ablation of Tregs increases IR and adipose tissue inflammation[23]. In our study, we report similar reductions in aTreg frequency in both WT and Blimp-1–deficient mice when these animals were placed on HFD. However, our data uniquely demonstrated that disruption of aTreg IL-10 secretion can reduce IR. Excluding IL-10, Tregs can secrete a number of other anti-inflammatory soluble mediators, including TGF-β, IL-35, amphiregulin, and methionine-enkephalin[161-164]. Hence, our findings suggest that the sum total of these Treg-derived mediators may need to be considered to accurately define how Tregs dictate whole-body metabolism and adipose tissue inflammation.

Together, our findings reveal that IL-10 secretion by Tregs is not limited solely to suppression of effector and autoreactive immune cells[157, 158], but rather that Tregs release IL-10 to promote the suppression of the beige gene program in adipocytes. Ultimately, these data have implications for the role of the immune cell-adipocyte axis in mediating systemic metabolism and protection from DIO.

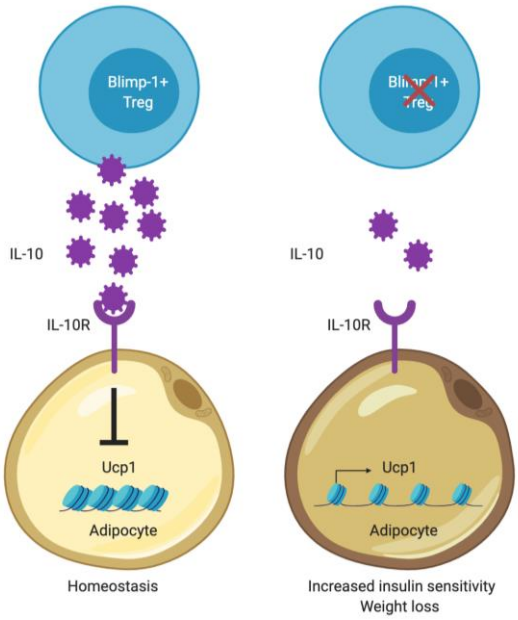

Figure 22. Tregs facilitate obesity and insulin resistance through a Blimp-1/IL-10 axis.

During diet-induced obesity, Blimp-1+ Tregs secrete IL-10 to suppress *Ucp1* thermogenesis gene expression in white adipose tissue. In the absence of Blimp-1+ Tregs, reduced IL-10 signaling leads to *Ucp1* up-regulation, increased adipocyte beiging, improved insulin sensitivity and limited weight gain.

2.5 Future Directions

In this project, we determined that Tregs facilitate obesity through a Blimp-1/IL-10 axis. Blimp-1 positively regulated IL-10 secretion in adipose Tregs, and IL-10 acted on beige adipocytes to suppress thermogenesis. In HFD mice, this resulted in increased weight gain, insulin resistance and glucose intolerance compared to mice lacking Blimp-1+ Tregs. Traditionally, Tregs have been viewed as critical for preserving insulin sensitivity and glucose tolerance[89-91]. However, in our study, we found that the Blimp-1+

Tregs can be detrimental during obesity. As described earlier in Chapter 1: Introduction, insulin sensitivity and thermogenesis are regulated by a multilateral network involving immune cells, adipocytes, and other endocrine organs (e.g. pancreas, liver, skeletal muscle) that communicate with one another at both the local and systemic level through secretory factors (e.g. cytokines, adipokines) and direct contact. Therefore, in order to understand the impact and significance of Blimp-1+ Tregs, these cells must be studied in relation to the other players that shape adipose immunobiology and metabolism.

2.5.1 Treg-intrinsic role of Blimp-1

2.5.1.1 Role of Blimp-1 in Treg activation, differentiation and function

In our project, we observed variable distributions of VAT, IAT and BAT Tregs in *Prdm1* $^{f/f}$ Foxp3-YFP-Cre+ mice (CKO) versus wild-type (WT) mice. Previous studies have shown that Blimp-1 is required for peripheral Treg homeostasis, and that loss of Blimp-1 leads to increased Tregs in organs such as the intestines and lungs[113, 116, 118]. This was attributable to increased Treg proliferation and decreased cell death[116]. In addition, it has been suggested that VAT Tregs undergo a 2-step differentiation process, in which thymic Tregs first traffic to the spleen, and then PPARg^{lo} Blimp-1^{lo} Tregs that become antigen-experienced proceed to migrate into the VAT where they acquire their full aTreg signature[100]. In our study, loss of Blimp-1 led to decreased VAT Treg frequency in SFD mice, and increased BAT Treg frequency in HFD mice. In addition, in both lean and obese mice, loss of Blimp-1 led to increased iLN and splenic Tregs. The higher frequency of secondary lymphoid organ Tregs suggests that they may be accumulating in these organs as a result of defective trafficking. Indeed, in our VAT Tregs, we saw that

loss of Blimp-1 led to decreased CCR2 expression. Our observations are in line with previously published research showing that Blimp-1 deficient VAT Tregs have decreased CCR2 and increased CCR7 (a secondary lymphoid organ targeting chemokine receptor)[80]. However, cell proliferation and apoptosis studies need to be performed to determine whether cellular turnover is affected.

In addition, Blimp-1 has been shown to play differing roles in peripheral effector Treg activation in inflamed versus non-inflamed tissue. In one study involving influenza infection, loss of Blimp-1 led to decreased ICOS+ lung Tregs[113]. However, in a different study under homeostatic conditions, loss of Blimp-1 led to increased ICOS+ Tregs across multiple peripheral tissues[116]. Obese adipose tissues experience chronic low-grade inflammation, and the degree of inflammation differs between VAT, scAT, and BAT[49-51]. Therefore, it would be interesting to examine whether the activation status differs between Blimp-1+ and Blimp-1- Tregs in the various adipose depots using our Blimp-1 YFP reporter mice. In particular, we could measure the expression of co-stimulatory molecules such as CD28, ICOS, OX40, 4-1BB, GITR and TNFR2 on adipose-resident Tregs[165].

As mentioned earlier, in addition to IL-10, Tregs can secrete TGF-β, IL-35, amphiregulin, methionine-enkephalin, Jagged 1 (Notch ligand) and cleave ATP to adenosine[161-164, 166-168]. Although in our study we observed that loss of Blimp-1+ Tregs helped maintain insulin sensitivity, other studies involving **total** loss of Tregs have found that it exacerbated insulin resistance[23, 31, 89-91]. Therefore, we should determine whether Blimp-1 deletion affects Treg function and systemic metabolism in an IL-10 independent manner. For example, IL-35 secreted from ST2+ Tregs have been shown to inhibit gamma-delta T cells in the lung during allergen exposure[169], and gamma-delta T cells

have been shown to support age-associated accumulation of VAT Tregs and promote cold-induced thermogenesis in the scAT and BAT[170]. In addition, amphiregulin can positively regulate PGC1a in the VAT[171], and PGC1a maintains metabolic homeostasis by regulating gluconeogenesis, fatty acid oxidation and preventing oxidative damage in the liver[172-174], and also by inducing scAT beiging[175]. Furthermore, administration of methionine-enkephalin to HFD mice has been shown to increase scAT beiging and decrease weight gain, insulin resistance, glucose intolerance and hepatic steatosis[176]. Finally, adenosine has been shown to induce lipolysis and thermogenesis in scAT and BAT[177].

Besides secretory factors, Tregs can use cell surface molecules such as CTLA4, TIGIT, TRAIL and PD-1 to directly suppress dendritic cells and conventional T cells[178]. In addition, it has been shown that although LAG3 does not affect Treg immunosuppressive capacity on a cellular level, it negatively regulates Treg maintenance and proliferation pathways, and hence loss of LAG3 leads to increased immunosuppressive capacity at the population level in pancreatic intra-islet Tregs during autoimmune Type 1 diabetes[179]. It will be interesting to investigate whether Blimp-1 regulates any of these inhibitory proteins in Tregs.

2.5.1.2 Blimp-1 mediated transcriptional regulation

In addition to determining whether or not Blimp-1 has an effect on non-IL10 related Treg function, it is important to identify the signaling networks that mediate Blimp-1 dependent changes in aTreg differentiation and function. For instance, researchers have previously observed that ß-adrenergic signaling induces naïve CD4 T cells in the BAT to

become Tregs through STAT6/PTEN signaling[94]. In VAT Tregs, TCR signaling induces the transcription factors BATF and IRF4 to directly bind and upregulate expression of *Pparg* and *Il1rl1* to promote cell proliferation and maintain VAT Treg identity[92]. As mentioned earlier, IRF4/Blimp-1 interaction is involved in generating lung effector Tregs during influenza infection[113]. It may be possible that a similar interaction occurs in aTregs as well. Besides these pathways, it has been shown that Bcl6 and Blimp-1 are reciprocal regulators of Tfh differentiation during LCMV infection[180], as well as in ST2+ Treg development during allergic asthma inflammation[181], indicative of a role for Bcl6.

2.5.2 Blimp-1+ Tregs in adipose tissue inflammation and metabolic regulation during obesity

2.5.2.1 Drivers of Blimp-1 expression in adipose Tregs during obesity

Besides examining the Treg-intrinsic role of Blimp-1, we should also consider how Blimp-1+ Tregs function within the adipose ecosystem and how they affect metabolic outcomes. As Blimp-1 expression in Tregs appears to be detrimental during diet-induced obesity, the first question we should address is what drives Blimp-1 expression in these cells, and how can we limit it? It has previously been established that Blimp-1 expression is driven by T cell receptor activation in the presence of IL-2, and that its expression can be further enhanced by cytokines such as IL-12, IL-4 and IL-6[113].

During excessive caloric intake, fats are stored as triglycerides in the adipose tissue[13]. However, when adipocytes become too hypertrophic, they risk the possibility of eventually rupturing and releasing free fatty acids into the environment[26-28]. In addition,

increased insulin resistance during obesity prevents uptake of ingested fats into cells resulting in increased circulating fatty acids[39-41].

It may be possible that these fatty acids serve as T cell receptor ligand and trigger Blimp-1 expression, or they may serve to enhance Blimp-1 expression once TCR stimulation occurs. Although, it has not been shown directly that fatty acids regulate Blimp-1 expression in Tregs, the fact that fatty acids have been shown to regulate IL-10 production suggests that a fatty acid/Blimp-1/IL-10 axis is possible.

For example, one study examined the role of monounsaturated omega-9 fatty acid oleic acid on Tregs during multiple sclerosis[182]. The researchers found that oleic acid was the most abundant long-chain fatty acid in the adipose tissue of their healthy donors, and that it was decreased in patients with multiple sclerosis (and inversely, circulating oleic acid was greater in patients with multiple sclerosis compared to healthy control)[182]. They also observed that circulating Tregs from multiple sclerosis patients had decreased IL-10 production and diminished suppressive capacity compared to their healthy counterparts[182]. However, when Tregs sorted from the PBMCs of multiple sclerosis and healthy controls were cultured with oleic acid, IL-10 production increased in both groups and the suppressive capacity of Tregs from multiple sclerosis patients was partially restored[182]. Mechanistically, they found that the effect of oleic acid on Treg suppressive capacity occurred through increased fatty acid oxidation[182]. Interestingly, it has been shown before that Blimp-1 positively regulates *Pparg*[80], and PPARG regulates lipid metabolism in VAT Tregs from male mice[85]. Adding additional support to the idea that fatty acids may induce Blimp-1 expression in Tregs is the finding that at least in Th1 cells, the microbiota-derived short-chain fatty acid butyrate can activate a G-protein coupled

receptor 43 (GPR43)/STAT3/mTOR/Blimp-1 pathway to ultimately induce IL-10 secretion[183]. Besides these two findings, it has also been demonstrated more generally that ex vivo stimulation of splenic T cells from mice fed polyunsaturated omega-3 fatty acid-rich diet produced more IL-10 than T cells from mice fed a polyunsaturated omega-6 fatty acid-rich diet[184]. It has also been shown that CD4 T cells stimulated ex vivo in the presence of omega-3 fatty acid eicosapentaenoic acid secreted higher levels of IL-10, whereas cells stimulated in the presence of omega-3 fatty acids docosahexaenoic acid produced less IL-10 relative to control cells that were stimulated in the absence of fatty acids[185]. Therefore, my initial hypothesis is that omega-3 fatty acid eicosapentaenoic, long-chain fatty acid oleic acid, and short-chain fatty acid butyrate can promote Blimp-1 expression in aTregs, whereas omega-3 fatty acid docosahexaenoic acid will suppress Blimp-1 expression.

It is also possible that fatty acids may act indirectly by activating non-Treg immune cells that then interact with Tregs to drive Blimp-1 expression and IL-10 secretion. For example, within the colon, macrophages and dendritic cells can respond to butyrate to produce IL-10, which in turn promotes differentiation of naïve T cells into Tregs and IL-10 producing T (Tr1) cells[186].

It has previously been reported that in humans, saturated fat and trans-fat intake is positively associated with increased weight gain, whereas poly-unsaturated fatty acid is not[187, 188]. The role of short-chain fatty acid butyrate in obesity is controversial with some studies demonstrating a protective role against obesity while others indicate an antagonistic effect[189]. Finally, the monounsaturated fatty acid oleic acid has been previously described to be protective against obesity, metabolic syndrome and Type 2

Diabetes[190]. It would be interesting to examine whether fatty acids differentially regulate Blimp-1 expression. To analyze the effect of dietary fat composition on Blimp-1 expression, the frequency and MFI of Blimp-1+ Tregs can be calculated in HFD mice and compared them to age-matched SFD control mice before their weights diverge. Commercially available diets for mice differ in their formulations, and they have been described to have different effects on obesity-associated disease pathology[191]. Therefore, in addition to the 60% HFD we utilized in this project, we can also repeat our experiments in mice fed 45% HFD, cafeteria diet[191], or Western diet[192].

Besides investigating whether free fatty acids drive Blimp-1 expression, it would be of interest to further characterize the cytokine milieu within the VAT, scAT and BAT in lean and obese tissue via qPCR and ELISA, and test whether the cytokine milieu drives differential levels of Blimp-1 expression in Tregs. A recent study by Vasanthakumar et al. (2020) found that IL-6 could induce Blimp-1 expression in VAT Tregs[80]. In addition, CD4 effector T cells, T follicular helper and NKT cells secrete IL-21. This cytokine may be another possible modulator of VAT Tregs, as IL-21 KO mice have been shown to have higher frequency of VAT Tregs[193] although whether IL-21 acts directly on adipose Tregs remains to be determined. VAT Tregs may also respond to insulin. Splenic Tregs can express insulin receptor, and treatment of these cells with insulin leads to AKT/mTOR signaling resulting in decreased IL-10 production[194]. Along those lines, VAT Tregs from hyperinsulinemic mice produce less IL-10 than VAT Tregs from lean mice[194]. In addition to cytokines, there are adipokines and miRNAs in the adipose that have been tied to insulin signaling and thermogenesis[15, 30, 31, 195, 196]. It may be possible that adipokines

such as leptin, adiponectin, IL-6, neuregulin 4, fibroblast growth factor 21, and adipocyte-derived miRNAs have a role in Blimp-1 expression.

Apart from fatty acids and the cytokine/adipokine milieu, hypoxia may also affect Blimp-1 expression in aTregs. It has previously been shown that hypoxia can induce Blimp-1 expression in human and mice pancreatic cancer cells[197]. During obesity, adipocyte hyperplasia and hypertrophy results in decreased oxygen availability[32, 33], and this may possibly lead to increased Blimp-1 expression in Tregs. This can be tested in vitro by culturing cells in a regular tissue culture incubator under decreased oxygen settings.

Recently, it has been suggested that the gut microbiota can play a role in determining one's susceptibility to obesity and metabolic syndrome[198]. It has previously been shown that Blimp-1+ Tregs can play a role in suppressing inflammation within the small intestines[119]. It would be interesting to isolate Tregs from clinical gut biopsies of obese and lean humans, and see whether Blimp-1 expression differs in people with different intestinal flora via fecal collection. In addition, these samples could then be used for fecal transplants into Blimp-1 reporter mice to see if Blimp-1 expression is altered in Tregs.

2.5.2.2 Effect of Blimp-1+ Tregs and IL-10 in the adipose during obesity

In this study, we elucidated the role of Treg-derived IL-10 on adipocytes during obesity. However, the adipose tissue contains other types of cells that can also respond to IL-10. Like many other types of adipokines and cytokines (e.g. IL-6, adiponectin and leptin), IL-10 is a pleiotropic cytokine that has differing effects depending on the cellular source, cell type that it's acting on, and the local microenvironment. Therefore, to

accurately understand how loss of Blimp-1+ Tregs and IL-10 affects adipose inflammation and systemic metabolism, one must take into consideration the other types of immune and stromal cells that exist within the tissue.

In addition to Tregs, lean adipose tissue in mice is populated by immune cells such as M2 macrophages, ILC2s, eosinophils, and Th2 cells that maintain an anti-inflammatory environment. ILC2- and Th2-derived cytokines, such as IL-5 and IL-13, support the maintenance of eosinophils, which through secretion of IL-4 can promote M2 macrophage polarization[21, 22]. Furthermore, adipose Tregs and a $NK1.1^{NEG}$ subclass of invariant natural killer T cells (iNKT) can secrete IL-10[23, 24 10], which can further promote M2 polarization, and also prohibit inflammatory signaling in adipocytes[25]. In contrast to lean adipose tissue, obese adipose tissue in mice skews towards housing pro-inflammatory immune cells such as M1 macrophages, CD8 T cells, T helper 1 cells (Th1) and T helper 17 cells (Th17)[30].

In this project, we showed that in the absence of Blimp-1, Tregs produce less IL-10. However, it has been found that macrophages, Th2 cells, and eosinophils can respond to as well as produce IL-10[199-201], and that ILC2s can secrete IL-10[202, 203]. Therefore, in lean mice, Treg-specific Blimp-1 deletion leads to decreased IL-10 production, but this may possibly be compensated for by other IL-10 producing cells. This would be in line with our observations that the changes in thermogenesis between Blimp-1 CKO and WT were more muted in lean mice relative to obese mice.

As mentioned earlier, macrophages play an important role in maintaining metabolic homeostasis[146]. In particular, IL-10 aids in M2 macrophage polarization[23-25]. Thus, we expected that in the absence of Blimp-1+ Tregs and decreased IL-10, our Blimp-1 CKO

mice will display changes in their macrophage populations. However, our data uncovered no differences in total macrophage frequency or the ratio of M1:M2 macrophages between Blimp-1 CKO and WT mice. However, we analyzed our cells using traditional macrophage markers F4/80, CD11c and CD206. In the future, it may be beneficial to include additional macrophage markers in our analyses to further sub-categorize these cells. For example, we can use M1 macrophage markers such as iNOS and Mcp-1, and M2 macrophage markers such as Arg1 and CD204[142]. Based off recent findings, it is now apparent that multiple macrophage subpopulations exist within the adipose tissue, and that their phenotypes change according to diet[75]. Therefore, utilizing single-cell RNA seq may yield clearer information on how the absence of Blimp-1+ Tregs may affect this heterogenous population. It may also be possible that Blimp-1+ Tregs affect their ability to produce TNFa, IL-1b, IL-6 or IL-10. Changes in cytokine production may be detected by LPS- or IL-4/IL-13 stimulating the adipose stromal vascular fraction ex vivo and analyzing cytokine production by flow.

Although there were no observable differences in macrophage frequency utilizing our current analysis strategy, surprisingly we saw that VAT CD8 T cells were increased in Blimp-1 CKO mice compared to WT controls. Previous studies have shown that CD8 T cells can cause insulin resistance and suppress BAT thermogenesis[204, 205]. At first glance, these details would suggest that the increase in CD8 T cells ran contrary to our working hypothesis of increased thermogenesis and improved insulin sensitivity in CKO mice compared to WT controls. However, it may be possible that these CD8 T cells are regulatory CD8 T cells, or given that they are in a chronically inflamed environment, we cannot rule out the possibility that they may be exhausted CD8 T cells. It has also been

previously demonstrated that IL-10 can enhance CD8 T cell function during gastric cancer[206]. Therefore, perhaps loss of Blimp-1+ Tregs leads to less IL-10, and dysfunctional CD8 T cells that have decreased capacity to suppress thermogenesis. Indeed, our lab has preliminary data suggesting that Blimp-1 deficient aTregs express more PD-1 (data not shown). We are currently performing extensive phenotyping of VAT, IAT and BAT CD8 T cells in our Blimp-1 CKO mice to see whether or not this is the case.

Although in our study, we examined a number of different immune cell subsets, four populations that we did not quantify were eosinophils, ILC2s, iNKT and regulatory B cells. ILC2 and eosinophils help promote thermogenesis, insulin sensitivity and glucose tolerance[56, 61]. IL-10 producing iNKT cells are enriched in lean scAT, and loss of iNKTs during DIO leads to increased insulin resistance[24, 207, 208]. In addition, in vivo iNKT activation by aGalCer or GLP1 peptide injection can increase scAT beiging[209]. Besides iNKT cells, loss of IL-10 producing regulatory B cells has also been shown to increase insulin resistance[210]. Given their connection to thermogenesis, insulin sensitivity and glucose tolerance, it would be interesting to study whether loss of Blimp-1+ Tregs affects any of these populations.

2.5.2.3 Effect of Blimp-1+ Tregs and IL-10 on systemic metabolism during obesity

In this study, the *Prdm1*$^{f/f}$ Foxp3-YFP-Cre+ mice and the *Il10*$^{f/f}$ Foxp3-YFP-Cre+ mice that were utilized affected all Tregs within the body. Other organs such as the liver, pancreas and skeletal muscle play critical roles in maintaining insulin sensitivity and glucose tolerance, and Tregs are present within these tissues as well. For example, one study found that non-alcoholic steatohepatitis patients have a higher hepatic Th17:resting Treg ratio compared to non-alcoholic fatty liver disease patients[211], and similarly in mice,

non-alcoholic steatohepatitis mice had an increased *Rorgt:Foxp3* hepatic mRNA ratio compared to normal diet mice[212] suggesting that a balance of Th17 and Tregs must be maintained to prevent abnormal liver pathology during obesity. To date, a role for pancreatic Tregs during DIO has not yet been described. However, it is worth noting that in Type 1 autoimmune diabetes NOD mice, CXCR3+ and ICOS+ pancreatic Tregs have been shown to suppress local inflammation as well as delay the onset and incidence of disease[213, 214]. Finally, skeletal muscle Tregs are decreased in HFD mice compared to standard chow mice[215]. Treatment of obese mice with resveratrol (an anti-inflammatory polyphenol) has been shown to be protective against obesity and correlated with increased M2 polarization and Treg infiltration into the skeletal muscle[216]. Therefore, the effect of Blimp-1 deletion on hepatic, pancreatic and skeletal muscle Tregs may be worth further examination.

Besides looking at inflammatory changes in the liver, pancreas and skeletal muscle, it would be interesting to examine whether Blimp-1+ Tregs affect metabolic processes within these organs. In our project, Blimp-1 CKO and IL-10 CKO mice exhibited improved insulin sensitivity, which is critical for regulating gluconeogenesis, glycogenolysis, de novo lipid synthesis in the liver, triglyceride synthesis and lipolysis. What's more, if we find that loss of Blimp-1+ Tregs results in decreased IL-10 in the blood, we cannot rule out the possibility that Treg IL-10 from one tissue may act distally on another organ to help maintain metabolic homeostasis. Although a role for IL-10 in the pancreas has not been described, it is known that IL-6 (another cytokine that signals through STAT3) enhances insulin secretion by pancreatic beta cells[217]. In addition, IL-10 has been shown to help maintain insulin sensitivity in skeletal muscle and prevent

macrophage infiltration and reduce IL-6 and TNFa within the muscle[218]. Although these findings by other labs can at first appear to conflict with our findings that loss of IL-10 improved insulin sensitivity, we must not forget to consider IL-10's effect on thermogenesis and how that affects systemic metabolism.

During BAT thermogenesis, BAT macrophages are in direct contact with BAT-innervating neurons and a plexin-semaforin signaling axis modulates norepinephrine activated thermogenesis[54]. It would be interesting to see whether loss of Blimp-1+ Tregs and its associated IL-10 has any effect on the frequency or phenotype of BAT macrophages as well as the concentration of BAT-innervating neurons, or their activity.

In addition to the BAT, loss of Blimp-1+ Tregs and IL-10 in the scAT may affect the local immune cell populations that ultimately affect thermogenesis. As mentioned earlier, M2 macrophages, eosinophils and ILC2s can induce scAT beiging[57-61]. Furthermore, macrophages and eosinophils can respond to as well as produce IL-10[199-201], and ILC2s can secrete IL-10[202, 203]. Therefore, it is possible that reduced IL-10 availability in Blimp-1 CKO mice might affect these cells' ability to carry out thermogenesis.

Finally, in our study, we performed thermogenic analysis on mice that were housed at 22°C. In both our short-term and long-term HFD mice, there were noticeable differences in IAT thermogenesis between our CKO and WT mice. However, with regard to BAT thermogenesis, we only observed an increase in one thermogenic gene in our CKO compared to WT. In addition, loss of Blimp-1+ Tregs had no effect on energy expenditure in both the short-term and long-term HFD mice. Moving forward, it may be worth conducting adaptive or ß-adrenergic studies to see whether a stronger phenotype is induced when the mice are placed under greater physiological stress. Furthermore, for

mice, the range for thermoneutrality is ~29-33ºC depending on the time of the day[219]. Performing experiments on mice raised at warmer temperatures may yield data that is more physiologically relevant to humans than performing pre-clinical studies in mice that are housed at the current temperature.

2.5.3 Therapeutic potential of Blimp-1+ Tregs during obesity

Some individuals tend to gain weight more readily than others. In order to determine how genetics may play a possible role, it may be worth isolating Tregs from the omental adipose of age- and sex-matched obese and healthy individuals to see whether single nucleotide polymorphisms within the Blimp-1 locus can be identified and utilized as a marker for reduced susceptibility towards obesity. Besides searching for correlations, we can also raise obese *Prdm*1$^{f/f}$ Foxp3$^{eGFP\text{-}Cre\text{-}ERT2}$ mice, then induce Blimp-1 deletion in Tregs with tamoxifen to see whether obesity can be reversed if Blimp-1+ Tregs are selectively removed.

2.5.4 Conclusion

In summary, loss of Treg-derived IL-10 may have protective or detrimental effects on metabolism depending on whether individuals are lean or obese. As a result, we cannot assume that findings in SFD mice will be replicable in HFD mice, and thus we must be diligent in performing experiments in each of the diet models before any conclusions are made. To address IL-10's possible pleiotropic effect during diet-induced obesity, immune cell and metabolic phenotyping should occur in both *Blimp-1*$^{f/f}$ Foxp3-

Cre+ and *Il10*$^{f/f}$ Foxp3-Cre+ mice both pre- and post- HFD diet intervention, and at various stages of obesity to account for differences in the adipose immune cell landscape.

Adipose Tregs do not exist in a vacuum. In order to have a true grasp on the role of these cells during diet-induced obesity, it is critical that we integrate our Blimp-1+ aTreg findings with the rest of the adipose microenvironment as well as with the systemic metabolic changes that are occurring during obesity. Traditionally, immunologists have examined Tregs in isolation and have attempted to make a direct link to insulin sensitivity, glucose tolerance and thermogenesis. However, based off the findings in this project indicating the antagonistic effects of Blimp-1+ Tregs, a paradigm shift may be required to understand the true nature of adipose-resident Tregs and their role in regulating metabolism.

Bibliography

1. Organization, W.H. *Obesity and Overweight*. 2020 [cited 2021 02/12]; Available from: https://www.who.int/news-room/fact-sheets/detail/obesity-and-overweight.

2. Prevention, C.f.D.C.a. *Prevalence of Overweight, Obesity, and Severe Obesity Among Children and Adolescents Aged 2–19 Years: United States, 1963–1965 Through 2017–2018*. 2018 [cited 2021 02/12]; Available from: https://www.cdc.gov/nchs/data/hestat/obesity-child-17-18/obesity-child.htm.

3. Prevention, C.f.D.C.a. *NCHS Data Brief*. 2020 [cited 2021 02/12]; Available from: https://www.cdc.gov/nchs/data/databriefs/db360_tables-508.pdf#page=4.

4. Prevention, C.f.D.C.a. *Obesity and Overweight*. 2018 [cited 2021 02/12]; Available from: https://www.cdc.gov/nchs/fastats/obesity-overweight.htm.

5. Cawley, J., et al., *Direct medical costs of obesity in the United States and the most populous states.* J Manag Care Spec Pharm, 2021: p. 1-13.

6. Goettler, A., A. Grosse, and D. Sonntag, *Productivity loss due to overweight and obesity: a systematic review of indirect costs.* BMJ Open, 2017. **7**(10): p. e014632.

7. Spieker, E.A. and N. Pyzocha, *Economic Impact of Obesity.* Prim Care, 2016. **43**(1): p. 83-95, viii-ix.

8. González-Muniesa, P., et al., *Obesity.* Nat Rev Dis Primers, 2017. **3**: p. 17034.

9. Maliszewska, K. and A. Kretowski, *Brown Adipose Tissue and Its Role in Insulin and Glucose Homeostasis.* Int J Mol Sci, 2021. **22**(4).

10. Drucker, D.J., *Diabetes, obesity, metabolism, and SARS-CoV-2 infection: the end of the beginning.* Cell Metab, 2021.

11. Becker, M., M.K. Levings, and C. Daniel, *Adipose-tissue regulatory T cells: Critical players in adipose-immune crosstalk.* Eur J Immunol, 2017. **47**(11): p. 1867-1874.

12. Zatterale, F., et al., *Chronic Adipose Tissue Inflammation Linking Obesity to Insulin Resistance and Type 2 Diabetes.* Front Physiol, 2019. **10**: p. 1607.

13. AlZaim, I., et al., *Adipose Tissue Immunomodulation: A Novel Therapeutic Approach in Cardiovascular and Metabolic Diseases.* Front Cardiovasc Med, 2020. **7**: p. 602088.

14. Asif, S., et al., *Understanding Dietary Intervention-Mediated Epigenetic Modifications in Metabolic Diseases.* Front Genet, 2020. **11**: p. 590369.

15. Wang, G.X., X.Y. Zhao, and J.D. Lin, *The brown fat secretome: metabolic functions beyond thermogenesis.* Trends Endocrinol Metab, 2015. **26**(5): p. 231-7.

16. Li, Y., Y. Meng, and X. Yu, *The Unique Metabolic Characteristics of Bone Marrow Adipose Tissue.* Front Endocrinol (Lausanne), 2019. **10**: p. 69.

17. Wolf, A.M., et al., *Adiponectin induces the anti-inflammatory cytokines IL-10 and IL-1RA in human leukocytes.* Biochem Biophys Res Commun, 2004. **323**(2): p. 630-5.

18. Ohashi, K., et al., *Adiponectin promotes macrophage polarization toward an anti-inflammatory phenotype.* J Biol Chem, 2010. **285**(9): p. 6153-60.

19. Spallanzani, R.G., et al., *Distinct immunocyte-promoting and adipocyte-generating stromal components coordinate adipose tissue immune and metabolic tenors.* Sci Immunol, 2019. **4**(35).

20. Mahlakõiv, T., et al., *Stromal cells maintain immune cell homeostasis in adipose tissue via production of interleukin-33.* Sci Immunol, 2019. **4**(35).

21. Molofsky, A.B., et al., *Innate lymphoid type 2 cells sustain visceral adipose tissue eosinophils and alternatively activated macrophages.* J Exp Med, 2013. **210**(3): p. 535-49.

22. Wu, D., et al., *Eosinophils sustain adipose alternatively activated macrophages associated with glucose homeostasis.* Science, 2011. **332**(6026): p. 243-7.

23. Feuerer, M., et al., *Lean, but not obese, fat is enriched for a unique population of regulatory T cells that affect metabolic parameters.* Nature medicine, 2009. **15**(8): p. 930-939.

24. LaMarche, N.M., et al., *Distinct iNKT Cell Populations Use IFNγ or ER Stress-Induced IL-10 to Control Adipose Tissue Homeostasis.* Cell Metab, 2020. **32**(2): p. 243-258.e6.

25. Saraiva, M., P. Vieira, and A. O'Garra, *Biology and therapeutic potential of interleukin-10.* J Exp Med, 2020. **217**(1).

26. Cinti, S., et al., *Adipocyte death defines macrophage localization and function in adipose tissue of obese mice and humans.* J Lipid Res, 2005. **46**(11): p. 2347-55.

27. Altintas, M.M., et al., *Mast cells, macrophages, and crown-like structures distinguish subcutaneous from visceral fat in mice.* J Lipid Res, 2011. **52**(3): p. 480-8.

28. Chylikova, J., et al., *Macrophages of the subcutaneous and omental fatty tissue in obese patients: Immunohistochemical phenotyping of M2 subtypes in relation to*

type 2 diabetes. Biomed Pap Med Fac Univ Palacky Olomouc Czech Repub, 2020. **164**(2): p. 133-137.

29. Suganami, T., J. Nishida, and Y. Ogawa, *A paracrine loop between adipocytes and macrophages aggravates inflammatory changes: role of free fatty acids and tumor necrosis factor alpha.* Arterioscler Thromb Vasc Biol, 2005. **25**(10): p. 2062-8.

30. Bradley, D., et al., *Adipose Tissue T Regulatory Cells: Implications for Health and Disease.* Adv Exp Med Biol, 2021. **1278**: p. 125-139.

31. Zhao, X.Y., et al., *The obesity-induced adipokine sST2 exacerbates adipose T(reg) and ILC2 depletion and promotes insulin resistance.* Sci Adv, 2020. **6**(20): p. eaay6191.

32. Ye, J., et al., *Hypoxia is a potential risk factor for chronic inflammation and adiponectin reduction in adipose tissue of ob/ob and dietary obese mice.* Am J Physiol Endocrinol Metab, 2007. **293**(4): p. E1118-28.

33. Rausch, M.E., et al., *Obesity in C57BL/6J mice is characterized by adipose tissue hypoxia and cytotoxic T-cell infiltration.* Int J Obes (Lond), 2008. **32**(3): p. 451-63.

34. Sung, H.K., et al., *Adipose vascular endothelial growth factor regulates metabolic homeostasis through angiogenesis.* Cell Metab, 2013. **17**(1): p. 61-72.

35. González-Muniesa, P., et al., *Effects of Hyperoxia on Oxygen-Related Inflammation with a Focus on Obesity.* Oxid Med Cell Longev, 2015. **2015**: p. 8957827.

36. Dowal, L., et al., *Intrinsic Properties of Brown and White Adipocytes Have Differential Effects on Macrophage Inflammatory Responses.* Mediators Inflamm, 2017. **2017**: p. 9067049.

37. Shankar, K., et al., *Role of brown adipose tissue in modulating adipose tissue inflammation and insulin resistance in high-fat diet fed mice.* Eur J Pharmacol, 2019. **854**: p. 354-364.

38. London, A., et al., *The Role of Hepatic Fat Accumulation in Glucose and Insulin Homeostasis-Dysregulation by the Liver.* J Clin Med, 2021. **10**(3).

39. Samuel, V.T. and G.I. Shulman, *Mechanisms for insulin resistance: common threads and missing links.* Cell, 2012. **148**(5): p. 852-71.

40. Browning, J.D. and J.D. Horton, *Molecular mediators of hepatic steatosis and liver injury.* J Clin Invest, 2004. **114**(2): p. 147-52.

41. Oh, Y.S., et al., *Fatty Acid-Induced Lipotoxicity in Pancreatic Beta-Cells During Development of Type 2 Diabetes.* Front Endocrinol (Lausanne), 2018. **9**: p. 384.

42. Fabbrini, E. and F. Magkos, *Hepatic Steatosis as a Marker of Metabolic Dysfunction.* Nutrients, 2015. **7**(6): p. 4995-5019.

43. Cypess, A.M., et al., *Identification and importance of brown adipose tissue in adult humans.* N Engl J Med, 2009. **360**(15): p. 1509-17.

44. White, J.D., R.S. Dewal, and K.I. Stanford, *The beneficial effects of brown adipose tissue transplantation.* Mol Aspects Med, 2019. **68**: p. 74-81.

45. Damal Villivalam, S., et al., *TET1 is a beige adipocyte-selective epigenetic suppressor of thermogenesis.* Nat Commun, 2020. **11**(1): p. 4313.

46. Guo, X., et al., *cAMP-MicroRNA-203-IFNγ network regulates subcutaneous white fat browning and glucose tolerance.* Mol Metab, 2019. **28**: p. 36-47.

47. Auffret, J., et al., *Beige differentiation of adipose depots in mice lacking prolactin receptor protects against high-fat-diet-induced obesity.* Faseb j, 2012. **26**(9): p. 3728-37.

48. Stine, R.R., et al., *EBF2 promotes the recruitment of beige adipocytes in white adipose tissue.* Mol Metab, 2016. **5**(1): p. 57-65.

49. McGregor, R.A., et al., *Time-course microarrays reveal modulation of developmental, lipid metabolism and immune gene networks in intrascapular brown adipose tissue during the development of diet-induced obesity.* Int J Obes (Lond), 2013. **37**(12): p. 1524-31.

50. Alcalá, M., et al., *Increased inflammation, oxidative stress and mitochondrial respiration in brown adipose tissue from obese mice.* Sci Rep, 2017. **7**(1): p. 16082.

51. Peterson, K.R., D.K. Flaherty, and A.H. Hasty, *Obesity Alters B Cell and Macrophage Populations in Brown Adipose Tissue.* Obesity (Silver Spring), 2017. **25**(11): p. 1881-1884.

52. Lettieri-Barbato, D. and K. Aquilano, *Aging and Immunometabolic Adaptations to Thermogenesis.* Ageing Res Rev, 2020. **63**: p. 101143.

53. Sakamoto, T., et al., *Macrophage infiltration into obese adipose tissues suppresses the induction of UCP1 level in mice.* Am J Physiol Endocrinol Metab, 2016. **310**(8): p. E676-e687.

54. Wolf, Y., et al., *Brown-adipose-tissue macrophages control tissue innervation and homeostatic energy expenditure.* Nat Immunol, 2017. **18**(6): p. 665-674.

55. Elieh Ali Komi, D., F. Shafaghat, and M. Christian, *Crosstalk Between Mast Cells and Adipocytes in Physiologic and Pathologic Conditions.* Clin Rev Allergy Immunol, 2020. **58**(3): p. 388-400.

56. Ding, X., et al., *IL-33-driven ILC2/eosinophil axis in fat is induced by sympathetic tone and suppressed by obesity.* J Endocrinol, 2016. **231**(1): p. 35-48.

57. Hui, X., et al., *Adiponectin Enhances Cold-Induced Browning of Subcutaneous Adipose Tissue via Promoting M2 Macrophage Proliferation.* Cell Metab, 2015. **22**(2): p. 279-90.

58. Qiu, Y., et al., *Eosinophils and type 2 cytokine signaling in macrophages orchestrate development of functional beige fat.* Cell, 2014. **157**(6): p. 1292-1308.

59. Nguyen, K.D., et al., *Alternatively activated macrophages produce catecholamines to sustain adaptive thermogenesis.* Nature, 2011. **480**(7375): p. 104-8.

60. Lee, M.W., et al., *Activated type 2 innate lymphoid cells regulate beige fat biogenesis.* Cell, 2015. **160**(1-2): p. 74-87.

61. Brestoff, J.R., et al., *Group 2 innate lymphoid cells promote beiging of white adipose tissue and limit obesity.* Nature, 2015. **519**(7542): p. 242-6.

62. Finlin, B.S., et al., *Mast Cells Promote Seasonal White Adipose Beiging in Humans.* Diabetes, 2017. **66**(5): p. 1237-1246.

63. Zhang, X., et al., *Functional Inactivation of Mast Cells Enhances Subcutaneous Adipose Tissue Browning in Mice.* Cell Rep, 2019. **28**(3): p. 792-803.e4.

64. Yabut, J.M., et al., *Genetic deletion of mast cell serotonin synthesis prevents the development of obesity and insulin resistance.* Nat Commun, 2020. **11**(1): p. 463.

65. Wang, G.X., et al., *The brown fat-enriched secreted factor Nrg4 preserves metabolic homeostasis through attenuation of hepatic lipogenesis.* Nat Med, 2014. **20**(12): p. 1436-1443.

66. Potthoff, M.J., et al., *FGF21 induces PGC-1alpha and regulates carbohydrate and fatty acid metabolism during the adaptive starvation response.* Proc Natl Acad Sci U S A, 2009. **106**(26): p. 10853-8.

67. Chartoumpekis, D.V., et al., *Brown adipose tissue responds to cold and adrenergic stimulation by induction of FGF21.* Mol Med, 2011. **17**(7-8): p. 736-40.

68. Burýsek, L. and J. Houstek, *beta-Adrenergic stimulation of interleukin-1alpha and interleukin-6 expression in mouse brown adipocytes.* FEBS Lett, 1997. **411**(1): p. 83-6.

69. Ellingsgaard, H., et al., *Interleukin-6 enhances insulin secretion by increasing glucagon-like peptide-1 secretion from L cells and alpha cells.* Nat Med, 2011. **17**(11): p. 1481-9.

70. Kurauti, M.A., et al., *Interleukin-6 increases the expression and activity of insulin-degrading enzyme.* Sci Rep, 2017. **7**: p. 46750.

71. Weisberg, S.P., et al., *Obesity is associated with macrophage accumulation in adipose tissue.* J Clin Invest, 2003. **112**(12): p. 1796-808.

72. Chung, K.J., et al., *A self-sustained loop of inflammation-driven inhibition of beige adipogenesis in obesity.* Nat Immunol, 2017. **18**(6): p. 654-664.

73. Goto, T., et al., *Proinflammatory cytokine interleukin-1β suppresses cold-induced thermogenesis in adipocytes.* Cytokine, 2016. **77**: p. 107-14.

74. Okla, M., et al., *Inhibitory Effects of Toll-Like Receptor 4, NLRP3 Inflammasome, and Interleukin-1β on White Adipocyte Browning.* Inflammation, 2018. **41**(2): p. 626-642.

75. Weinstock, A., et al., *Single-Cell RNA Sequencing of Visceral Adipose Tissue Leukocytes Reveals that Caloric Restriction Following Obesity Promotes the Accumulation of a Distinct Macrophage Population with Features of Phagocytic Cells.* Immunometabolism, 2019. **1**.

76. Pacella, I. and S. Piconese, *Immunometabolic Checkpoints of Treg Dynamics: Adaptation to Microenvironmental Opportunities and Challenges.* Front Immunol, 2019. **10**: p. 1889.

77. Mancuso, P. and B. Bouchard, *The Impact of Aging on Adipose Function and Adipokine Synthesis.* Front Endocrinol (Lausanne), 2019. **10**: p. 137.

78. Blaszczak, A.M., et al., *Obesogenic Memory Maintains Adipose Tissue Inflammation and Insulin Resistance.* Immunometabolism, 2020. **2**(3).

79. Cipolletta, D., et al., *Appearance and disappearance of the mRNA signature characteristic of Treg cells in visceral adipose tissue: age, diet, and PPARγ effects.* Proc Natl Acad Sci U S A, 2015. **112**(2): p. 482-7.

80. Vasanthakumar, A., et al., *Sex-specific adipose tissue imprinting of regulatory T cells.* Nature, 2020. **579**(7800): p. 581-585.

81. Ishikawa, A., et al., *Estrogen regulates sex-specific localization of regulatory T cells in adipose tissue of obese female mice.* PLoS One, 2020. **15**(4): p. e0230885.

82. Medrikova, D., et al., *Brown adipose tissue harbors a distinct sub-population of regulatory T cells.* PLoS One, 2015. **10**(2): p. e0118534.

83. Lira, F.S., et al., *Both adiponectin and interleukin-10 inhibit LPS-induced activation of the NF-κB pathway in 3T3-L1 adipocytes.* Cytokine, 2012. **57**(1): p. 98-106.

84. Morris, D.L., et al., *Adipose tissue macrophages function as antigen-presenting cells and regulate adipose tissue CD4+ T cells in mice.* Diabetes, 2013. **62**(8): p. 2762-72.

85. Cipolletta, D., et al., *PPAR-gamma is a major driver of the accumulation and phenotype of adipose tissue Treg cells.* Nature, 2012. **486**(7404): p. 549-53.

86. Ip, W.K.E., et al., *Anti-inflammatory effect of IL-10 mediated by metabolic reprogramming of macrophages.* Science, 2017. **356**(6337): p. 513-519.

87. Tiemessen, M.M., et al., *CD4+CD25+Foxp3+ regulatory T cells induce alternative activation of human monocytes/macrophages.* Proc Natl Acad Sci U S A, 2007. **104**(49): p. 19446-51.

88. Liu, X., et al., *Tim-3 Regulates Tregs' Ability to Resolve the Inflammation and Proliferation of Acute Lung Injury by Modulating Macrophages Polarization.* Shock, 2018. **50**(4): p. 455-464.

89. Ilan, Y., et al., *Induction of regulatory T cells decreases adipose inflammation and alleviates insulin resistance in ob/ob mice.* Proc Natl Acad Sci U S A, 2010. **107**(21): p. 9765-70.

90. Priceman, S.J., et al., *Regulation of adipose tissue T cell subsets by Stat3 is crucial for diet-induced obesity and insulin resistance.* Proc Natl Acad Sci U S A, 2013. **110**(32): p. 13079-84.

91. Han, J.M., et al., *IL-33 Reverses an Obesity-Induced Deficit in Visceral Adipose Tissue ST2+ T Regulatory Cells and Ameliorates Adipose Tissue Inflammation and Insulin Resistance.* J Immunol, 2015. **194**(10): p. 4777-83.

92. Vasanthakumar, A., et al., *The transcriptional regulators IRF4, BATF and IL-33 orchestrate development and maintenance of adipose tissue-resident regulatory T cells.* Nat Immunol, 2015. **16**(3): p. 276-85.

93. Bapat, S.P., et al., *Depletion of fat-resident Treg cells prevents age-associated insulin resistance.* Nature, 2015. **528**(7580): p. 137-41.

94. Kälin, S., et al., *A Stat6/Pten Axis Links Regulatory T Cells with Adipose Tissue Function.* Cell Metab, 2017. **26**(3): p. 475-492.e7.

95. Becker, M., et al., *Short-term cold exposure supports human Treg induction in vivo.* Mol Metab, 2019. **28**: p. 73-82.

96. Kolodin, D., et al., *Antigen- and cytokine-driven accumulation of regulatory T cells in visceral adipose tissue of lean mice.* Cell Metab, 2015. **21**(4): p. 543-57.

97. DiSpirito, J.R., et al., *Molecular diversification of regulatory T cells in nonlymphoid tissues.* Sci Immunol, 2018. **3**(27).

98. Cipolletta, D., et al., *Appearance and disappearance of the mRNA signature characteristic of Treg cells in visceral adipose tissue: age, diet, and PPARgamma effects.* Proc Natl Acad Sci U S A, 2015. **112**(2): p. 482-7.

99. Lynch, L., et al., *Regulatory iNKT cells lack expression of the transcription factor PLZF and control the homeostasis of T(reg) cells and macrophages in adipose tissue.* Nat Immunol, 2015. **16**(1): p. 85-95.

100. Li, C., et al., *TCR Transgenic Mice Reveal Stepwise, Multi-site Acquisition of the Distinctive Fat-Treg Phenotype.* Cell, 2018. **174**(2): p. 285-299.e12.

101. Frias, A.B., Jr., et al., *The Transcriptional Regulator Id2 Is Critical for Adipose-Resident Regulatory T Cell Differentiation, Survival, and Function.* J Immunol, 2019. **203**(3): p. 658-664.

102. Wara, A.K., et al., *KLF10 Deficiency in CD4(+) T Cells Triggers Obesity, Insulin Resistance, and Fatty Liver.* Cell Rep, 2020. **33**(13): p. 108550.

103. Keller, A.D. and T. Maniatis, *Identification and characterization of a novel repressor of beta-interferon gene expression.* Genes Dev, 1991. **5**(5): p. 868-79.

104. Turner, C.A., Jr., D.H. Mack, and M.M. Davis, *Blimp-1, a novel zinc finger-containing protein that can drive the maturation of B lymphocytes into immunoglobulin-secreting cells.* Cell, 1994. **77**(2): p. 297-306.

105. Crotty, S., R.J. Johnston, and S.P. Schoenberger, *Effectors and memories: Bcl-6 and Blimp-1 in T and B lymphocyte differentiation.* Nat Immunol, 2010. **11**(2): p. 114-20.

106. Kim, S.J., *Immunological function of Blimp-1 in dendritic cells and relevance to autoimmune diseases.* Immunol Res, 2015. **63**(1-3): p. 113-20.

107. Chang, D.H., C. Angelin-Duclos, and K. Calame, *BLIMP-1: trigger for differentiation of myeloid lineage.* Nat Immunol, 2000. **1**(2): p. 169-76.

108. Martins, G.A., et al., *Transcriptional repressor Blimp-1 regulates T cell homeostasis and function.* Nat Immunol, 2006. **7**(5): p. 457-65.

109. Kallies, A., et al., *Transcriptional repressor Blimp-1 is essential for T cell homeostasis and self-tolerance.* Nat Immunol, 2006. **7**(5): p. 466-74.

110. Kallies, A., et al., *Blimp-1 transcription factor is required for the differentiation of effector CD8(+) T cells and memory responses.* Immunity, 2009. **31**(2): p. 283-95.

111. Rutishauser, R.L., et al., *Transcriptional repressor Blimp-1 promotes CD8(+) T cell terminal differentiation and represses the acquisition of central memory T cell properties.* Immunity, 2009. **31**(2): p. 296-308.

112. Ji, Y., et al., *Repression of the DNA-binding inhibitor Id3 by Blimp-1 limits the formation of memory CD8+ T cells.* Nat Immunol, 2011. **12**(12): p. 1230-7.

113. Cretney, E., et al., *The transcription factors Blimp-1 and IRF4 jointly control the differentiation and function of effector regulatory T cells.* Nat Immunol, 2011. **12**(4): p. 304-11.

114. Sciammas, R., et al., *Graded expression of interferon regulatory factor-4 coordinates isotype switching with plasma cell differentiation.* Immunity, 2006. **25**(2): p. 225-36.

115. Kwon, H., et al., *Analysis of interleukin-21-induced Prdm1 gene regulation reveals functional cooperation of STAT3 and IRF4 transcription factors.* Immunity, 2009. **31**(6): p. 941-52.

116. Bankoti, R., et al., *Differential regulation of Effector and Regulatory T cell function by Blimp1.* Sci Rep, 2017. **7**(1): p. 12078.

117. Vasanthakumar, A., et al., *The TNF Receptor Superfamily-NF-κB Axis Is Critical to Maintain Effector Regulatory T Cells in Lymphoid and Non-lymphoid Tissues.* Cell Rep, 2017. **20**(12): p. 2906-2920.

118. Cretney, E., et al., *Characterization of Blimp-1 function in effector regulatory T cells.* J Autoimmun, 2018. **91**: p. 73-82.

119. Ogawa, C., et al., *Blimp-1 Functions as a Molecular Switch to Prevent Inflammatory Activity in Foxp3(+)RORγt(+) Regulatory T Cells.* Cell Rep, 2018. **25**(1): p. 19-28.e5.

120. Garg, G., et al., *Blimp1 Prevents Methylation of Foxp3 and Loss of Regulatory T Cell Identity at Sites of Inflammation.* Cell Rep, 2019. **26**(7): p. 1854-1868.e5.

121. Zhou, X., et al., *Instability of the transcription factor Foxp3 leads to the generation of pathogenic memory T cells in vivo.* Nat Immunol, 2009. **10**(9): p. 1000-7.

122. Floess, S., et al., *Epigenetic control of the foxp3 locus in regulatory T cells.* PLoS Biol, 2007. **5**(2): p. e38.

123. Wan, Y.Y. and R.A. Flavell, *Identifying Foxp3-expressing suppressor T cells with a bicistronic reporter.* Proc Natl Acad Sci U S A, 2005. **102**(14): p. 5126-31.

124. Shapiro-Shelef, M., et al., *Blimp-1 is required for the formation of immunoglobulin secreting plasma cells and pre-plasma memory B cells.* Immunity, 2003. **19**(4): p. 607-20.

125. Rubtsov, Y.P., et al., *Regulatory T cell-derived interleukin-10 limits inflammation at environmental interfaces.* Immunity, 2008. **28**(4): p. 546-58.

126. Mooli, R.G.R., et al., *Sustained mitochondrial biogenesis is essential to maintain caloric restriction-induced beige adipocytes.* Metabolism, 2020. **107**: p. 154225.

127. Panduro, M., C. Benoist, and D. Mathis, *Tissue Tregs.* Annu Rev Immunol, 2016. **34**: p. 609-33.

128. Deng, T., et al., *Adipocyte adaptive immunity mediates diet-induced adipose inflammation and insulin resistance by decreasing adipose Treg cells.* Nature Communications, 2017. **8**(1): p. 15725.

129. Yuan, X., G. Cheng, and T.R. Malek, *The importance of regulatory T-cell heterogeneity in maintaining self-tolerance.* Immunological reviews, 2014. **259**(1): p. 103-114.

130. Toomer, K.H., et al., *Essential and non-overlapping IL-2Rα-dependent processes for thymic development and peripheral homeostasis of regulatory T cells.* Nat Commun, 2019. **10**(1): p. 1037.

131. Ronchetti, S., et al., *Glucocorticoid-induced tumour necrosis factor receptor-related protein: a key marker of functional regulatory T cells.* J Immunol Res, 2015. **2015**: p. 171520.

132. Onodera, T., et al., *Adipose tissue macrophages induce PPARγ-high FOXP3(+) regulatory T cells.* Scientific reports, 2015. **5**: p. 16801-16801.

133. Rajbhandari, P., et al., *Single cell analysis reveals immune cell-adipocyte crosstalk regulating the transcription of thermogenic adipocytes.* Elife, 2019. **8**.

134. Caspar-Bauguil, S., et al., *Adipose tissues as an ancestral immune organ: site-specific change in obesity.* FEBS Lett, 2005. **579**(17): p. 3487-92.

135. Caspar-Bauguil, S., et al., *Weight-dependent changes of immune system in adipose tissue: importance of leptin.* Exp Cell Res, 2006. **312**(12): p. 2195-202.

136. Miller, A.M., et al., *Interleukin-33 induces protective effects in adipose tissue inflammation during obesity in mice.* Circ Res, 2010. **107**(5): p. 650-8.

137. Patel, H., C.C. Kerndt, and A. Bhardwaj, *Physiology, Respiratory Quotient*, in *StatPearls*. 2020, StatPearls Publishing

Copyright © 2020, StatPearls Publishing LLC.: Treasure Island (FL).

138. Kühn, R., et al., *Interleukin-10-deficient mice develop chronic enterocolitis.* Cell, 1993. **75**(2): p. 263-74.

139. Chaudhry, A., et al., *Interleukin-10 signaling in regulatory T cells is required for suppression of Th17 cell-mediated inflammation.* Immunity, 2011. **34**(4): p. 566-78.

140. Keubler, L.M., et al., *A Multihit Model: Colitis Lessons from the Interleukin-10-deficient Mouse.* Inflamm Bowel Dis, 2015. **21**(8): p. 1967-75.

141. Griesenauer, B. and S. Paczesny, *The ST2/IL-33 Axis in Immune Cells during Inflammatory Diseases.* Front Immunol, 2017. **8**: p. 475.

142. Morita, Y., et al., *Impact of tissue macrophage proliferation on peripheral and systemic insulin resistance in obese mice with diabetes.* BMJ Open Diabetes Res Care, 2020. **8**(1).

143. Wang, Y., et al., *Improvement of obesity-associated disorders by a small-molecule drug targeting mitochondria of adipose tissue macrophages.* Nat Commun, 2021. **12**(1): p. 102.

144. Antony, A., et al., *Deficiency of Stat1 in CD11c(+) Cells Alters Adipose Tissue Inflammation and Improves Metabolic Dysfunctions in Mice Fed High-Fat Diet.* Diabetes, 2020.

145. Brestoff, J.R., et al., *Intercellular Mitochondria Transfer to Macrophages Regulates White Adipose Tissue Homeostasis and Is Impaired in Obesity.* Cell Metab, 2020.

146. Orliaguet, L., et al., *Mechanisms of Macrophage Polarization in Insulin Signaling and Sensitivity.* Front Endocrinol (Lausanne), 2020. **11**: p. 62.

147. Matta, B.M., et al., *IL-33 is an unconventional Alarmin that stimulates IL-2 secretion by dendritic cells to selectively expand IL-33R/ST2+ regulatory T cells.* J Immunol, 2014. **193**(8): p. 4010-20.

148. Macdougall, C.E., et al., *Visceral Adipose Tissue Immune Homeostasis Is Regulated by the Crosstalk between Adipocytes and Dendritic Cell Subsets.* Cell Metab, 2018. **27**(3): p. 588-601.e4.

149. Srikakulapu, P. and C.A. McNamara, *B Lymphocytes and Adipose Tissue Inflammation.* Arterioscler Thromb Vasc Biol, 2020. **40**(5): p. 1110-1122.

150. Sattler, S., et al., *IL-10-producing regulatory B cells induced by IL-33 (Breg(IL-33)) effectively attenuate mucosal inflammatory responses in the gut.* J Autoimmun, 2014. **50**(100): p. 107-22.

151. Li, Y., et al., *Natural Killer Cells: Friend or Foe in Metabolic Diseases?* Front Immunol, 2021. **12**: p. 614429.

152. Wang, L., et al., *Metabolic tissue-resident CD8(+) T cells: A key player in obesity-related diseases.* Obes Rev, 2021. **22**(3): p. e13133.

153. Rajbhandari, P., et al., *IL-10 Signaling Remodels Adipose Chromatin Architecture to Limit Thermogenesis and Energy Expenditure.* Cell, 2018. **172**(1-2): p. 218-233.e17.

154. Laakso, M., et al., *The Metabolic Syndrome in Men study: a resource for studies of metabolic and cardiovascular diseases.* J Lipid Res, 2017. **58**(3): p. 481-493.

155. Wu, D., et al., *T reg-specific insulin receptor deletion prevents diet-induced and age-associated metabolic syndrome.* J Exp Med, 2020. **217**(8).

156. He, K., et al., *Blimp-1 is essential for allergen-induced asthma and Th2 cell development in the lung.* J Exp Med, 2020. **217**(7).

157. Ouyang, W. and A. O'Garra, *IL-10 Family Cytokines IL-10 and IL-22: from Basic Science to Clinical Translation.* Immunity, 2019. **50**(4): p. 871-891.

158. Vignali, D.A., L.W. Collison, and C.J. Workman, *How regulatory T cells work.* Nat Rev Immunol, 2008. **8**(7): p. 523-32.

159. Seale, P., et al., *Transcriptional control of brown fat determination by PRDM16.* Cell Metab, 2007. **6**(1): p. 38-54.

160. Wu, J., et al., *Beige adipocytes are a distinct type of thermogenic fat cell in mouse and human.* Cell, 2012. **150**(2): p. 366-76.

161. Bettini, M. and D.A. Vignali, *Regulatory T cells and inhibitory cytokines in autoimmunity.* Curr Opin Immunol, 2009. **21**(6): p. 612-8.

162. Shime, H., et al., *Proenkephalin(+) regulatory T cells expanded by ultraviolet B exposure maintain skin homeostasis with a healing function.* Proc Natl Acad Sci U S A, 2020. **117**(34): p. 20696-20705.

163. Ito, M., et al., *Brain regulatory T cells suppress astrogliosis and potentiate neurological recovery.* Nature, 2019. **565**(7738): p. 246-250.

164. Fahlén, L., et al., *T cells that cannot respond to TGF-beta escape control by CD4(+)CD25(+) regulatory T cells.* J Exp Med, 2005. **201**(5): p. 737-46.

165. Wing, J.B., C. Tay, and S. Sakaguchi, *Control of Regulatory T Cells by Co-signal Molecules.* Adv Exp Med Biol, 2019. **1189**: p. 179-210.

166. Maj, T., et al., *Oxidative stress controls regulatory T cell apoptosis and suppressor activity and PD-L1-blockade resistance in tumor.* Nat Immunol, 2017. **18**(12): p. 1332-1341.

167. Deaglio, S., et al., *Adenosine generation catalyzed by CD39 and CD73 expressed on regulatory T cells mediates immune suppression.* J Exp Med, 2007. **204**(6): p. 1257-65.

168. Ali, N., et al., *Regulatory T Cells in Skin Facilitate Epithelial Stem Cell Differentiation.* Cell, 2017. **169**(6): p. 1119-1129.e11.

169. Faustino, L.D., et al., *Interleukin-33 activates regulatory T cells to suppress innate γδ T cell responses in the lung.* Nat Immunol, 2020. **21**(11): p. 1371-1383.

170. Kohlgruber, A.C., et al., *γδ T cells producing interleukin-17A regulate adipose regulatory T cell homeostasis and thermogenesis.* Nat Immunol, 2018. **19**(5): p. 464-474.

171. Yang, B., et al., *Transgenic mice specifically expressing amphiregulin in white adipose tissue showed less adipose tissue mass.* Genes Cells, 2018. **23**(3): p. 136-145.

172. Besse-Patin, A., et al., *PGC1A regulates the IRS1:IRS2 ratio during fasting to influence hepatic metabolism downstream of insulin.* Proc Natl Acad Sci U S A, 2019. **116**(10): p. 4285-4290.

173. Estall, J.L., et al., *Sensitivity of lipid metabolism and insulin signaling to genetic alterations in hepatic peroxisome proliferator-activated receptor-gamma coactivator-1alpha expression.* Diabetes, 2009. **58**(7): p. 1499-508.

174. Besse-Patin, A., et al., *Estrogen Signals Through Peroxisome Proliferator-Activated Receptor-γ Coactivator 1α to Reduce Oxidative Damage Associated With Diet-Induced Fatty Liver Disease.* Gastroenterology, 2017. **152**(1): p. 243-256.

175. Kleiner, S., et al., *Development of insulin resistance in mice lacking PGC-1α in adipose tissues.* Proc Natl Acad Sci U S A, 2012. **109**(24): p. 9635-40.

176. Suo, J., et al., *Met-enkephalin improves metabolic syndrome in high fat diet challenged mice through promotion of adipose tissue browning.* Toxicol Appl Pharmacol, 2018. **359**: p. 12-23.

177. Gnad, T., et al., *Adenosine activates brown adipose tissue and recruits beige adipocytes via A2A receptors.* Nature, 2014. **516**(7531): p. 395-9.

178. Shevyrev, D. and V. Tereshchenko, *Treg Heterogeneity, Function, and Homeostasis.* Front Immunol, 2019. **10**: p. 3100.

179. Zhang, Q., et al., *LAG3 limits regulatory T cell proliferation and function in autoimmune diabetes.* Sci Immunol, 2017. **2**(9).

180. Johnston, R.J., et al., *Bcl6 and Blimp-1 are reciprocal and antagonistic regulators of T follicular helper cell differentiation.* Science, 2009. **325**(5943): p. 1006-10.

181. Koh, B., et al., *Bcl6 and Blimp1 reciprocally regulate ST2(+) Treg-cell development in the context of allergic airway inflammation.* J Allergy Clin Immunol, 2020. **146**(5): p. 1121-1136.e9.

182. Pompura, S.L., et al., *Oleic acid restores suppressive defects in tissue-resident FOXP3 Tregs from patients with multiple sclerosis.* J Clin Invest, 2021. **131**(2).

183. Sun, M., et al., *Microbiota-derived short-chain fatty acids promote Th1 cell IL-10 production to maintain intestinal homeostasis.* Nat Commun, 2018. **9**(1): p. 3555.

184. Sierra, S., et al., *Dietary fish oil n-3 fatty acids increase regulatory cytokine production and exert anti-inflammatory effects in two murine models of inflammation.* Lipids, 2006. **41**(12): p. 1115-25.

185. Ly, L.H., et al., *Dietary n-3 polyunsaturated fatty acids suppress splenic CD4(+) T cell function in interleukin (IL)-10(-/-) mice.* Clin Exp Immunol, 2005. **139**(2): p. 202-9.

186. Singh, N., et al., *Activation of Gpr109a, receptor for niacin and the commensal metabolite butyrate, suppresses colonic inflammation and carcinogenesis.* Immunity, 2014. **40**(1): p. 128-39.

187. Field, A.E., et al., *Dietary fat and weight gain among women in the Nurses' Health Study.* Obesity (Silver Spring), 2007. **15**(4): p. 967-76.

188. Raatz, S.K., et al., *Relationship of the Reported Intakes of Fat and Fatty Acids to Body Weight in US Adults.* Nutrients, 2017. **9**(5).

189. Liu, H., et al., *Butyrate: A Double-Edged Sword for Health?* Adv Nutr, 2018. **9**(1): p. 21-29.

190. Palomer, X., et al., *Palmitic and Oleic Acid: The Yin and Yang of Fatty Acids in Type 2 Diabetes Mellitus.* Trends Endocrinol Metab, 2018. **29**(3): p. 178-190.

191. Lang, P., et al., *Effects of different diets used in diet-induced obesity models on insulin resistance and vascular dysfunction in C57BL/6 mice.* Sci Rep, 2019. **9**(1): p. 19556.

192. Hasegawa, Y., et al., *Long-term effects of western diet consumption in male and female mice.* Sci Rep, 2020. **10**(1): p. 14686.

193. Fabrizi, M., et al., *IL-21 is a major negative regulator of IRF4-dependent lipolysis affecting Tregs in adipose tissue and systemic insulin sensitivity.* Diabetes, 2014. **63**(6): p. 2086-96.

194. Han, J.M., et al., *Insulin inhibits IL-10-mediated regulatory T cell function: implications for obesity.* J Immunol, 2014. **192**(2): p. 623-9.

195. Thomou, T., et al., *Adipose-derived circulating miRNAs regulate gene expression in other tissues.* Nature, 2017. **542**(7642): p. 450-455.

196. Heyn, G.S., L.H. Corrêa, and K.G. Magalhães, *The Impact of Adipose Tissue-Derived miRNAs in Metabolic Syndrome, Obesity, and Cancer.* Front Endocrinol (Lausanne), 2020. **11**: p. 563816.

197. Chiou, S.H., et al., *BLIMP1 Induces Transient Metastatic Heterogeneity in Pancreatic Cancer.* Cancer Discov, 2017. **7**(10): p. 1184-1199.

198. Huda, M.N., M. Kim, and B.J. Bennett, *Modulating the Microbiota as a Therapeutic Intervention for Type 2 Diabetes.* Front Endocrinol (Lausanne), 2021. **12**: p. 632335.

199. Makita, N., et al., *IL-10 enhances the phenotype of M2 macrophages induced by IL-4 and confers the ability to increase eosinophil migration.* Int Immunol, 2015. **27**(3): p. 131-41.

200. Hill, A.A., W. Reid Bolus, and A.H. Hasty, *A decade of progress in adipose tissue macrophage biology.* Immunol Rev, 2014. **262**(1): p. 134-52.

201. Poholek, A.C., et al., *IL-10 induces a STAT3-dependent autoregulatory loop in T(H)2 cells that promotes Blimp-1 restriction of cell expansion via antagonism of STAT5 target genes.* Sci Immunol, 2016. **1**(5).

202. Howard, E., et al., *IL-10 production by ILC2s requires Blimp-1 and cMaf, modulates cellular metabolism, and ameliorates airway hyperreactivity.* J Allergy Clin Immunol, 2021. **147**(4): p. 1281-1295.e5.

203. Bando, J.K., et al., *ILC2s are the predominant source of intestinal ILC-derived IL-10.* J Exp Med, 2020. **217**(2).

204. Nishimura, S., et al., *CD8+ effector T cells contribute to macrophage recruitment and adipose tissue inflammation in obesity.* Nat Med, 2009. **15**(8): p. 914-20.

205. Moysidou, M., et al., *CD8+ T cells in beige adipogenesis and energy homeostasis.* JCI Insight, 2018. **3**(5).

206. Bedke, T., et al., *Title: IL-10-producing T cells and their dual functions.* Semin Immunol, 2019. **44**: p. 101335.

207. Lynch, L., et al., *Adipose tissue invariant NKT cells protect against diet-induced obesity and metabolic disorder through regulatory cytokine production.* Immunity, 2012. **37**(3): p. 574-87.

208. Sag, D., et al., *IL-10-producing NKT10 cells are a distinct regulatory invariant NKT cell subset.* J Clin Invest, 2014. **124**(9): p. 3725-40.

209. Lynch, L., et al., *iNKT Cells Induce FGF21 for Thermogenesis and Are Required for Maximal Weight Loss in GLP1 Therapy.* Cell Metab, 2016. **24**(3): p. 510-519.

210. Nishimura, S., et al., *Adipose Natural Regulatory B Cells Negatively Control Adipose Tissue Inflammation.* Cell Metab, 2013. **18**(5): p. 759-766.

211. Rau, M., et al., *Progression from Nonalcoholic Fatty Liver to Nonalcoholic Steatohepatitis Is Marked by a Higher Frequency of Th17 Cells in the Liver and an Increased Th17/Resting Regulatory T Cell Ratio in Peripheral Blood and in the Liver.* J Immunol, 2016. **196**(1): p. 97-105.

212. He, B., et al., *The imbalance of Th17/Treg cells is involved in the progression of nonalcoholic fatty liver disease in mice.* BMC Immunol, 2017. **18**(1): p. 33.

213. Kornete, M., E. Sgouroudis, and C.A. Piccirillo, *ICOS-dependent homeostasis and function of Foxp3+ regulatory T cells in islets of nonobese diabetic mice.* J Immunol, 2012. **188**(3): p. 1064-74.

214. Tan, T.G., D. Mathis, and C. Benoist, *Singular role for T-BET+CXCR3+ regulatory T cells in protection from autoimmune diabetes.* Proc Natl Acad Sci U S A, 2016. **113**(49): p. 14103-14108.

215. Khan, I.M., et al., *Intermuscular and perimuscular fat expansion in obesity correlates with skeletal muscle T cell and macrophage infiltration and insulin resistance.* Int J Obes (Lond), 2015. **39**(11): p. 1607-18.

216. Shabani, M., et al., *Resveratrol alleviates obesity-induced skeletal muscle inflammation via decreasing M1 macrophage polarization and increasing the regulatory T cell population.* Sci Rep, 2020. **10**(1): p. 3791.

217. Suzuki, T., et al., *Interleukin-6 enhances glucose-stimulated insulin secretion from pancreatic beta-cells: potential involvement of the PLC-IP3-dependent pathway.* Diabetes, 2011. **60**(2): p. 537-47.

218. Hong, E.G., et al., *Interleukin-10 prevents diet-induced insulin resistance by attenuating macrophage and cytokine response in skeletal muscle.* Diabetes, 2009. **58**(11): p. 2525-35.

219. Symonds, M.E., et al., *Adipose tissue growth and development: the modulating role of ambient temperature.* J Endocrinol, 2021. **248**(1): p. R19-r28.